# Near Earth Asteroids associated with meteor showers

Bogdan Alexandru Dumitru

PSL UNIVERSITÉ PARIS

THÈSE DE DOCTORAT
DE L'UNIVERSITÉ PSL

Préparée à l'Observatoire de Paris
Dans le cadre d'une cotutelle avec Université de Bucarest,
Faculté de Physique

# Etude d'astéroïdes géocroiseurs à l'origine des pluies de météores

## Physical properties of Near Earth Asteroids at the origin of meteor showers


Soutenue par
**Bogdan Alexandru Dumitru**
Le 26.09.2018


Ecole doctorale n° 127
**Astronomie et astrophysique d'Île-de-France**

Spécialité
**SYSTEME SOLAIRE, ASTEROIDS**

Composition du jury :

| | |
|---|---|
| Prof. Dr. Daniela Dragoman<br>Université de Bucarest, Roumanie | *Président* |
| Dr. Remus Stefan Boata<br>Romanian Academy - Timisoara Branch, Romania | *Rapporteur* |
| Prof. Dr. Philippe Rousselot<br>Observatoire de Besançon, France | *Rapporteur* |
| Dr. Agnieszka Kryszczynska<br>Observatoire de Poznan, Pologne | *Examinateur* |
| Dr. William Thuillot<br>Observatoire of Paris, France | *Examinateur* |
| Prof. Dr. Sabina Stefan<br>Université de Bucarest, Roumanie | *Examinateur* |
| Prof. Dr. Mirel BIRLAN<br>Observatoire of Paris, France | *Directeur de thèse* |
| Prof. Dr. Mihai DIMA<br>Université de Bucarest, Roumanie | *Directeur de thèse* |

l'Observatoire de Paris | PSL


**THÈSE DE DOCTORAT**

DE L'UNIVERSITÉ PSL

# Contents

# Abstract

Meteoroids, asteroids, and comets have been permanently interacting with Earth during its existence. When an object, such as a comet or an asteroid, revolve around the Sun it may leave fragments of matter behind it and if this object is in Earth's proximity, those fragments are gathered by the planet gravity. The study of these objects and the link between them can help in the understanding of the formation and evolution conditions of the Solar System, the conditions of developing the life on Earth, the chaotic processes in the Solar System, Earth security and maybe, in future, space industry.

All objects within the Solar System are characterized by their orbits and the meteoroid streams have similar orbits with the objects that produce them. For that reason the most common method of parent body identification is based on orbits similarities, also known as discrimination criteria or D-Criteria. In my work I used three D-Criteria metrics for parent body association. I set a threshold for each metric by using a new threshold selection method. Moreover, I investigated the associated objects orbital stability, in the Lyapunov time sense and their physical properties.

Due to the similarities between meteoroid streams and their parent bodies, it is required for the associations to belong to Near Earth Asteroids population. But for this population is difficult to obtain data. The favorable geometry for these objects observations occurs five times per century. For this reason was created an observational program, that aims to obtain physical data for the associated objects that do not have physical data.

My results consist from a sample of 296 asteroids that were associated with 28 meteor showers, from which 73 asteroids satisfied all the criteria used. From the dynamical perspective, my sample contains 82% of Apollo asteroids and 7% are classified as potential hazardous, 15.3% are on commentary orbits and 84.3% are on asteroidal orbits. From the physical data perspective, I found two asteroids that are fast-rotators, therefore they can not generate meteors. On the other hand, I also found associated one binary asteroid and one tumbling asteroid, objects with a high probability of being parent bodies.

I also managed to find similarities between 5 meteorites and 5 associated asteroids with physical data and I obtained observational data for three associated asteroids.

# Résumé

Les météoroïdes, les astéroïdes et les comètes ont été en interaction permanente avec la Terre pendant son existence. Lorsqu'un objet, tel qu'une comète ou un astéroïde, tourne autour du Soleil, il peut laisser des fragments de matière derrière lui. Il y a une relation implicite entre les fragments et leurs corps parents. Le champ gravitationnel de la Terre capte les fragments et quelques fois le matériel extraterrestre est retrouve au sol sous la forme des météorites.. L'étude de ces objets et le lien entre eux peuvent aider comprendre les conditions de formation et d'évolution du Système solaire, les conditions de développement de la vie sur Terre, les processus chaotiques dans le Système solaire, la sécurité de la Terre et peut-être , l'industrie spatiale.

Tous les objets dans le Système solaire sont caractérisés par leurs orbites et les flux de météoroïdes ont des orbites similaires avec les objets qui les produisent. Pour cette raison, la méthode la plus courante d'identification du corps parental est basée sur les similarités des orbites, également appelées critères de discrimination ou critères-D. Dans mon travail, j'ai utilisé trois critères D-Criteria pour l'association des corps parents. Je définis un seuil pour chaque mesure en utilisant une nouvelle méthode de sélection de seuil. En outre, j'ai étudié les objets associés stabilité orbitale, dans le sens du temps de Lyapunov et leurs propriétés physiques.

En raison des similitudes entre les flux de météorites et leurs corps parents, il est nécessaire que les associations appartiennent à la population d'astéroïdes géocroiseurs. L'observation de cette population d'objets est cependant difficile. La géométrie favorable pour les observations d'un géocroiseur est limité a trois ou cinq fois par siècle. Pour cette raison j'ai créé un programme d'observation, qui vise à obtenir des données physiques pour les objets associés qui n'ont pas de données physiques.

Lors de mes recherches, j'ai pu associé 296 géocroiseurs à 28 pluies de météores; parmi eux, 73 astéroïdes satisfaisant les trois critères utilisés. Du point de vue dynamique, mon échantillon contient 82% d'astéroïdes de type Apollo et 7% sont classés comme potentiellement dangereux, 15,3% sont sur des orbites cométaires et 84,3% sur des orbites d'astéroïdes. Du point de vue des données physiques, j'ai trouvé deux astéroïdes qui sont des rotateurs rapides, donc ils ne peuvent pas générer de météores. D'un autre côté, j'ai également trouvé un astéroïde binaire associé et un astéroïde tumbling, des objets avec une forte probabilité d'être des corps parents. J'ai également réussi à trouver des similitudes entre 5 météorites et 5 astéroïdes associés avec des données physiques et j'ai obtenu des données d'observation pour

trois astéroïdes associés.

# Abstract

Meteoroizii, asteroizii și cometele au interacționat permanent cu Pământul în timpul existenței sale. Când un obiect, cum ar fi o cometă sau un asteroid, orbitează în jurul Soarelui, poate lăsa fragmente de materie în urma lui, iar dacă acest obiect este în proximitatea Pământului, aceste fragmente sunt adunate de gravitația planetei. Studiul acestor obiecte și legătura dintre ele pot contribui la înțelegerea condițiilor de formare și evoluție a Sistemului Solar, a condițiilor de dezvoltare a vieții pe Pământ, a proceselor haotice din Sistemul Solar, a securității Pământului și, poate, în viitor, industria spațială.

Toate obiectele din Sistemul Solar sunt caracterizate de orbitele lor, iar curenții meteorici au orbite similare cu obiectele care le produc. Din acest motiv, cele mai comune metode de identificare a corpului părinte se bazează pe similaritățile orbitelor, cunoscute și ca criterii de discriminare sau criteriul-D. În această lucrarea am folosit trei metrici ale criteriului-D pentru asocierea corpului părinte. Am stabilit o valuare de prag pentru fiecare metrică folosind o nouă metodă de selectare a acestor valori. Mai mult, am investigat stabilitatea orbitală a obiectelor asociate, în sensul timpului Lyapunov și proprietăților fizice.

Datorită asemănărilor orbitale dintre curenților meteorici și corpurile care le produc, este necesar ca obiectele asociate să aparțină populației de asteroizi din apropierea Pământului. Dar pentru această populație este dificil să se obțină date. Geometria favorabilă pentru observațiile acestor obiecte are loc de cinci ori pe secol. Din acest motiv a fost creat un program observațional, care vizează obținerea datelor fizice pentru obiectele asociate care nu au date fizice.

Rezultatele mele constau intr-un eșantion care conține 296 asteroizi care au fost asociați cu 28 de curenți meteorici, dintre care 73 de asteroizi au fost asociați de toate metricile folosite. Din perspectiva dinamică, eșantionul meu conține 82% de asteroizii Apollo, 7% sunt clasificați ca potențiali periculoși, 15,3% sunt pe orbite cometare, iar 84,3% sunt pe orbite asteroidale. Din perspectiva datelor fizice, am găsit doi asteroizi care se rotesc foarte repede in jurul propriei axe, deci nu pot genera meteori. Pe de altă parte, am descoperit asociați, un asteroid binar și un asteroid care se rostogolește, obiecte care au o probabilitate mare de a fi corpuri părinte.

De asemenea, am reușit să găsesc asemănări între 5 meteoriți și 5 asteroizi asociați cu date fizice și am obținut date observaționale pentru trei asteroizi asociați.

# Acknowledgments

I would like to express my sincere gratitude to my advisers, Prof. Dr. Mirel Birlan and Prof. Dr. Mihai Dima, for the continuous support of my Ph.D study and related research, for their patience, motivation, and immense knowledge. Their guidance helped me in all the time of research, career and writing of this thesis. I could not have imagined having a better advisors and mentors for my Ph.D study.

My sincere thanks also goes to Dr. Dan Alin Nedelcu and Dr. Marcel Popescu for Astronomical Institute of the Academy, Bucharest, who provided me an opportunity to join their team and who gave access to their telescopes and funded part of my work. Without their precious support it would not be possible to conduct this research.

My gratitude goes as well to Dr. Sorin Ion Zgura, director of the Institute of Space Science, Magurele, for the same reasons, the opportunity to join their team and for funding a part of my work.

And finally I would like to express special gratitude for the colleagues from Institute of Celestial Mechanics and Ephemerides Calculations (IMCCE), Paris, for all their help and moral, scientific and financial support.

Last but not the least, I would like to thank my family and friends for supporting me spiritually throughout writing this thesis and my life in general.

# Key words

**Astronomical unit (a.u.)** – the distance between Sun and Earth. 1 a.u. = 149 597 871 km

**Comets** – objects similar with asteroids, that orbits around the Sun on eccentric orbits, largely composed of volatile materials. The main difference between comets and asteroids is that near the Sun, the comet evolve a tail.

**Dwarf planets** – objects which are similar with planets, but have not cleared the neighborhood around its orbit and is not a satellite.

**Lagrangian point** – the position in orbit between two objects (e.g. Sun and a planet) where a small object can maintain a stable position (against these two objects)

**Meteoroids** – fragments of matter produced by asteroids and comets through various processes. Those fragments orbits are similar to the parent bodies object and as long as they are in orbit their name will be meteoroids.

**Meteors** – the light path of a meteoroid that burns in atmosphere.

**Meteorite** – if the meteoroid survives to the passing through the atmosphere, then it will hit the Earth's surface. The object found on the surface is called meteorite.

**Meteoroids stream** – a conglomeration of meteoroids.

**Meteor showers** – a number of meteorites which appears to originate from a single point of the sky at a particular time of year, due to regular passing of Earth through o meteoroid stream.

**Minor planets (Asteroids)** – objects with irregular shape, without atmosphere, often pitted or cratered, which can have a variable sizes, from hundreds of kilometers to only a few tens of meters in diameter.

**Perihelion and aphelion distances** – the points in orbit where an object is located at a minimum distance from the Sun (perihelion) or the largest (aphelion).

**Planets** – objects in orbit around the Sun, have sufficient mass for itself-gravity to overcome rigid body forces so that it assumes a hydrostatic equilibrium

(nearly round) shape, and has cleared the neighborhood around its orbit.

**Satellites** – objects in orbit around a planet or minor planet.

**Small Solar System Body (SSSB)** – this category includes objects such as minor planets, comets, etc. More specifically, if the object is not a planet, a dwarf planet or natural satellite, that object will be classified as a SSSB object. The term SSSB was defined by the International Astronomical Union in 2006.

**Tisserand parameter (TJ)** – the computation value between a relatively small object and a larger body orbital elements. With this parameter one can distinguish different kinds of orbits. It can be applied to restricted three-body problems in which the three objects all differ greatly in mass. The mathematical expression is:

$$TJ = \frac{a_P}{a} + 2\sqrt{\frac{a}{a_P}(1 - e^2)\cos i} \tag{1}$$

where a, e, and i are the orbital elements of the small body and $a_P$ is the semi-major axis of the larger one.

# Chapter 1

# Introduction

Our Solar System is a gravitationally bounded complex which includes one star and its planetary system. The last one includes eight known planets, five known dwarf planets, 470 known natural satellites (173 for planets and 297 for minor planets), approximately 750 000 known minor planets (or asteroids) and about 4 000 known comets. In short, a very complex system hold it all in place by one star, the Sun (see Fig. 1.1).

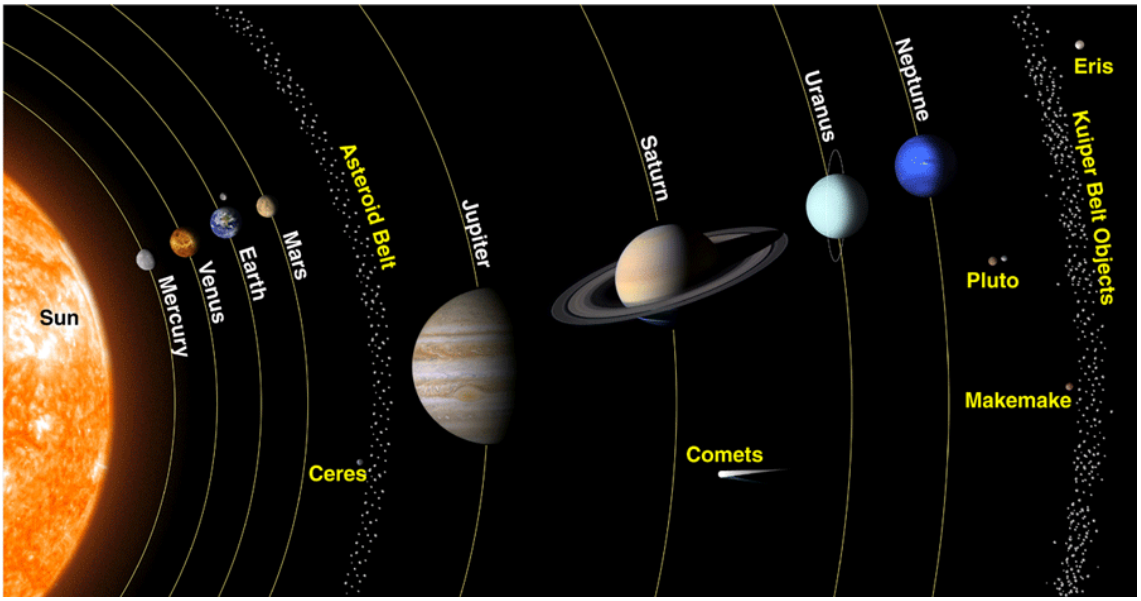


**Figure 1.1:** Our Solar System view. Credit *https* : *//theplanets.org/solar − system/*.

An interesting and important research subject is represented by the Small Solar System Body (SSSB). This category contains comets, asteroids, objects from Kuiper Belt and Oort cloud, small planetary satellites and interplanetary dust. The interesting part of these objects is that some of them have suffered minimal alteration during the conception of the Solar System and may provide important information about its formation and evolution (see Section 1.4).

In this thesis I will focus on the SSSB and the links between them, mainly

on the link between meteor showers (Section1.1) and asteroids (Section 1.2).

This concept, the existence of a link between SSSB objects, appeared in 1861, when Daniel Kirkwood suggested a connection between comets and meteor showers. Schiaparelli (1867) identified the first pairing of the Perseid meteor shower and comet 109P/Swift–Tuttlle and also tried to link Leonids meteor shower and comet 55P/Temple-Tuttle but failed due to the poor orbital elements (the honors for this association going to Peters (1867)). The most important event was the prediction of a large storm of Andromedids meteor shower made by Weiss (1868), that associated this meteor shower with comet 3D/Biela. In 1872 this prediction was confirmed and the relationship comet-meteor shower was largely accepted (for an account of these early developments see Williams 2011).

After a few decades, Olivier (1925) and Hoffmeister (1937) suggested that asteroids may also be linked to the meteor showers. At first, was presumed that asteroids generate the sporadic meteorites and comets generate the meteor showers (Lovell 1954; Levin 1956). The discovery of new asteroids in Earth's proximity, new meteoroids observations and new studies on this matter increased the possibility that a relationship between meteor showers and asteroids exist (Sekanina 1973, 1976; Drummond 1982; Babadzhanov & Obrubov 1983; Clube & Napier 1984; Porubčan et al. 2004, and others).

A very important step in the relationship between meteor showers, asteroids and comets was represented by the investigation of their dynamical and physical properties and links between them. It facilitated the understanding of the formation of meteor showers and of the parent bodies. In order to have a relationship between the meteor shower and the asteroids, it is necessary for the asteroid to be in the proximity of Earth's orbit. Those asteroids are called Near Earth Asteroids(NEA). Their source is divided. From one point of view, the origin is the main belt (Farinella et al. 1992). The other point of view, proposed by Opik in 1963 is that the majority of NEAs are extinct comets. Matter confirmed also by Weissman et al. (1989).

The most important discovery might be the existence of asteroids that have activity like comets (Fig. 1.2), know a new population, evidence found by Jewitt et al. (2015). The active asteroids are defined as small bodies with the semi-major axis being smaller than the Jupiter's semi-major axis (5.2 a.u.), a TJ larger than 3.08 and shows evidence of mass loss (Jewitt et al. 2015). This TJ value was set to avoid many ambiguous cases such as Encke-type comets (TJ = 3.02), quasi-Hilda comets (TJ between 2.9 and 3.04), etc. From the total number of active asteroids found, I will specify two that have orbits in the Earth's vicinity, ((3200)Phaethon and (2201)Oljato).

Today it becomes obvious that there is a direct relation between comets, asteroids and meteor shower (see Jopek & Williams 2013, and all references herein).

The main objective of this study is to determinate the asteroids that can produce or feed the meteor showers using a global process. The outcome of such a global process is useful for the fundamental science on Solar System evolution and also for mitigation or space awareness. For more information about the motivation

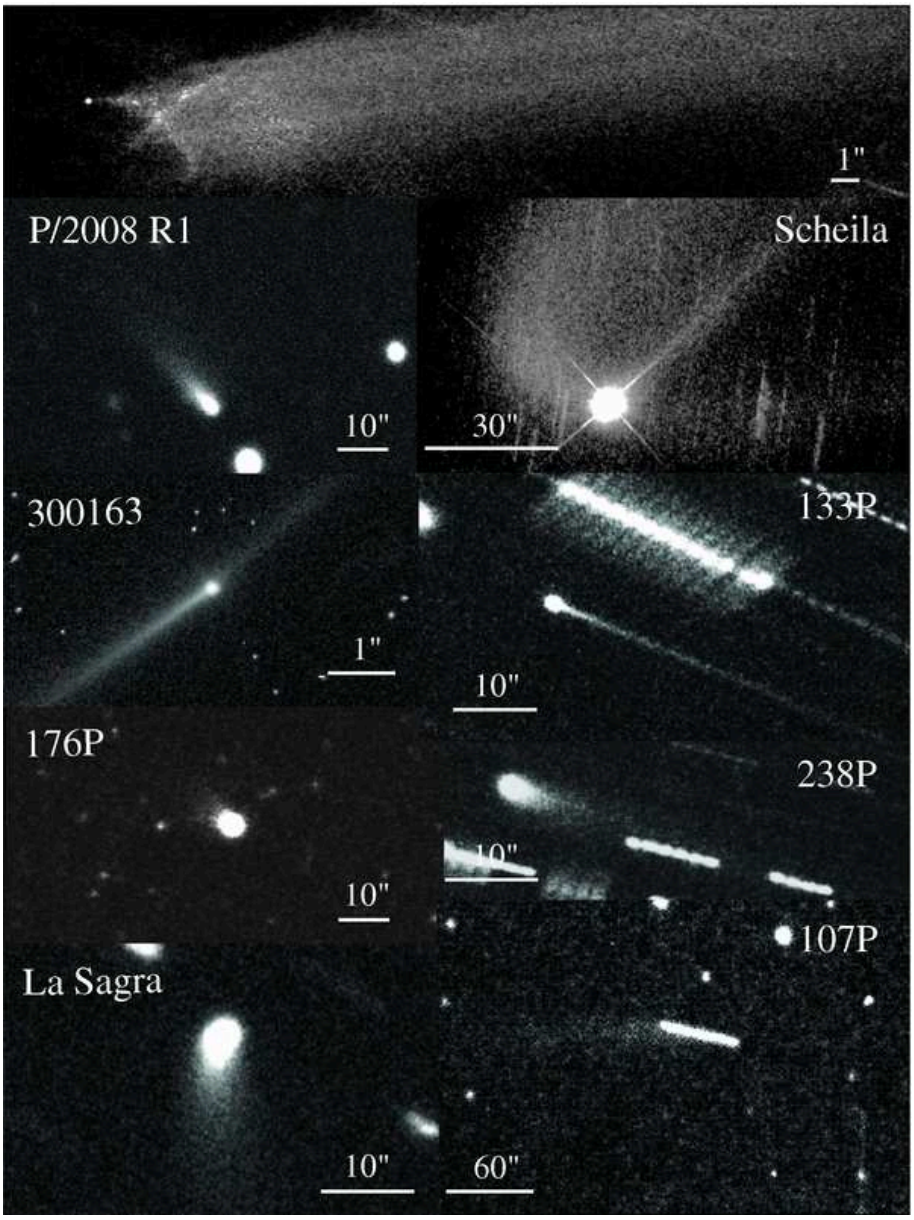


**Figure 1.2:** Active asteroids Jewitt (2012).

of this study please see Section 1.4.

## 1.1 Meteor showers

Before talking about meteor showers we need to understand what is a meteoroid, a meteor and a meteorite and also the difference between meteor showers and meteoroid streams.

### 1.1.1 Meteoroids

When an object revolves around the Sun (comet or asteroid), could leave fragments of mater behind it (see Fig. 1.3). The processes which generate these fragments are: ejection and disintegration at impacts, rotational instabilities, electrostatic repulsion, radiation pressure, dehydration stresses and thermal fracture, in addition to sublimation of ice (Jewitt et al. 2015). The fragments are called meteoroids, and are in the size range from 10 microns to 1 meters (Rubin & Grossman 2010). These meteoroids are gathered in confined tours, namely meteoroid stream and when the object that produces these meteoroids intersects Earth's orbit (see Fig. 1.3), the fragments are collected by gravity.

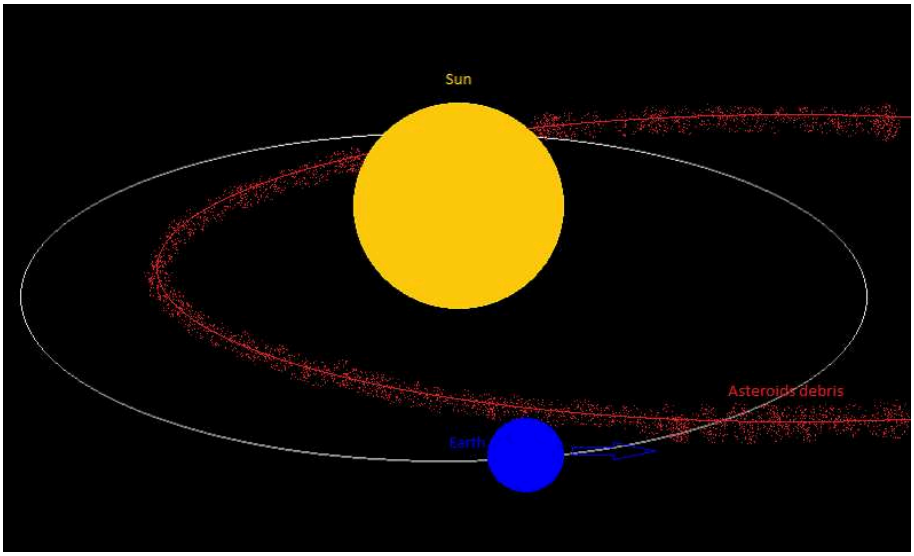


**Figure 1.3:** Earth moving through meteoroid debris

### 1.1.2 Meteors

When the meteoroids enter in Earth's atmosphere, they burn up and produce flashes of light that can be observed on the night sky. The flashes are called meteors. If a number of meteors appears on the same time of the year on the same place of the sky, then that phenomenon is called a meteor shower. The meteors from a meteor shower have the same velocity and parallel paths, but from the observer perspective from Earth the meteor shower appears to originate from a single point of the sky. This point is called radiant. This radiant receives the name of the constellation in which is located (e.g. Geminids shower has radiant in the Gemini constellation, the Leonids shower radiant is in the Leo constellation). If several meteor showers have the radiant in the same constellation then the current name gets a Greek letter as prefix (e.g. $\alpha$-Draconid, $\Omega$-Draconid, etc.) (see Fig. 1.4).

Taking into account that no instrument is needed to observe them, the meteor showers were observed by humans since millennia. However, even if this phenomenon can be seen with the naked eye, the first scientific study appeared only two centuries ago, when a great storm of Leonids shower was observed in November

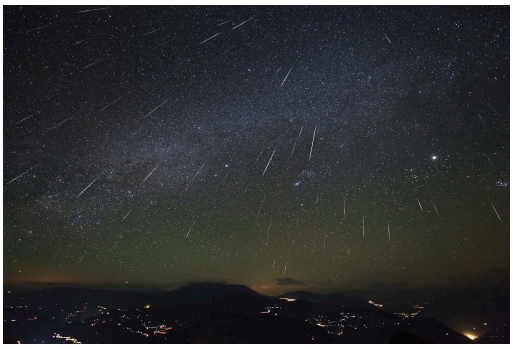

**(a)** Geminids meteor shower. Credit: Jeff Dai


**(b)** Meteor showers radiant. Credit: Stellarium

**Figure 1.4:** Geminids meteor shower (radiant in Fig. 1.4b and real picture in Fig. 1.4a)

1833. Denison Olmsted explained this event with highest accuracy and speculated that this phenomenon originates from space (Olmsted 1836, 1835, 1834).

Today we know 112 established meteor showers and other 25 temporary (version from 16-12-2017, IAU Meteor Data Center[1]).

### 1.1.3 Meteorites

The meteoroids which survive the atmosphere transitions and reach the ground, are called meteorites. These are of two types: the fall meteorites are that which are observed and recovered and the find meteorites are the others (they can not be associated with an observation).

The name of the meteorite is given after the closest human location where it was found (e.g. the Allende meteorite is a fall from Pueblito de Allende, Mexico). If the meteorite is found in the desert or uninhabited place, it will have been attributed a name and a number (e.g., Allan Hills (ALH) 84001 meteorite was found in Allan Hills mountain, in Antarctica).

The terms stony meteorites (rocky material), iron meteorites (metallic material) and stony-–iron meteorites (mixtures) are used from early $19^{th}$ century but do not have much genetic significance today. Weisberg et al. (2006) created a new approach for meteorites division: chondrites (undifferentiated meteorites) and achondrites (differentiated meteorites) (see Fig. 1.5).

Chondrites are the meteorites with solar-like compositions (without the highly volatile elements) and are derived from asteroids or comets that did not experienced planetary differentiation. This group of meteorites is divided in classes and groups. The main classes of this group are:

1. Carbonaceous chondrites (with groups CI, CM, CO, CV, etc) that have in

[1] $http://pallas.astro.amu.edu.pl/\ jopek/MDC2007/$

composition minerals such as olivine and serpentine (silicates, oxides and sulfides). The finding rate of this type of asteroid is about 4.6% (Bischoff & Geiger 1995)

2. Ordinary chondrites (with groups H, L and LL) are stony chondritic meteorites composed of olivine, orthopyroxene and more or less oxidized nickel-iron (depends of the group) and represents about 87% of all found meteorites[2].

3. Estatite chondrites (with groups EH and EL) are a rare type of meteorites with high percentage of enstatite($MgSiO_3$) mineral that contain almost no iron oxide. This type represent about 2% of the fallen meteorites (Norton & Chitwood 2008)

Achondrites are igneous rock (melts, partial melts, melt residues) or breccias of igneous rock fragments from differentiated asteroids and planetary bodies (Mars, Moon) (Gnos et al. 2004; Treiman et al. 2000). It consists of terrestrial materials such as basalts or plutonic rocks due to their melting and recrystallization on or within meteorite parent body (Gupta & Sahijpal 2010). The same meteorites can have achondritic textures (igneous or recrystallized) and a primitive chemical affinity to their chondritic precursors. This class is called primitive achondrites and contains nonchondritic meteorites, but are closer to their primitive chondritic parent than other achondrites (Weisberg et al. 2006).

As it was mentioned there are two groups of this meteorites:

1. Achondrites meteorites are stony meteorites that do not contain chondrules. In this group, one can find meteorites which came from asteroids (such as EUC, HED, HOW, etc), Moon and Mars (such as SHE, NAK, etc.). The asteroidal achondrites or evolved achondrites are the meteorites with mineralogical and chemical composition changed from the original parent body by melting and crystallization processes.

2. Primitive achondrites, also called PAC group, contain meteorites with primitive chemical affinity to their chondritic precursors, but with igneous texture (indicative of melting processes)

There is also a similarity between asteroids and meteorite spectra. Those associations are between: Ch, Cgh types asteroids with CM meteorites, K types asteroids with CV, CO, CR, CK meteorites, X types asteroids with iron meteorites, V types asteroids with HED meteorites, Xc types asteroids with ECs and aubrites meteorites, T types asteroids with Tagish Lake meteorite, K types asteroids with mesosiderites, A types asteroids with pallasites and brachinites, S types asteroids with ordinary chondrites (Vernazza et al. 2016).

In December 2017 the Meteoritical Bulletin Database[3] had approximately 57200 meteorites.

[2] http://www.nhm.ac.uk/our-science/data/metcat/search/metsPerGroup.dsml
[3] https://www.lpi.usra.edu/meteor/metbull.php

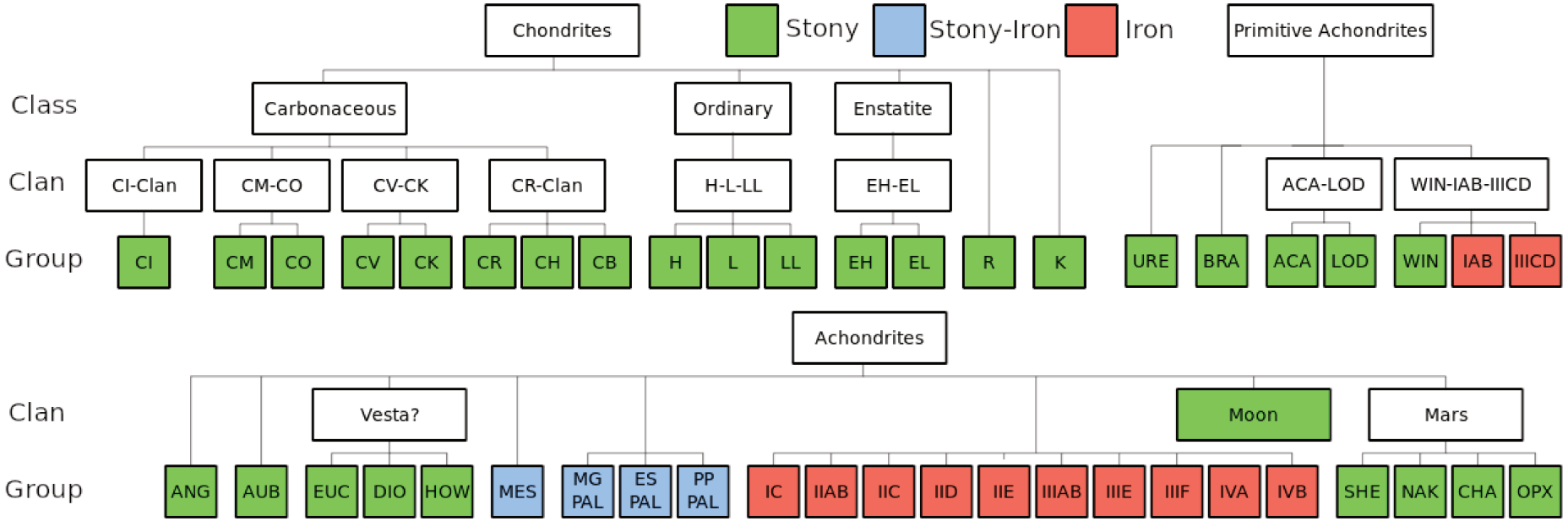


**Figure 1.5:** Meteorites classification (Weisberg et al. 2006)

## 1.2 Asteroids and Comets

### 1.2.1 Asteroids

Asteroids or minor planets are fragments of matter which have remained since the early formation of our Solar System about 4.6 billion years ago (Tsirvoulis & Michel 2016).

They are objects with irregular shape, without atmosphere, often pitted or cratered and can have variable sizes between from hundreds of kilometers to only a few tens of meters in diameter. Also, they revolve around the Sun on elliptical orbits and rotate around its own axis, sometimes quite erratically, tumbling as they go.

The term asteroid appear after the discovery of the planet Uranus by Sir William Herschel in 1781, who used the Titius–Bode law. The law says that at the distance 2.8 a.u. there must be a planet (Graner & Dubrulle 1994).

The first object of its kind was discovered on 01 January 1801 by the astronomer Giuseppe Piazzi, namely Ceres[4], and was considered a new planet (Ureche 1982). After Ceres discovery, other objects were found, (2) Pallas, (3) Juno, and (4) Vesta, over the next few years, and a new category appeared namely asteroids. The term asteroid was proposed by Sir William Herschel, meaning star-like (Cunningham & Hughes 1988).

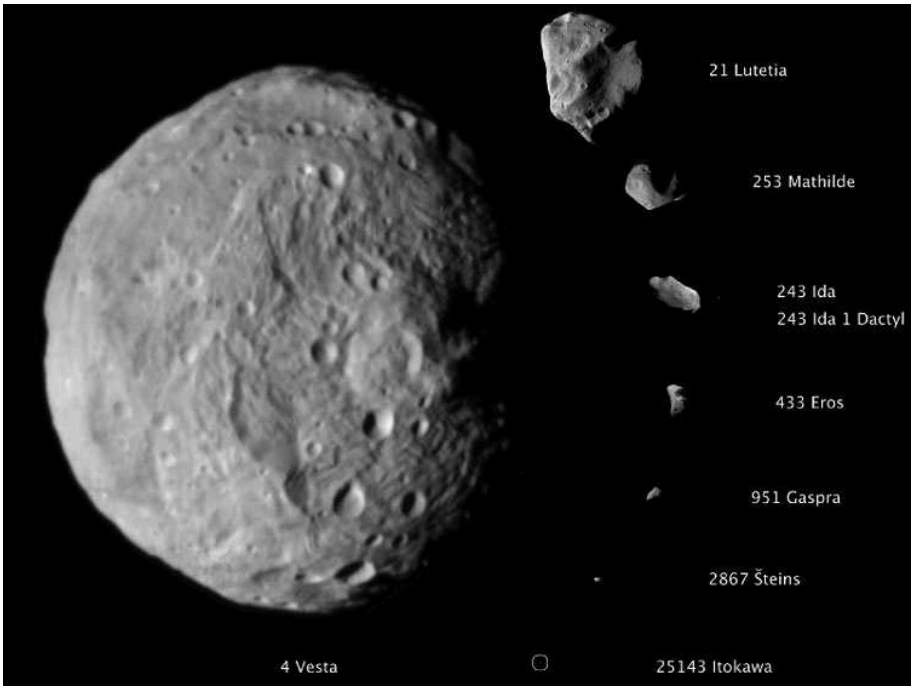


**Figure 1.6:** Some asteroids visited by spacecraft by 2011. Image Credit $NASA/JPL - Caltech/JAXA/ESA$.

[4]This object is now classified as a dwarf planet, because is the largest object in the main belt.

Today we know approximate by 750 000 asteroids in IAU Minor Plane Center[5] database and every month over 4 000 new asteroids are discovered.

In order to highlight the discovered asteroids, rules of nomenclature were imposed and accepted by astronomical community worldwide. Thus, each well known asteroid has a serial number and a proper name (1 Ceres, 2 Pallas, 3 Juno, etc.). The new findings are reported to the Minor Planet Center, were are assigned provisional indicative until their confirmation. The indicative consists of two parts: the year of discovery and a group of two letters (the first letter indicates the time of year expressed in half of the calendar month in which they made the discovery, and the second designates the number of discovery from the time interval deliberate of the first letter). For example, the asteroid 1979 DA was discovered in 1979 in the second half of February (D indicate the 4th interval of 15 days of the year) and is the first discovery in the mentioned interval (A). The final name of the asteroid is given in the board of IAU nomenclature and the name is chosen from proposals made previously by researchers in the field, after its orbit is very well known.

There are two criteria for classifying asteroids: by their orbits and by their physical parameters.

### Dynamical classification

The asteroids classification after there dynamical elements is presented below (Fig. 1.7):

1. Main belt asteroids: asteroids located between Mars and Jupiter (at 2–4 a.u. from Sun, see Fig. 1.7b). Here are the most of the asteroids. Their existence today is due to the birth of Jupiter, which prevented the formation of another planetary bodies between Mars and Jupiter. Also, they are divided in sub-groups, namely families: Hungarias, Floras, Phocaea, Koronis, Eos, Themis, Cybeles and Hildas. The family name is given after the main asteroid in the group.

2. Trojan asteroids: asteroids that have identical orbit with those of planets. These asteroids are located in L4 and L5 of the Lagrangian points of the planets. Today we know six planets that have Trojans asteroids:

   (a) Venus has four Trojan asteroids: 2001CK32, 2002VE68, 2012XE133 and 2013ND15 (de la Fuente Marcos & de la Fuente Marcos 2014).

   (b) Earth has just one confirmed Trojan asteroids, namely 2010TK7 (Connors et al. 2011).

   (c) Mars has seven Trojan asteroids: (5261)Eureka, (101429)1998VF31, (211514)1999UJ7, (311999)2007NS2, 2001DH47, 2011SC191 and 2011UN63. Also another candidate for this category is 2011SL25 (de la Fuente Marcos & de la Fuente Marcos 2013).

[5] *http : //www.minorplanetcenter.net/*

(d) Jupiter has over 6 500 of Trojan asteroids. The entire list can be found on Minor Planet Center website[6].

(e) Uranus has two Trojan asteroids: 2011QF99 and 2014YX49 (de la Fuente Marcos & de la Fuente Marcos 2017).

(f) And finally, Neptune has 17 Trojan asteroids. The entire list can be found on Minor Planet Center website[7].

3. Near Earth Asteroids (NEA's). Are the objects in Earth's proximity. There are known over 17 500 such objects. These objects are classified after their orbital elements in five categories (see Fig. 1.7a):

   - Atiras or Apohele asteroids are the objects that have orbits inside Earth orbit. These objects have the aphelion distance smaller then the perihelion distance of Earth. That means that semi-major axis is also smaller than Earth's semi-major axis.

   - Atens asteroids are objects that have semi-major axis smaller then 1 a.u., but intersect the Earth's orbit. Also these objects have the aphelion distance bigger than 0.983 a.u.

   - Appolo asteroids are the objects that intersect the Earth's orbit. These objects are between semi-major axis bigger than 1 a.u. and perihelion distance smaller than 1.017 a.u., were the value of 1.017 is the Earth's aphelion distance.

   - Amor asteroids are objects that orbits outside the Earth's orbit. These objects have perihelion distance greater than Earth's aphelion distance.

   - Potentially Hazardous Asteroids (PHA) are the asteroids that have Minimum Orbit Intersection Distance (MOID) with Earth smaller than 0.05 a.u.

4. Centaurus asteroids: are the asteroids that orbit between Jupiter and Neptune. These are very interesting objects due to their asteroidal and commentary features. Also have unstable orbits due to their orbital cross of gas giants and unexpected surface color variations.

5. Kuiper belt (KBOs) and trans–Neptunian objects (TNOs): The KBOs are objects composed mainly of frozen water, methane and ammonia, and orbit between Neptune and up to 50 a.u. from the Sun. Also these objects belong to a family namely trans-Neptunian Objects (TNOs) (see Lee et al. 2007, and all ref.). This family contains all objects that orbit between Neptune and Oort Cloud (objects from Oort Cloud are also included). The name Kuiper belt, was given in honor of the astronomer Gerard Peter Kuiper, who predicted and demonstrated the existence of this disk of matter. Also, the Oort Cloud was named after astronomer Jan Oort, who concluded that at the commentary origin lies a vast cloud of matter, at approximate one light year from the Sun (at the gravitational boundary of the Solar System, see Fig. 1.7c).

[6] https://minorplanetcenter.net/iau/lists/t_jupitertrojans.html
[7] https://minorplanetcenter.net/iau/lists/NeptuneTrojans.html

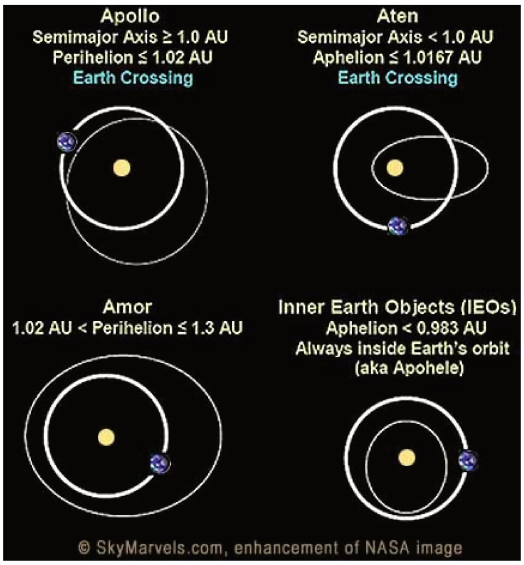


**(a)** Near Earth Asteroids Orbits.

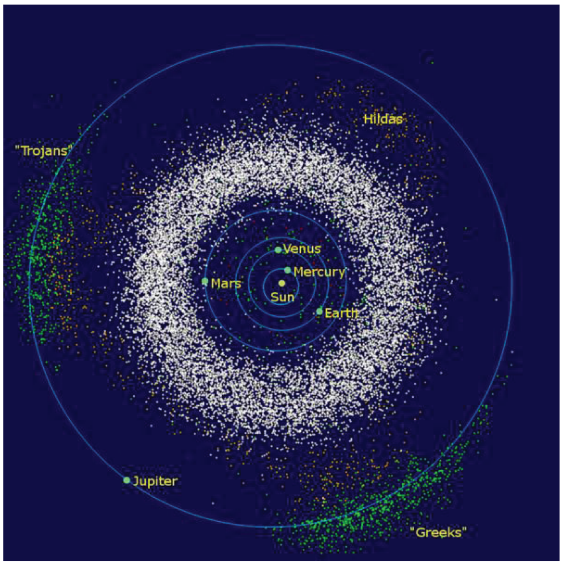


**(b)** Main Belt and Trojan asteroids

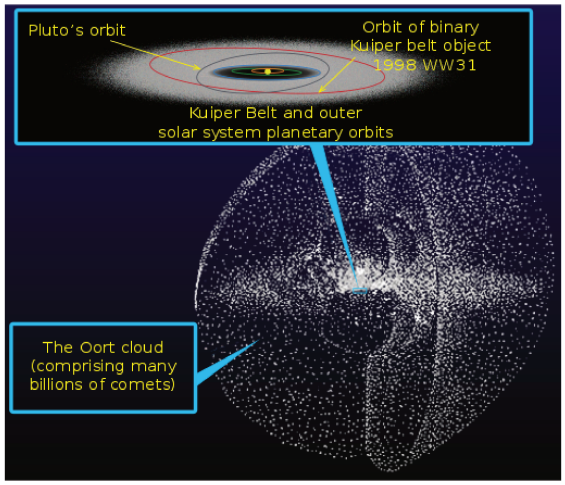


**(c)** Kuiper belt and Oort Cloud

**Figure 1.7:** Positions of all SSSB objects in our Solar System. 1.7a). The NEAs orbits around Earth's orbit. 1.7b). The Main Belt(white) and Jupiter Trojan(green) asteroids. 1.7c). The Kuiper belt and the Oort Cloud.

### Physical classification

In this classification the asteroids are grouped after their spectral shape, colors or albedo. Asteroid surfaces have specific reflective properties which could be characterized by their spectra (see Fig. 1.8). Visible and near-infrared spectra helps us to identify chemical and mineralogical properties of asteroid surfaces (Reddy et al. 2015).

The first spectrum classification or taxonomic classification was published in 1975 and contained three groups of asteroids: **C** objects associated with carbon-rich material, **S** objects rich in compounds of silicon and **U** for items that do not fit in the other two categories (Chapman et al. 1975). This taxonomy was further developed and today there is a number of classification schemes (Tholen 1989; Bus

& Binzel 2002a; Lazzaro et al. 2004, etc.). The last and most used taxonomic class was published in 2009 and contains 24 asteroids classes divided in three groups: C objects associated with carbon-rich material, S objects rich in compounds of silicon and X for metallic objects (DeMeo et al. 2009a) (see Fig. 1.8).

With the help of the albedo one can determinate the surface composition. An albedo smaller than 0.15 (excluding the metallic ones) is akin to primitive objects belonging to taxonomic class such as C, D, B or G (Fulchignoni et al. 2000) while an albedo larger than 0.15 could be associated to objects closer to ordinary chondrites (S–complex), or to objects which experienced partial or total melting (V, O, A, or X taxonomic classes).

The asteroids colors are used to determine some characteristics of asteroid's surface and to make a first order estimation of its taxonomic type (Fulchignoni et al. 2000). The systems of filters, commonly used are Johnson-Cousins U, B, V, R and I (see Bessell 1979; Cousins 1974; Johnson & Morgan 1953) and Sloan Digital Sky Survey (SDSS) u, g, r, i and z (York et al. 2000). But today this method is just for estimations. This type of classification can use up to five points (from 0.3 to 1.0 $\mu$m, visible) to assign taxonomic class, compared to the spectral classification, where the range of the wavelengths can be between 0.4 to 2.4 $\mu$m (visible and near-infrared) and can have hundreds of points.

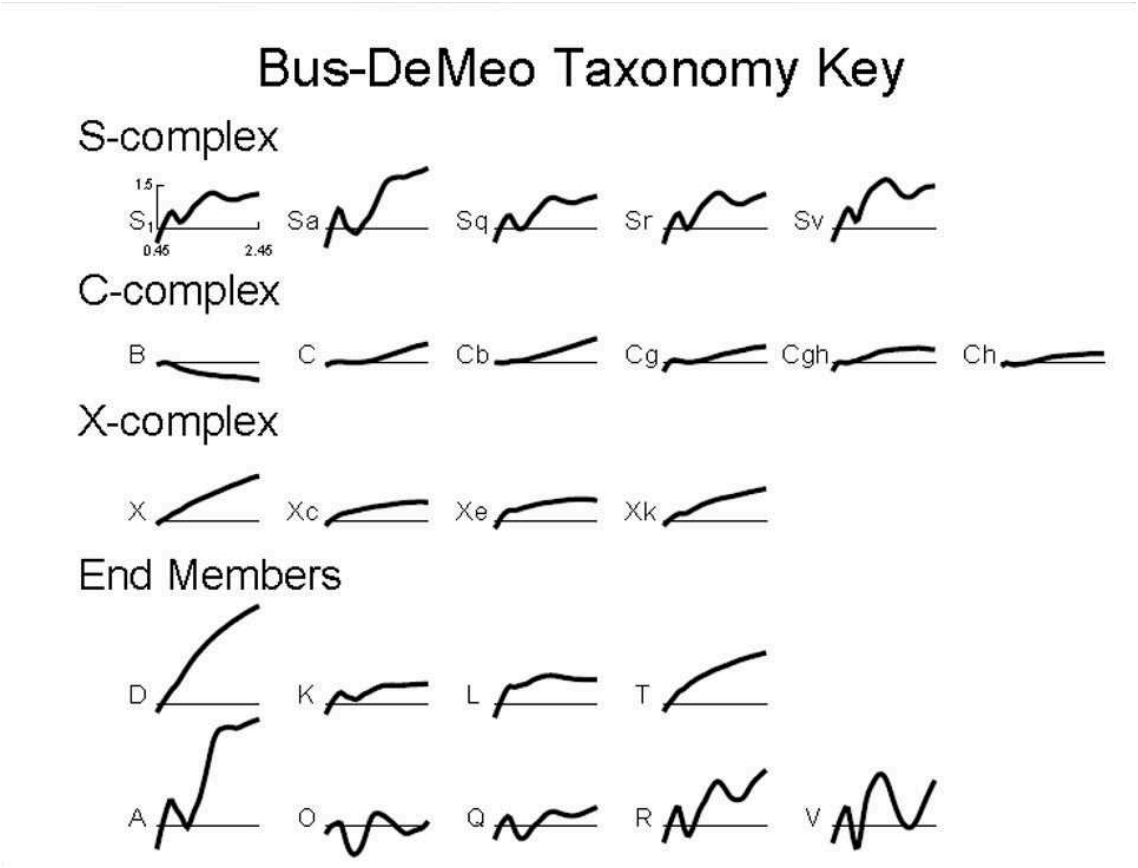


**Figure 1.8:** Bus–DeMeo taxonomy (DeMeo et al. 2009a)

### 1.2.2 Comets

Comets are also small bodies of the Solar System, being composed by nucleus, comma and tail. These objects have large eccentricities and when approaching the Sun, they begin to warm up and they start to release gasses. This process is known as outgassing and it is generated by the solar radiation and solar wind acting on the nucleus.

Until 1994, the system of naming the comets was composed of two steps. The first step was the provisional designation which consists of the discovery year and an alphabetic letter, in the order of discovery (e.g. Comet 1973f was discovered in year 1973 and was the sixth comet discovered in that year). The second step is the permanent designation that is composed of the year of its perihelion and a roman number that indicates the order of the perihelion passage in that year (e.g. Comet 1969i became Comet 1970 II, second comet that pass on perihelion in 1970).

But after 1994, the International Astronomical Union decided to change the naming system, due to the increasing number of discoveries. Now the comets are designated by the discovery year, a letter (indicate the half-month of the discovery) and a number (indicate the order of the discovery). If now one discovers a comet, for example in the first-half of march 2016 and is the first discovery on this time it will be named 2016 E1. Also, prefixes were added to indicate the comet nature:

1. P/ for periodic comets
2. C/ for non periodic comets
3. X/ for comets that orbit that could be calculated
4. D/ for periodic comets that disappeared, broken up, or were lost
5. A/ for minor planets mistaken as comets
6. I/ for interstellar objects (like 1I/Oumuamua[8])

The principal components of a comet that can be studied are: nucleus, coma and tail.

The nucleus is the solid part of a comet and can have dimensions between hundred of meters up to tens of kilometers (see Fig. 1.9). This is composed of rock, dust, ice and frozen gases (carbon dioxide, carbon monoxide, methane, and ammonia) (Greenberg 1998). The nucleus can also be named ”dirty snowballs” or ”icy dirtballs”, depending on the concentration of dust. This theory on comet composition starts from Fred Whipple in 1950.

When the comet reaches an approximate distance of 3 or 4 a.u.(solar radiation and solar wind start to act on the nucleus) the volatile elements start to outgas, creating a layer of dust and gas, like an atmosphere around the comet, namely coma.

[8] https://www.minorplanetcenter.net/mpec/K17/K17V17.html

In general, it is composed by water and dust, water being 90% of the volatiles that outflow (Combi et al. 2004) and can reach up to 15 times the Earth diameter.

As the comet approach the inner Solar System and the volatile matter start to outburst from the nucleus, the mater is left behind, forming two tails (the dust tail and the gas tail). The dust tail is left behind the comet orbit, indicating the inverse direction of movement of the comet. In case of the gas tail or ion tail, because it is strongly affected by the solar wind, it points away from the Sun (Lang 2011). The tail may stretch up to one astronomical unit.

Due to their highly eccentric elliptical orbits, the comets can be dynamical classified in two categories: short-period comets and long-period comets. It is believed that short-period comets originate form Kuiper belt while long-period comets originate from Oort cloud (Randall 2015).

Also, an interesting topic is Jupiter family comets. Those objects are short-period comets with low inclination and an orbital period of 20 years. They are called Jupiter family comets because their orbits are primary determined by Jupiter's gravity and they are believed to originate from Kuiper belt. There are known over 400 objects that belong to this family (objects such as Encke and Halley), but due to their short period, most of them are very faint. Their volatile materials are rapidly depleted due to their multiple trips to the inner Solar System (Lowry et al. 2008).

Today are known about 4 000 comets on IAU Minor Planet Center.

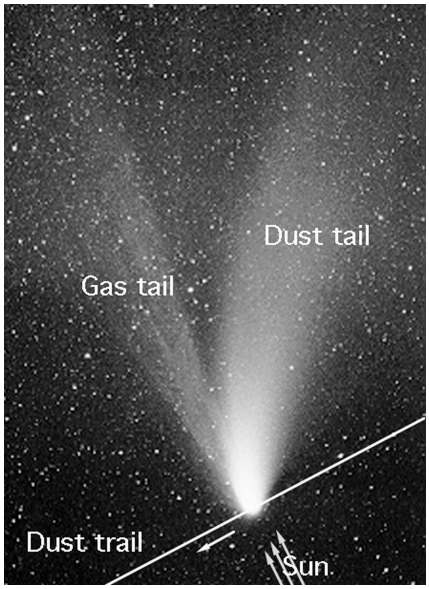


**(a)** Parts of a comet. Image Credit K. Jobse, P. Jenniskens and NASA Ames Research Center.

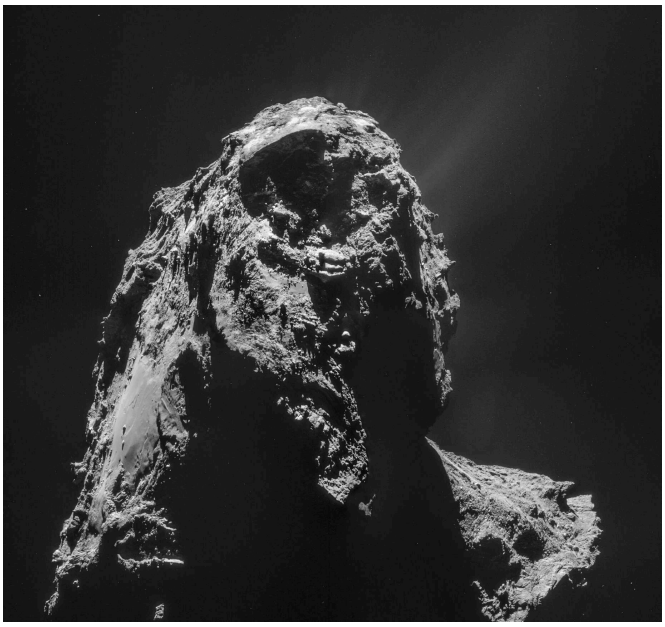

**(b)** Comet 67P/Churyumov Gerasimenko observed in Rosetta mission. Image Credit Rosetta mission

**Figure 1.9:** Comets observed from ground and from space.

## 1.3 Known asteroids parent bodies of meteor showers

As specified in Chapter 1 the first suggestions about a link between asteroids and meteor streams were made by Olivier (1925) and Hoffmeister (1937). After this assumption many studies have been made on this topic. Here are present only some of them.

An important stimulant in the investigation of the relation between asteroids and meteor showers was the discovery of (3200) Phaethon, which orbits near Geminids meteor shower (Olsson-Steel 1988; Fox et al. 1984; Whipple 1983).

The study of (2329) Orthos orbit shows that it intersects the Earth's orbit eight times. After a search, four meteor showers were confirmed from IAU Meteor Data Center archive, and the connection between those meteor showers and the (2329) Orthos asteroid leads to the conclusion that it's an extinct comet (Babadzhanov 1996).

The study of the (2101) Adonis orbital evolution through Halphne-Goryachev method, leads to its association with four meteor showers. Published data show that theoretical prediction of the meteor showers are similar with those from observations ($\alpha$ Capricornids, $\chi$ Sagittariids , $\chi$ Capricornids and Capricornids-Sagittariids ). The existence of those associations provides evidence that supports the hypothesis of (2101) Adonis asteroid being of commentary nature (Babadzhanov 2003).

Until 2004, Quadrantids meteor shower has supposedly evolved far from the observational power from an old and widely stream. From a new data-set, was found that this stream does not have more than 500 years, and it's parent body is 2003 EH1 that has a commentary like orbit and coincides with the meteor shower orbit. The final conclusion was that 2003 EH1 is an intermittent comet (Jenniskens 2004).

Another study proposes that asteroids (69230) Hermes and 2002 SY50 have associated meteor showers. In order to confirm this, the geometric parameters of the orbital approach (theoretical radiant) and a distance function were used (Valsecchi et al. 1999). The final conclusion was that these asteroids do not have similarities with associated meteor showers from IAU (Jopek et al. 2004).

In 2007 the idea that some NEA's are extinct or dormant comets is already an accepted concept. A study that aims to detect NEA's in Piscids meteor shower, found four asteroids with similar orbits (1997 GL3, 2000 PG3, 2002 GM2 and 2002 JC9). Also, in this study were performed theoretical parameters calculations of the meteor shower. They searched and compared the result with data from existing meteor showers catalog and confirmed all theoretical calculations. The conclusion was that these objects are fragments form a larger commentary body (Babadzhanov et al. 2008b).

A study was conducted also on Taurid Complex. This consists of many streams and it is based on the 2P/Enke comet and some NEA's, that orbits in the complex. This study aims to find new objects, to investigate orbital evolution and the association with the meteor showers. The asteroids found in this complex are between 0.11 and 7.55 km, and are fragments of 2P/Encke comet or the fragments and the comet come from a larger body (Babadzhanov et al. 2008c).

Everhart RADAU19 method of numerical integration was used for 2003 EH1 asteroid evolution. This asteroid belongs to Amor group and has a commentary like orbit. The theoretical computations indicate that this asteroid intersects the Earth's orbit eight times and for every intersection it produces a meteor shower. Comparing with published data, the observed meteor showers are identical with the predicted ones. The orbital characteristic and the existence of associated meteor showers with this asteroid indicates an extinct comet (Babadzhanov et al. 2008a).

A study of the orbital evolution under the influence of planetary perturbations was made on three NEA's (2002 JS2, 2002 PD11 and 2003 MT9), which are supposed to have the same origin, that have similar orbits with the Aquariids meteor shower. In the end it was concluded that the asteroid-meteor shower relationship is the result of commentary breakdown (Babadzhanov et al. 2009).

Also, another study on Taurid Complex was made in 2014 on the mineralogical surface of the associated asteroids (Popescu et al. 2014). The spectra for six asteroids were studies: ((2201) Oljato, (4183) Cuno, (4486) Mithra, (5143) Heracles, (6063) Jason si (269690) 1996 RG3). The observational data were obtained with the IRTF telescope equipped with an SpeX spectrometer, and the taxonomic classification was made by using the Bus-DeMeo taxonomy. To learn the composition at the asteroid's surface, the spectra were compared with Relab (meteor spectra database). From six studied asteroids, five of them have spectra which are similar with the taxonomic class S. The asteroid (269690) 1996 RG6 was associated with the taxonomic class C, and the geometric albedo was set at 0.03. The conclusion of this study recognizes the importance of the dynamical groups on Taurid Complex asteroids, but the spectral data of larger asteroids do not support the hypothesis of commentary origin, and the study on this complex needs to continue (Popescu et al. 2014).

One of the actual problem in the association of parent bodies is the identification method. A study on this case was made by comparing four methods based on the D-Criterion ($D_{SH}$ – Sowthworth and Hawkins from 1963, $D_H$ – Jopek in 1993, $D_V$ – Jopek in 2008 and $D_J$ – Jenniskens in 2008). This comparison was made in order to determinate a threshold value that can help in the process of searching the parent bodies of observed meteor showers by French meteorites network, developed under the project CABERNET. The final result do not provide a threshold value for all asteroids classes, but a few meteorites were associated with asteroid 2005 UW6 and an asteroid was removed from parent bodies candidates for the Taurid Complex (Rudawska et al. 2012a).

The most recent on this subject was made by Šegon et al. (2017), who tried to identify the parent bodies for several newly identified showers. The authors

combined data from the new meteor showers with the Croatian Meteor Network and SonotaCo meteor databases. They also used D-criteria metrics to identify the parent bodies, stimulated the particles ejected form the associated object and compared them with real meteor shower observations. The study results found connections between three meteor showers and comets (2001W2–49 Andromedids(FAN), C/1964N1–July $\xi$ Arietids(JXA), P/255 Levy–$\alpha$ Cepheids(ACP))and four with asteroids (2001XQ–66 Draconids(SSD), 2009SG18–$\kappa$ Cepheids(KCE), 2009WN25–November Draconids(NED), 2008GV–$\psi$ Draconids(POD)). Also four associations were inconclusive and two associations need more observational data.

But even with different known methods of associations, many unsolved problems remain in this field. We know that the meteor showers are produced by larger objects such as comets and asteroids. In some cases the meteor showers can be produced by a comet or an asteroid or both. But are also meteor showers that do not have an associated parent body or the association is unreliable (the appointed parent body do not produce meteoroids or the rate is to small, or it is unstable and the time on that orbit do not coincide with the meteor shower, etc.).

## 1.4 Motivation of this thesis

The objectives of my thesis are ticked to:

1. Formation and evolution conditions of the Solar System. An accepted hypothesis in the scientific community is that the Solar System was formed from a dust and gas nebula which began to collapse due to gravitational instability. The asteroids are the reminiscent of the accretion process, objects that have not substantially changed their mineralogical structure. The study of asteroids allows us to answer questions related to the nebula type from Solar System formation, the amounts of material, of its homogeneity, the temperature and pressure conditions of the nebula.

2. Conditions for life development on Earth. Our planet contains two essential constituents for life: excess of water, carbon and compounds based on its bonds. This is presumed to be due to excessive collisions of asteroids and comets with the Earth. From the studies conducted on asteroid mineralogical parameters, it has been observed that approximately 60% of them have a composition similar to the carbon rich mineral (Birlan et al. 1996; Barucci et al. 1987).

3. Chaotic processes in the Solar System. In a system where the bodies operate in the gravitational interactions, one of the major problems is their stability. The population of over three quarters of a million of celestial bodies represents a laboratory in natural size where chaotic processes can be studied (Grazier et al. 2005).

4. Earth and civilization protection from natural risks related to NEA's. Meteoroids, asteroids, and comets were permanently interacting with Earth during

its existence. In the Earth Impactors Database[9] there are 188 confirmed impact structures. The biggest cataclysmic event, highly influencing the life on Earth, is considered the impact of an asteroid in Chicxulub, Mexico. This took place about 65.5 million years ago (Smit 1980; Alvarez et al. 1980). The crater produced was between 180-200 km (Hildebrand et al. 1991) and a huge amount of carbon and sulfur was released into the atmosphere. On a long term this new atmospheric composition produced extended darkness, global cooling and acid rain (Toon et al. 1997; Pierazzo et al. 2003). Another recent event is the Tunguska one in 1908 when an explosion estimated at 10 to 15 megatons of trinitrotoluene (TNT), occurred near Podkamennaya Tunguska river. The cause of the event was supposed to be the impact of a comet (Shapley 1930) or an asteroid (Kulik 1938). Other studies conclude that there is a high probability that at the origin of the Tunguska event was an asteroid (Farinella et al. 2001). More recently the Chelyabinsk[10] event in Russia, in February 2013 was associated with the impact of an asteroid estimated between 17 to 20 meter in size. The estimated energy of this event was around 440 kilotons of TNT and the shock-wave made 1,100 injuries (Popova et al. 2013).

5. Space industries. Today we can not imagine life without space technology: movement using GPS, mobile phone, Internet, etc. The difference between the technologies used on the ground and the spatial ones is that the last must meet standards to work in extreme conditions, keeping in mind that their repair are very unlikely. Because the supply of spare parts from the ground is very expensive, it was raised the issue of developing space industries, based on raw materials obtained from asteroids, which are used to build in space the devices.

[9] http://www.passc.net/EarthImpactDatabase/
[10] http://neo.jpl.nasa.gov/news/fireball_130301.html

# Chapter 2

# Analysis procedure based on dynamical parameters

Any object from the Solar System, such as planets, asteroids, comets, etc., can be characterized by its orbit. In order to understand the methods used to associate distinct objects in the Solar System, one needs to know what an orbit is and how it can be characterized.

The orbit is the path of an object in the gravitational field of a larger object. Johannes Kepler described the motion of an object on an orbit as follows: "the motion of an object in our Solar System is made on elliptical orbit" (not circular) and "the Sun is located in one of the focal points". Also, "the speed of the object on the orbit is not constant", its speed depends on the distance between the object and the Sun (the shorter the distance the object velocity is higher and vice versa). And finally, he found a relationship between the orbital properties of all objects that orbit the Sun. Today we know this as Kepler laws or as laws of planetary motion.

But Johannes Kepler did not explain these laws. They were inferred from observations. The mathematical base for those mechanisms was made by Isaac Newton. Today we know them under the name of the law of universal attraction and the three Newtonian principles.

An orbit is also characterized by its orbital elements. They help to uniquely identify the orbit of an object. Those elements are known as classical or Keplerian elements and can be classified as follows (Fig. 2.1):

1. Orbital elements that define the shape and size of the orbit:

   (a) semi–major axis (noted with a in Fig. 2.1) – this element gives us the size of the orbit. It represents the half distance between perihelion (the point on the orbit that is the closest from the Sun ) and aphelion (the point on the orbit that is the furthest from the Sun) distances. It is measured in a.u. .

   (b) eccentricity (e) – is the orbital parameter that characterizes the shape of

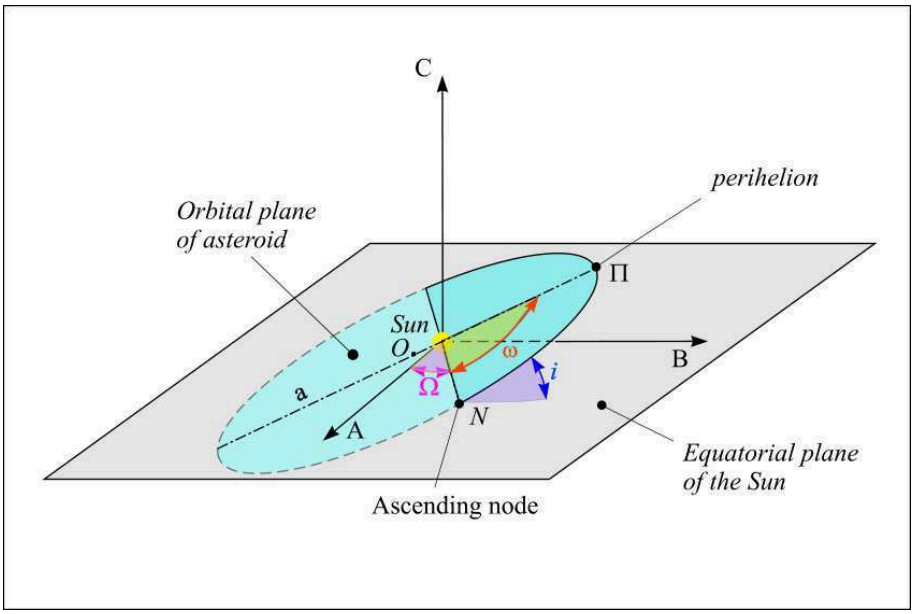


**Figure 2.1:** Orbital elements of an orbit (a - semimajor axa, e - eccentricity, i - inclination, Ω - longitude of the ascending node, $\omega$ - argument of periapsis, Π - perihelion distance) (Dumitru et al. 2017).

the orbit. This value quantifies the deviation of the orbit from a perfect circle. If the eccentricity is 0, then the orbital trajectory will have a perfect circle shape. If the value is between 0 and 1, then the orbital trajectory will be an ellipse shape, if the value is equal to 1 the orbital trajectory will be a parabola shape and if the eccentricity is larger than 1 the orbital trajectory will be a hyperbola shape.

2. Orbital elements that define the tilt and the swivel of the orbital plane:

   (a) inclination (noted with i in Fig. 2.1) – with the help of this element we know the vertical tilt of the orbital plain with respect to the equatorial plane of the Sun. Its measurement is made perpendicular to the intersection line between these two plans (the intersection is noted with N in Fig. 2.1). It is measured in degrees or radians.

   (b) longitude of the ascending node (noted with Ω in Fig. 2.1) – represents the swivel of the orbit. This is the angle between the vernal point (the point on the ecliptic where the Sun crosses from the Southern to the Northern celestial hemisphere, noted with A in Fig. 2.1) and the ascending node. Is measured in degrees or radians.

3. Orbital elements that define the location and position of the object:

   (a) argument of periapsis (noted with $\omega$ in Fig. 2.1) – this element defines the location of the perihelion on the orbit. It represents the angle between the ascending node and the perihelion (noted with Π in Fig. 2.1). Also, this angle is measured in degrees.

   (b) true anomaly ($\mu$) – it gives us the position of the object on its orbit at

a certain time and represents the angle between the perihelion distance and the object.

Taking into account the above definitions and that the objects that generate the meteor showers have similar orbits with the meteorite stream, the most common method of measuring the degree of similarity between the orbits is the so called discrimination criteria or D–criterion.

## 2.1 D-criteria associations

Discrimination criteria or D–criterion is a distance defined in the orbital elements space. Depending on the authors, the number of parameters and their weights differ: n = 3 in the case of Asher et al. (1993) and n = 5 in case of Southworth & Hawkins (1963) and Jopek (1993). A threshold value $D_c$ is defined, and if $D(X,Y) < D_c$ the orbits are similar and the comet or the asteroid can be associated with the meteor shower. Also the D–criterion can be divided in two categories: based on orbit's shape and size, and based on orbital dynamics. We will present them in this section.

The first metric using this approach was introduced by Southworth & Hawkins (1963). Several other metrics were defined by Drummond (1981), Steel et al. (1991), Jopek (1993), Asher et al. (1993), Valsecchi et al. (1999), Jopek et al. (2008), Jenniskens (2008), etc.

We briefly introduce these metrics.

D–criteria introduced by Southworth & Hawkins (1963) ($D_{SH}$) has the mathematical expression:

$$[D_{SH}]^2 = (q_X - q_Y)^2 + (e_X - e_Y)^2 + \left(2\sin\frac{I_{XY}}{2}\right)^2 + \left(\frac{e_X + e_Y}{2}\right)^2 \left(2\sin\frac{\Pi_{XY}}{2}\right)^2 \quad (2.1)$$

where $I_{XY}$ is the angle between the planes of the orbits given by:

$$I_{XY} = \arccos[\cos i_X \cos i_Y + \sin i_X \sin i_Y \cos(\Omega_X - \Omega_Y)] \quad (2.2)$$

and $\Pi_{XY}$ is the angle between perihelion points:

$$\Pi_{XY} = \omega_X - \omega_Y + 2\Gamma \arcsin\left(\cos\frac{i_X - i_Y}{2} \sin\frac{\Omega_X - \Omega_Y}{2} \sec\frac{I_{XY}}{2}\right) \quad (2.3)$$

where $\Gamma$ is defined by:

$$\Gamma = -1 \Rightarrow |\Omega_X - \Omega_Y| > 180^0$$
$$\Gamma = +1 \Rightarrow |\Omega_X - \Omega_Y| \leq 180^0$$

The notations used in Eq. 2.1 to define the orbital elements are: $q$ (perihelion distance), $e$ (eccentricity), $i$ (inclination), $\Omega$ (longitude of the ascending node), $\omega$ (argument of perihelion).

Drummond (1981) made some modifications to $D_{SH}$ and created a new D-criteria metric:

$$[D_D]^2 = \left(\frac{q_X - q_Y}{q_X + q_Y}\right)^2 + \left(\frac{e_X - e_Y}{e_X + e_Y}\right)^2 + \left(\frac{I_{XY}}{180^\circ}\right)^2 + \left(\frac{e_X + e_Y}{2}\right)^2 \left(\frac{\theta_{XY}}{180^\circ}\right)^2 \quad (2.4)$$

where $I_{XY}$ is the angle between the planes specified in eq. 2.2 and $\theta_{XY}$ is the angle between perihelion points with the expression:

$$\theta_{XY} = \arccos(\sin\beta_X \sin\beta_Y + \cos\beta_X \cos\beta_y \cos(\lambda_X - \lambda_Y)) \quad (2.5)$$

where $\beta$ and $\lambda$ are the ecliptic longitude and latitude of perihelion with the expressions:

$$\lambda = \Omega + \arctan(\cos(i)\tan(\omega)) \quad and \quad \beta = \arcsin(\sin(i)\sin(\omega)) \quad (2.6)$$

if $\cos(\omega) < 0$, $\lambda = \lambda + 180^\circ$

Jopek (1993) studied the methods introduced by Southworth & Hawkins (1963) and Drummond (1981) and concluded that they depend mostly on the orbital elements $q$ (in the case of criterion $D_{SH}$ ) and $e$ (in the case of criterion proposed by Drummond). Based on the above considerations, he proposed a new criterion, $D_H$, defined by:

$$[D_H]^2 = (e_X - e_Y)^2 + \left(\frac{q_X - q_Y}{q_X + q_Y}\right)^2 + \left(2\sin\frac{I_{XY}}{2}\right)^2 + \left(\frac{e_X + e_Y}{2}\right)^2 \left(2\sin\frac{\Pi_{XY}}{2}\right)^2 \quad (2.7)$$

As the orbital elements $\omega$ and $\Omega$ evolve rapidly with time, Steel et al. (1991) and Asher et al. (1993) used only three orbital elements and developed a D-criterion metric. The difference between them is represented by the orbital elements used. The D-criteria of Steel et al. (1991) is defined as:

$$[D_{SAC}]^2 = (q_X - q_Y)^2 + (e_X - e_Y)^2 + \left(2\sin\frac{i_X - i_Y}{2}\right) \quad (2.8)$$

while Asher et al. (1993) defined his metric as:

$$[D_{ACS}]^2 = \left(\frac{a_X - a_Y}{3}\right)^2 + (e_X - e_Y)^2 + \left(2\sin\frac{i_X - i_Y}{2}\right) \tag{2.9}$$

where $a$ is the semi–major axis.

Valsecchi et al. (1999) function is the most transparently based on the physical difference between the orbits. The mathematical expression is:

$$[D_N]^2 = (U_X - U_Y)^2 + w_1(\cos(\theta_X) - \cos(\theta_Y))^2 + \Delta\xi^2 \tag{2.10}$$

where

$$\cos(\theta) = \frac{1 - U^2 - \frac{1}{a}}{2U} \tag{2.11}$$

$$\Delta\xi^2 = \min(w_2\Delta\phi_A^2 + w_3\Delta\lambda_A^2, w_2\Delta\phi_B^2 + w_3\Delta\lambda_B^2) \tag{2.12}$$

$$\Delta\phi_A = 2\sin\frac{\phi_X - \phi_Y}{2} \tag{2.13}$$

$$\Delta\phi_B = 2\sin\frac{180^\circ + \phi_X - \phi_Y}{2} \tag{2.14}$$

$$\Delta\lambda_A = 2\sin\frac{\lambda_X - \lambda_Y}{2} \tag{2.15}$$

$$\Delta\lambda_B = 2\sin\frac{180^\circ + \lambda_X - \lambda_Y}{2} \tag{2.16}$$

where U is the unperturbed geocentric speed just prior to impact, $(\theta, \phi)$ define the direction of the radiant in a frame moving with the Earth about the Sun, $\lambda$ is the ecliptic longitude of the Earth at meteoroid impact, $\cos\theta$ is the orbital energy and $w_i$ is the weighting factors.

Jopek et al. (2008) proposed a new metric that used vectorial elements for meteoroid stream identification:

$$\begin{aligned}[D_V]^2 = {} & w_{h1}(h_{x1} - h_{y1})^2 + w_{h2}(h_{x2} - h_{y2})^2 + 1.5w_{h3}(h_{x3} - h_{y3})^2 \\ & + w_{e1}(e_{x1} - e_{y1})^2 + w_{e2}(e_{x2} - e_{y2})^2 + w_{e3}(e_{x3} - e_{y3})^2 \\ & + 2w_E(E_x + E_y)^2 \end{aligned} \tag{2.17}$$

where w are weight coefficients, h are the angular momenta, e are the Laplace vectors and E is the energy constant.

Another metric based on dynamical invariants for meteoroid stream identification was proposed by Jenniskens (2008):

$$[D_J]^2 = \left(\frac{C_{x1} - C_{y1}}{0.13}\right)^2 + \left(\frac{C_{x2} - C_{y2}}{0.06}\right)^2 + \left(\frac{C_{x3} - C_{y3}}{14^\circ.2}\right)^2 \quad (2.18)$$

where the first invariant ($C_1$) corresponds to the z–component of the orbital angular momentum, $C_2$ is taken from the secular model of Lidov and $C_3$ is the longitude of perihelion:

$$C_1 = (1 - e^2)\cos^2 i \quad (2.19)$$
$$C_2 = e^2(0.4sin^2isin^2\omega) \quad (2.20)$$
$$C_3 = \pi = \omega + \Omega \quad (2.21)$$

## 2.2 Databases used in the simulations

For these statistics, I used various databases and programs. For orbital elements of asteroids I used the IAU Minor Planet Data Center[1] -– MPCORB.DAT file (version from 13.02.2018). This file is daily updated and contains orbital elements for all minor planets (numbered and unnumbered).

Its header contains more useful information, such as: the number or provisional designation, the name (for the well known asteroids), the absolute magnitude and slope parameter, the mean anomaly and the epoch when the mean anomaly was computed (is necessary in order to infer the asteroid location on the orbit), the orbital elements of the asteroids (a, e, i, $\Omega$, $\omega$, presented above), mean daily motion, uncertainty parameter for the orbit (classified between 0 and 9, where 0 represents a very stable orbit and 9 represents a very unstable orbit), the number of observations and oppositions, the first and last year of observation, indicators of perturbation, etc.

I decided to use all the MPCORB.DAT file (755 619 objects), in order to test the association programs as well. For the associations to be reliable, all objects need to belong to NEAs population.

For orbital elements of meteor showers we used the IAU Meteor Data Center[2] (version from 13.02.2018) (Jopek & Kaňuchová 2014; Jopek & Jenniskens 2011). In this case we selected only the established meteor showers (112, last updated 13 Jan 2018 by R. Rudawska, Z. Kanuchova and T.J. Jopek).

This database contains the orbital elements of the radiant points for all established meteor showers. Also, besides the orbital elements, the database contains the coordinates of the radiant, the geocentric speed, number of objects used in computation for the determination of the mean orbital elements for the radiant, the known parent body, etc.

[1] http://www.minorplanetcenter.net
[2] http://www.astro.amu.edu.pl/~jopek/MDC2007

I have searched for the meteor activity as well. The main source for this task is the book of Kronk (2014), but we also made a comparison with the data found at IMO, Shower Calendar 2018 and the web site Meteor Shower Online[3] based on Kronk (1988). If a recent source for a certain meteor shower was found, the last publication was taken into account. I only used the maximum activity period, because the probability of a meteor falling from a particular stream is highest then.

For asteroids, physical data were used from multiple databases:

1. European Asteroid Research Node[4] (E.A.R.N.) – this database contains numerous physical data of known NEAs such as albedo, diameter, taxonomic class, rotation period, etc. The database was last updated in 01.02.2018.

2. Small Bodies Data Ferret[5] – this is a searching tool for physical data of asteroids, comets and satellites.

3. Asteroid Lightcurve Photometry Database[6] (ALCDEF) – is a size made by Brian D. Warner with the help of NASA and hosted by International Asteroid Warning Network (IAWN) which allowed to the researchers to upload their observations and make them available for others to use in independent studies. The database contains observational data for over 13000 objects and growing.

4. SMASS MIT database[7] for NEO (Rayner et al. 2003) – is a database of spectroscopic data for NEAs. The resources and asteroid observing expertise for this database belongs to those from MIT, from the University of Hawaii, and from the NASA IRTF.

5. NEOWISE: The Wide–field Infrared Survey Explorer (WISE) database[8] (Mainzer et al. 2016) – This database contains physical data of asteroids detected by NEOWISE, such as diameters, optical and near-infrared albedos and beaming parameters.

I also searched for fall meteorites. The search was made in the Meteoritical Bulletin database[9] over a period of approximate 150 years (approximate 362). The database contains 57 395 meteorite with valid names, 7 993 meteorites with provisional names and was last updated in 09.02.2018

Also, the asteroids spectral data were reviewed using the Modeling for Asteroids (M4AST[10]) tool. M4AST is an online tool devoted to the analysis and interpretation of visible and near–infrared reflection spectra of asteroids by querying databases containing more than 6 000 spectra (Popescu et al. 2012; Birlan et al. 2016).

[3] http://www.meteorshowersonline.com
[4] *http://earn.dlr.de/nea/*
[5] *https://sbnapps.psi.edu/ferret/*
[6] *http://alcdef.org/*
[7] *http://smass.mit.edu/minus.html*
[8] https://sbn.psi.edu/pds/resource/neowisediam.html
[9] http://www.lpi.usra.edu/meteor/
[10] http://spectre.imcce.fr/m4ast/index.php/index/home

From the databases of meteor showers and asteroids I chose seven fields (name + six orbital elements: a, e, i, q, $\Omega$ and $\omega$) that were useful for these statistics. A C++ code was developed (the data and program flow is presented in Fig. 2.2a and 2.2b) in order to use the D–criteria metrics from Eq. 2.1, 2.7, and 2.9. The program can be downloaded from my git-hub page[11].

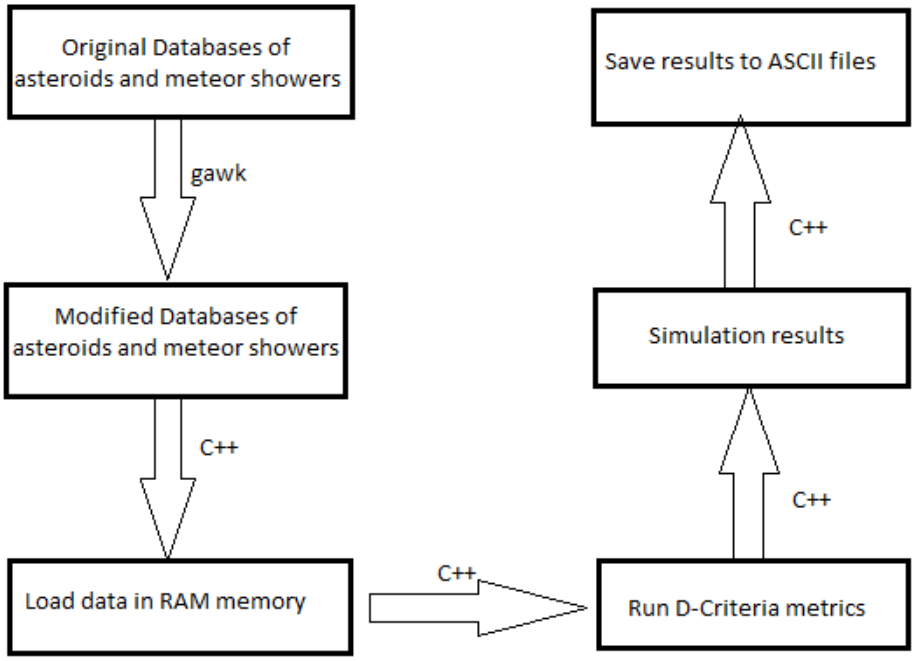


**(a)**

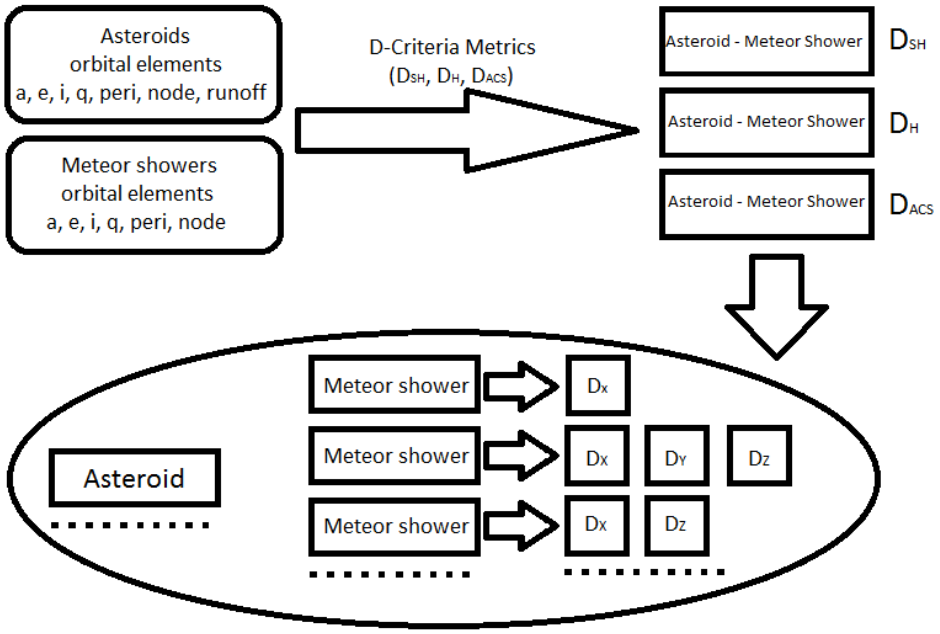


**(b)**

**Figure 2.2:** Program and data flow.

[11] https://github.com/dbogdy/D-Criteria

The program starts by loading objects from a list. Every object contains the name, its orbital elements and a variable which separates the object type (see Listing A.1). In this list were put all the elements from the meteor showers and asteroids databases.

After all objects are loaded, I computed the similarities with the mentioned metrics (the code for Eq. 2.7 in Listing A.2). In the first part of the code the metrics were splitted in separate elements in order to avoid mistakes. After each element is computed the final result is returned.

The results consist of the two objects (the associated asteroid and the meteor shower) and the calculated distance for all metrics ($D_{SH}$, $D_H$ and $D_{ACS}$). The structure for each pair is presented in Listing A.3.

## 2.3 Thresholds selections

In order to identify the possible parents (Y) of a meteor shower (X) with the help of the D–criteria metrics listed above, we need to establish a limit value ($D_C$). If the distance $D(X, Y)$ between $X$ and $Y$ is smaller than $D_C$, it is possible that the object is a parent. If $D(X, Y) > D_C$, then the object will be ignored.

In the literature there are different methods for setting the threshold.

In Asher et al. (1993) the authors calculated the associations for Taurid Complex (TC) using the $D_{ACS}$ metric with a threshold of 0.26 and obtained 25 associated asteroids (see Asher et al. 1993, Table 1). They suggested that a threshold of 0.2 corresponds to the minimum probability for the TC asteroids.

In Porubčan et al. (2006) the authors use the $D_{SH}$ metric with a threshold set to 0.3 in order to determinate the associations for TC from 3 380 NEOs and they obtained 91 associated objects. In a second step a computation backward in time for 5 000 years allows nine associated NEOs to remain.

Rudawska et al. (2012a) tests D–criterion metrics, $D_{SH}$ and $D_H$, using the model for the generation and evolution of meteoroid streams in the Solar System from Vaubaillon et al. (2005). They determined a threshold of 0.084 for $D_{SH}$ and 0.077 for $D_H$, when a meteor is associated to the meteoroid stream.

In Šegon et al. (2014), the authors used the $D_{SH}$ and $D_H$ metrics with cutoff values set to 0.15 to find asteroids associated with meteor showers. They found 43 associated asteroids with inclination $> 15°$ that can be associated to streams containing ten or more meteor orbits. The cutoff values for this paper were selected following Lindblad (1971a), Lindblad (1971b), and Jenniskens (2006).

Ryabova (2016) use the $D_{SH}$ metric to evaluate the dispersion of a Geminids stream model composed by a sample with three different meteoroid masses. The integration of orbits backward in time for 2 000 years shows that for this popu-

lation the $D_{SH}$ do not exceed 0.2. Also, this is less than 0.046 when it is estimated for the meteor shower (Ryabova 2016).

The number of associated asteroids is highly dependent on the selected threshold. Each metric requires a different threshold, because the method of computation will generate different statistical distances (see Jopek 1993, Table 1).

Also, Jopek & Bronikowska (2017) studied the probability of a random similarity between two orbits. In this study, the authors tested the influences of several factors using multiple methods for the generation of orbital samples and the threshold method presented by Lindblad (1971a). They came to the conclusion that the threshold method gives to much high values and as a remedy same modification was proposed.

For this analysis I used a new algorithm in two steps for defining a threshold value (Dumitru et al. 2017).

Firstly, was ran the metrics for different values, between 0 and 0.5 for several values of $D_C$. From these runs were selected the number of associations and the meteor showers that have corresponding objects. Then a global parameter which could characterize all the meteor showers was defined (Eq. 2.22).

$$AV_{D_C} = \frac{N_{D_C}}{M_{D_C}} \tag{2.22}$$

where $N_{D_C}$ is the total number of associated asteroids for a metric, and $M_{D_C}$ is the number of meteor showers that could be produced by these asteroids. $AV_{D_C}$ is the average number of associated asteroids per meteor shower and is dimensionless with no physical meaning. It only represents a way to qualify the evolution of the clustering.

This average dimensionless parameter was used further for the definition of the threshold value (Fig. 2.3).

One can observe an important change in slope in Fig. 2.3a that occurs approximately at AV = 18, for all metrics. After this point, the number of associations increases exponential, which indicates unreliable associations. The difference between them is the number of the associated meteor showers. So, in this case, the selected value was AV = 18 as a reference point in the threshold selection.

The final step is to establish the cutoff for each used metric, using the reference point and the Fig. 2.3b. For each metric, were selected the cutoff from x axis at the reference point and the obtained values are: $D_{ACS} = 0.06$, $D_{SH} = 0.21$, and $D_H = 0.19$.

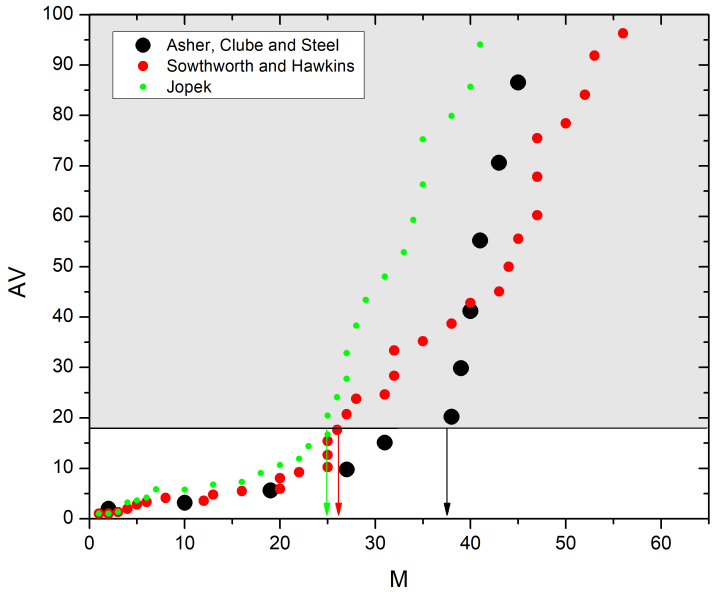


**(a)**

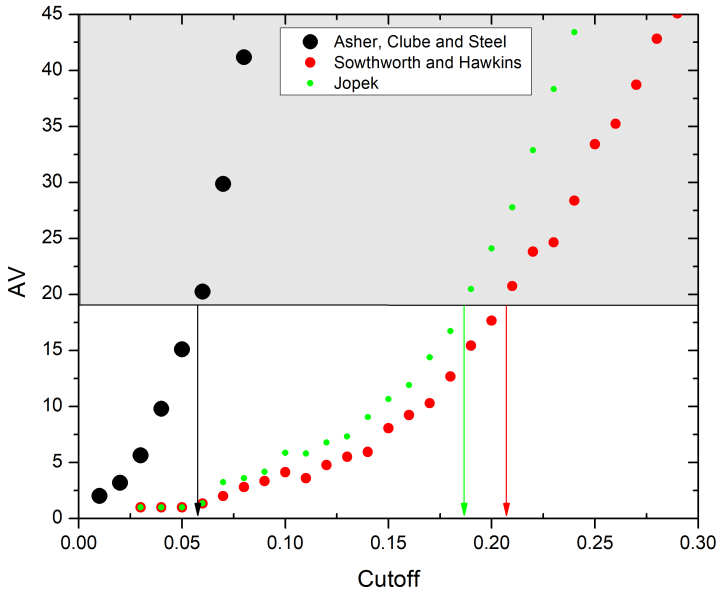


**(b)**

**Figure 2.3:** Threshold selection. 2.3a). The representation of the average number of associated asteroids per meteor shower (AV) versus the number of meteor showers (M) that could be produced by the asteroids. 2.3b). The representation of the average number of associated asteroids per meteor shower (AV) versus the cutoff value (Dumitru et al. 2017).

## 2.4 Orbital evolution and Lyapunov time

A supplementary investigation was done for the determination of orbital stability of asteroids using clones (Nedelcu et al. 2014). Also, this step is presented in (Dumitru et al. 2017).

For each asteroid were generated ten clones using a Gaussian distribution in the space of the six orbital elements with the corresponding standard deviation:

$$\sigma_{clones} = 3\sigma_{asteroid},$$

with $\sigma_{asteroid}$ for each element obtained from NEODYS service (Chesley & Milani 1999). For each asteroid the clones were integrated backward in time for 10 000 years using a realistic dynamical model of the Solar System described by Nedelcu et al. (2010) modified to use an 80–bit extended precision data type. Examples of my numerical integration are in Figs. 2.5a and 2.5b.

The orbital dispersion of clones is due both to the current uncertainty of the orbital elements and to the inherently chaotic nature of NEO dynamics. Backward numerical integrations of meteoroids orbits along with their presumed parent body may be able to identify the epoch of stream formation by finding the intersection of orbits, meteoroids and the one of the asteroid (Gustafson 1989).

This kind of approach is, however, complicated when one includes the current uncertainties of meteoroids orbital elements (Ryabova et al. 2008). Highly accurate orbits are required in order to infer a reliable stream age using the above method.

For relatively well constrained orbits of the showers, the stochastic nature of NEO orbital evolution is a second limiting factor that has to be considered and it motivates my numerical study (Abedin et al. 2017). A meaningful parent–shower association cannot be determined beyond few Lyapunov times in the past.

This kind of analysis can be reliably employed only for a few Lyapunov times back in time. For this reason the Lyapunov time was computed ($T_L$) from the solution of the variational equations that were integrated backward in time together with the equations of motion (Tancredi et al. 2001). This integration run was limited to 2 000 years, which is approximately ten times the typical value of $T_L$ for NEA (near–Earth asteroids).

The results are presented in Fig. 2.4. 85% of asteroids have a $T_L$ shorter than 200 years, a result in agreement with Tancredi (1998). According to the values of the $T_L$ I propose two distinct categories of NEA:

1. If $T_L > 100$ years, the asteroid has stable orbit. These asteroids may be long–time contributors to the meteor flux.

2. If $T_L < 100$ years, the asteroid has unstable orbit. These asteroids may be the current contributors to the supply of that meteor shower.

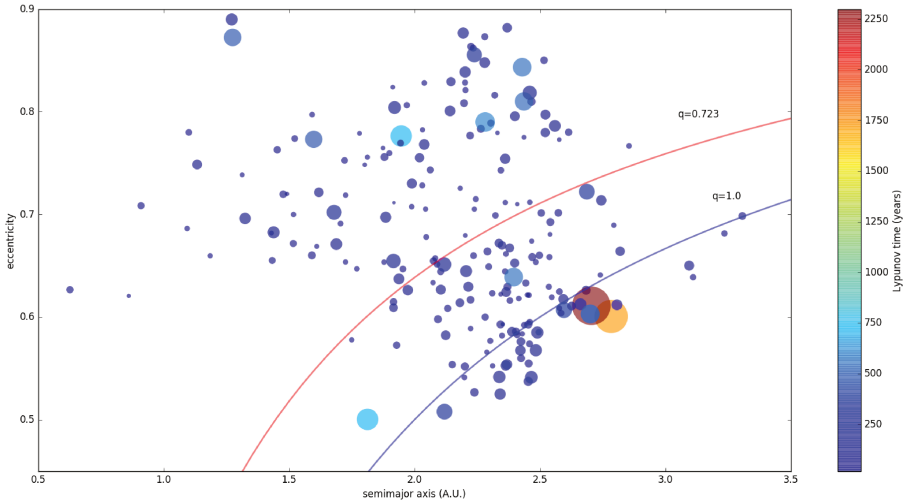


**Figure 2.4:** Lyapunov time ($T_L$) for all associated asteroids.

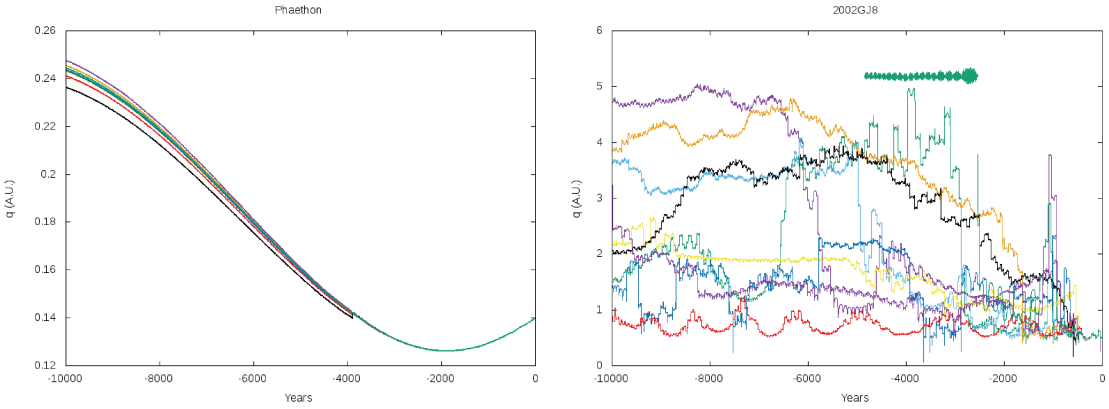


**(a)** **(b)**

**Figure 2.5:** Asteroids orbital stability according to my criteria of stable (a) or unstable (b) orbit. 2.5a). The asteroid (3200)Phaethon's perihelion evolution. This asteroid has a stable orbit ($T_L$ = 226 years). 2.5b). The asteroid 2002GJ8 perihelion evolution. This asteroid has an unstable orbit ($T_L$ = 63 years).

## 2.5 Objects association probability

In this study, I consider parent body objects with high probability those asteroids which were associated to a meteor shower by all three metrics. The medium probability will be considered for the asteroids which were associated by two metrics, while the low probability represents the amount of asteroids associated to a meteor shower just by one metric. By using several metrics for my statistics, it seems more appropriate to consider several clustering approaches giving similar results.

# Chapter 3

# Planning and telescopic observations

In this study, I used the D–Criteria metrics, a new threshold selection method and other filters to create a sample of objects that can be associated with the meteor shower, from the dynamical view. For a robust association, one has to look at the physical parameters of the associated parent bodies. The main source for the asteroids physical parameters was the literature, but many of them do not have all the necessary data.

It is very difficult to make observations for this sample of asteroids, only NEAs. For this kind of asteroids, the opportunity to get an observing window is approximately one or two weeks during their close approach to Earth. The favorable geometry for this objects occurs, in average, five times per century(Birlan et al. 2015).

So, with that in mind, was created an observational program. The goal of the program is to obtain colors and lightcurves for my sample objects. Besides the opportunity to get an observing window, the visibility criteria are also needed in order to get observational data. Some of them are presented below.

### 3.0.1 Visible magnitude limit of telescopes

First criteria of visibility is the visible magnitude limit which can be observed on a certain telescope. This helped to establish what telescope diameter is needed to see a certain target. The best formula to establish the limit of a telescope magnitude was presented by North (1997) and the mathematical expression is:

$$\lim(m_v) = 4.5 + 4.4\log(D) \tag{3.1}$$

where $m_v$ is the magnitude limit and D is the telescope diameter in millimeters. As one can see from Fig. 3.1, the observable magnitude limit of a telescope is linear dependent of the log diameter.

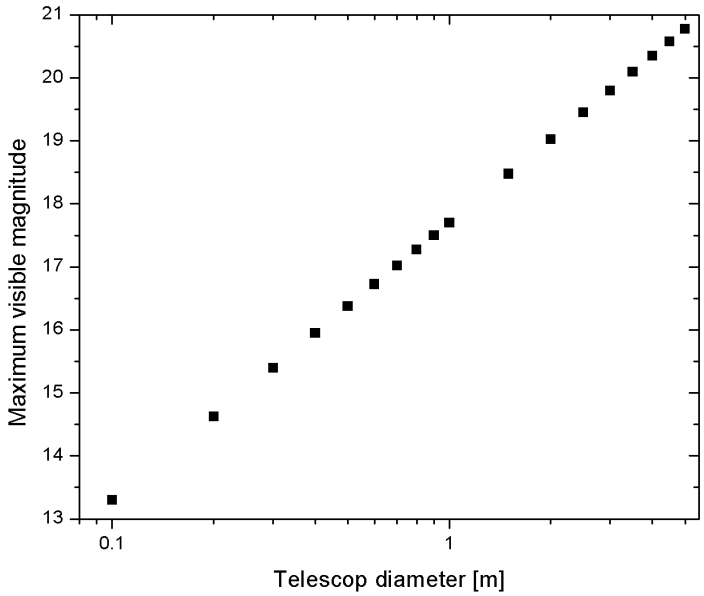


**Figure 3.1:** The observable magnitude limit that depends on the telescope diameter using Eq. 3.1.

This equation is designed to serve as a guide to predict the visible magnitude limit of a telescope viewed through a eyepiece. The real limit depends on many other factors such as, atmosphere conditions (seeing and transparency), the magnification used, exposure time, the quantum efficiency of the detector etc. Nevertheless, this method is often useful to predict the visual magnitude limit of a telescope.

### 3.0.2 Airmass

In astronomy, the airmass, represents the light path length through the atmosphere. This is measured by the amount of air that light needs to traverse. If the observed object is at zenith (imaginary point directly above a particular location, at 90°), then the airmass is equal to 1 and grows as it moves away from it.

For example, when the photons from a certain object pass through the atmosphere, it could hit atoms, dust particles, water molecules, etc. and may be absorbed or scattered on a different path. When the photons are absorbed the observed object becomes dimmer than in reality. In astronomy, this effect is also known as extinction. When the photons are scattered, the object becomes blurry. In astronomy, this effect is also known as seeing.

Considering those effects (extinction and seeing), in order to obtain the best data, is needed to make observations when between the telescope and the target is as less airmass as possible. In order to start the acquisition process it is required to know the minimum altitude which the data are reliable.

If one considers that the atmosphere is homogeneous and the Earth is flat, then one can use Eq. 3.2 to see how much airmass (x) is at different distances from the zenith point (z = 90° - object altitude).

$$x = \frac{1}{cos(z)} \tag{3.2}$$

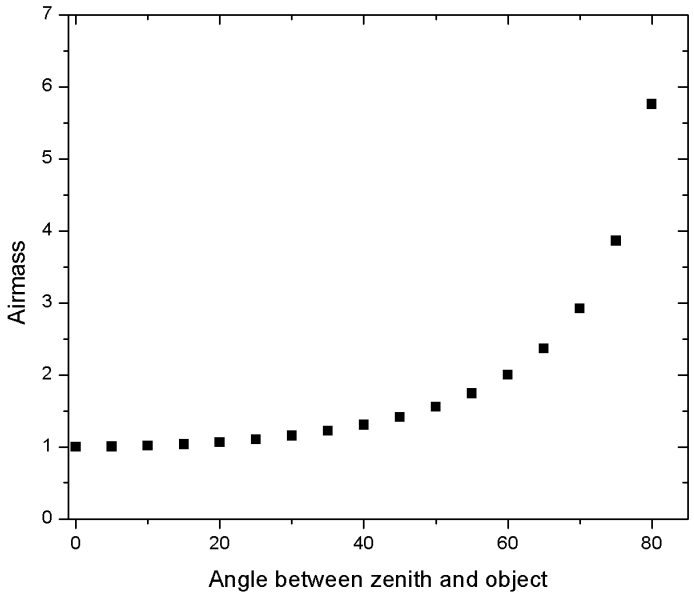


**Figure 3.2:** Airmass vs zenith distance using Eq. 3.2.

As one can see from the Fig. 3.2, until the 60° the airmass is approximate 2. However, this equation can be used for small zenith distances (up to 60°) depending on the necessary accuracy (Mathar 2015).

## 3.1 Observation planing for targets selection

As it was explained at the beginning of this chapter, the objects sample consist only of NEAs and for those objects the observational window is one or two weeks during their close approach. To obtain the period in which my objects sample can be observed we need to compute the ephemerides.

For my observation targets we used a web-based tool from Euronear, namely Long Planing[1]. This tool used the orbital parameters from the Asteroid Orbital Elements Database (Astorb)[2] and the computation is based on a simple two-body orbital model. To get the list with the targets that can be observed the tool needs some input parameters:

[1]http://www.euronear.org/tools/longplan.php
[2]http://www.naic.edu/ nolan/astorb.html

1. A list with all the objects of interest (in my case, the list with all the associated asteroids to the meteor showers). The list needs to be a text file and on every line it has to contain the name or the number of an asteroid.

2. The location where the observations will be made (here we need to input the IAU code for the observatory site). The IAU code is assigned by the MPC for each registered observatory. This code consists of three digit, from 000 to Z99.

3. The period during which we want to make observations. For this, are assigned two parameters: the start date and the number of nights we wish to search the visible targets.

4. Some constraining parameters, such as: the limit of apparent magnitude, the maximum motion of the object, the minimum altitude for observations and the minimum number of hours that the object can be observed.

The results are shown on the web page or can be downloaded in a csv format file. The information resulted from this computation are: the period in which a object can be observed, the night in which the object has the brightest magnitude and the highest number of hours in which it is observable, etc.

But this tool do not provide the coordinates, because the two body problem method is a simplified calculation that does not count perturbations caused by other objects and various corrections were ignored. This method is useful for seeing the objects which can be observed, but for a precise coordinates of the object, a dedicated ephemeris service is needed (Vaduvescu et al. 2017).

### 3.1.1 Ephemeride computation

As specified in Section 3.1, for my target selection, I used a simple two-body orbital model, which is described below (Ureche 1982).

I will start with the determination of the object position on the orbital plane. First parameter needed is the mean anomaly (M), for which the mathematical expression is presented in Eq. 3.3).

$$M = n(t - t_0) \tag{3.3}$$

where $n = \frac{2\pi}{P}$, and P is the sidereal revolution of the object.

Sometimes instead of the moment $t_0$, it is given the value of the mean anomaly ($M_\tau$) at the time at which the orbital elements were determined. Eq. 3.3 becomes

$$M = M_\tau + n(t - \tau) \tag{3.4}$$

Using M, one can determine the eccentric anomaly (E) by solving:

$$E - e\sin(E) = M \tag{3.5}$$

Eq. 3.5 can be solved by several methods, but in this case (elliptical orbits) it is applied the method of successive approximations. If one sets $E_0 = M$, the successive approximations will be computed as follows:

$$E_0 = M \tag{3.6}$$
$$E_1 = M + e\sin(E_0) \tag{3.7}$$
$$E_2 = M + e\sin(E_1) \tag{3.8}$$
$$..... \tag{3.9}$$
$$E_n = M + e\sin(E_{n-1}) \tag{3.10}$$

These equations are convergent for each M $\in \Re$ and e $< 1$. The convergence is faster as the e is lower. The iteration process is stopped when the difference of two successive approximations is below the admissible error, taking the value of E as the last computed approximation.

The position on the orbital plane will be determined by the polar coordinates ($r$ and $\beta$), which are given by:

$$r = a(1 - e\cos(E)) \tag{3.11}$$
$$\tan\frac{\beta}{2} = \sqrt{\frac{1+e}{1-e}}\tan\frac{E}{2} \tag{3.12}$$

Then one needs to obtain the heliocentric coordinates of the object.

For this computation one takes two reference systems. First, S–$x_o$–$y_o$–$z_o$ (Sun (S) - the origin, $x_o$–S–$y_o$ - the ecliptic plane, S–$x_o$ - North line axis (Fig. 3.3, $\Psi$), $\Psi$–S–$z_o$ - direction of ecliptic North pole (PNO)) and second S–$x_1$–$y_1$–$z_1$ (Sun (S) - the origin, $x_1$–S–$y_1$ - the ecliptic plane, S–$x_1$ - orientated to the vernal point ($\nu$), S–$z_1$ coincide with S–$z_o$).

Now the angle between the northern line and the ray of the object vectors (u) for S–$x_o$–$y_o$–$z_o$ system will be:

$$u = \beta + \omega \tag{3.13}$$

From Fig. 3.3 it can be seen that the coordinates $x_o$–$y_o$–$z_o$ of the object are:

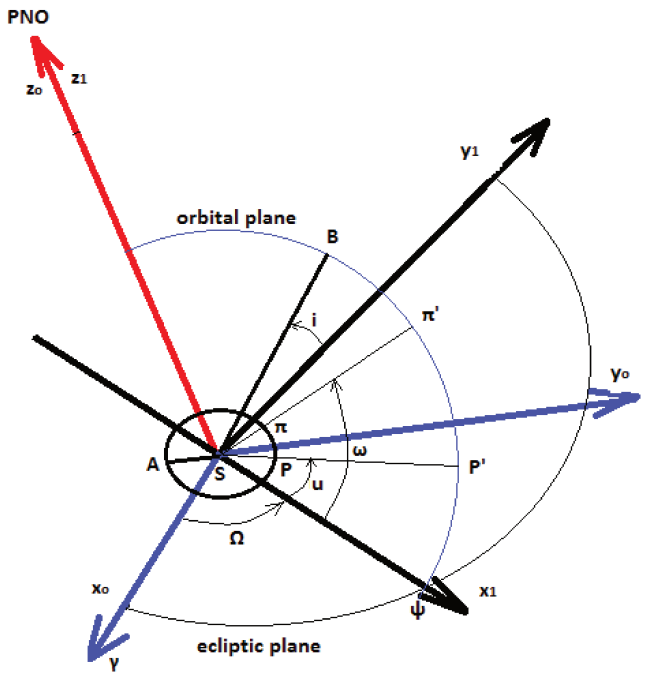


**Figure 3.3:** Ecliptic reference system

$$x_1 = r\cos(u) \tag{3.14}$$
$$y_1 = r\sin(u)\cos(i) \tag{3.15}$$
$$z_1 = r\sin(u)\sin(i) \tag{3.16}$$

Now one can move from the system S–$x_1$–$y_1$–$z_1$ to S–$x_o$–$y_o$–$z_o$ through a rotation in the ecliptic plane, of $\Omega$ angle. The new coordinates are:

$$x_1 = r(\cos(u)\cos(\Omega) - \sin(u)\sin(\Omega)\cos(i)) \tag{3.17}$$
$$y_1 = r(\cos(u)\sin(\Omega) + \sin(u)\cos(\Omega)\cos(i)) \tag{3.18}$$
$$z_1 = r\sin(u)\sin(i) \tag{3.19}$$

By performing a final rotation (the angle between the ecliptic plane and the equatorial plane), the new coordinates are:

$$x_2 = r(\cos(u)\cos(\Omega) - \sin(u)\sin(\Omega)\cos(i)) \tag{3.20}$$
$$y_2 = r(\cos(u)\sin(\Omega)\cos(\varepsilon) - \sin(u)\cos(\Omega)\cos(\varepsilon) - \sin(u)\sin(i)\sin(\varepsilon)) \tag{3.21}$$
$$z_2 = r(\cos(u)\sin(\Omega)\sin(\varepsilon) + \sin(u)\cos(\Omega)\cos(i)\sin(\varepsilon) + \sin(u)\sin(i)\cos(\varepsilon) \tag{3.22}$$

Now are defined two auxiliary variables ($\gamma$ and N) and the Gauss constants a, b, c, A, B, C through the equations:

$$\gamma \sin(N) = \sin(i) \tag{3.23}$$
$$\gamma \cos(N) = \cos(\Omega)\cos(i) \tag{3.24}$$
$$a \sin(A) = \cos(\Omega) \tag{3.25}$$
$$a \cos(A) = -\sin(\Omega)\cos(i) \tag{3.26}$$
$$b \sin(B) = \sin(\Omega)\cos(\varepsilon) \tag{3.27}$$
$$b \cos(B) = \cos(\Omega)\sin(i)\cos(\varepsilon) - \sin(i)\sin(\varepsilon) = \gamma \cos(N+\varepsilon) \tag{3.28}$$
$$c \sin(C) = \sin(\Omega)\sin(\varepsilon) \tag{3.29}$$
$$c \cos(C) = \cos(\Omega)\sin(i)\sin(\varepsilon) + \sin(i)\cos(\varepsilon) = \gamma \sin(N+\varepsilon) \tag{3.30}$$

Equatorial heliocentric coordinates have now the simple form:

$$x_2 = ra \sin(u + A) \tag{3.31}$$
$$y_2 = rb \sin(u + B) \tag{3.32}$$
$$z_2 = rc \sin(u + C) \tag{3.33}$$

The final spherical equatorial geocentric coordinates of the object are obtained after a translation from the heliocentric reference system to the geocentric one. In this system we have:

$$x_3 = \varphi \cos(\beta)\cos(\alpha) \tag{3.34}$$
$$y_3 = \varphi \cos(\beta)\sin(\alpha) \tag{3.35}$$
$$z_3 = \varphi \sin(\beta) \tag{3.36}$$

where $\alpha$ is the right ascension, $\beta$ is the declination, and $\varphi$ is the geocentric distance of the object. From this one obtains:

$$\tan(\alpha) = \frac{y_3}{x_3} \tag{3.37}$$
$$\tan(\beta) = \frac{z_3}{y_2}\sin(\alpha) \tag{3.38}$$
$$\varphi = \frac{z_3}{\sin(\beta)} \tag{3.39}$$

### 3.1.2 Apparent magnitude computation

The apparent magnitude represents the brightness of an object observed from Earth. Its magnitude depends on: the distance between the object and the Sun, the distance

between object and Earth, the size of the object, the surface composition, etc. The strength in brightness of an object is inversely proportional to the square distance form the Sun and also the radiation flux of an object at a certain distance from the Sun decreases with square distance between the object and Earth.

To compute the apparent magnitude (V) one needs the absolute magnitude (H) and the slope parameter (G). Also, because the apparent magnitude depends on the distances between Sun, Earth and the object, it must be taken into account the phase angle.

The mathematical expression for the apparent magnitude at a certain phase angle is:

$$V = H - 2.5 \log(((1 - G)\Phi_1 - G\Phi_2)) \tag{3.40}$$

where $\Phi_1$ and $\Phi_2$ are two basis functions normalized at unity for a 0° phase angle (Muinonen et al. 2010).

### 3.1.3 Two bodies orbital method vs. full numerical integration

As a check, a comparison was made between the performance of two methods of ephemeride computation on three NEAs (a simple two-body orbital method presented in Subsection 3.1.1 and the full numerical integration method that uses a realistic dynamical model of Solar System (Nedelcu et al. 2014)).

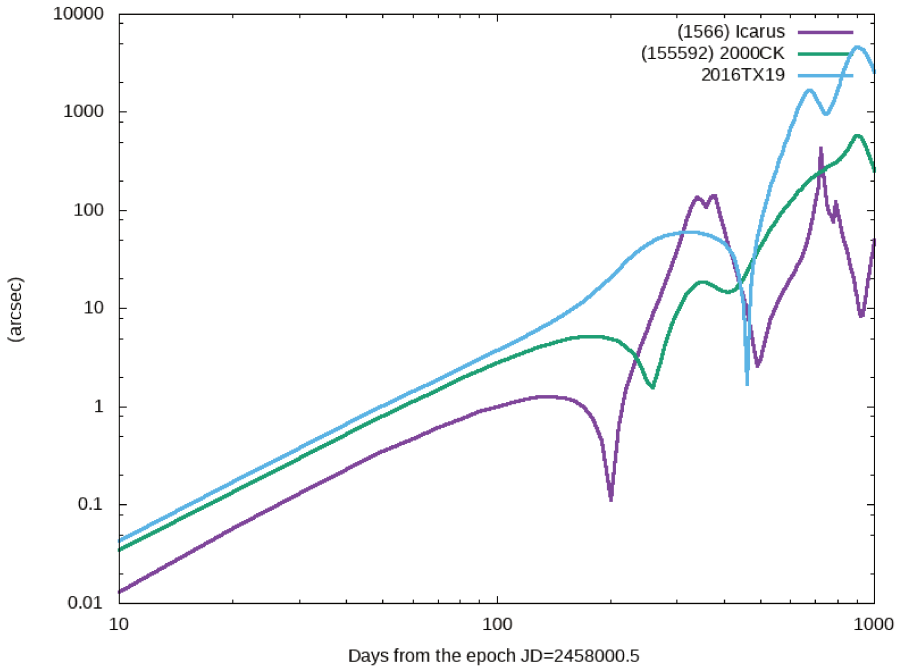


**Figure 3.4:** Analytic–numerical integration positions difference

Fig. 3.4 shows the differences between near-Earth asteroids sky positions obtained using the 2 bodies approximation and the full, numerical integration model. Close to the epoch of orbital elements (JD=2458000.5 in this case), the faster, 2 bodies method has a sufficient accuracy for observations planning purposes. For the actual run and target identification were used the precise positions obtained by numerical integrations.

## 3.2 Data extraction from observation

### 3.2.1 Photometry with charge coupled devices (CCD)

The CCD is a detector (silicon base) which is electrically divided into independent pieces, called pixels. The chip can have between 0.5 cm to 10 cm in linear size on which can be up to 16 777 216 (4 096 x 4 096) individual pixels. In astronomy, the CCD is used to measure the light that falls on each pixel and the output is a digital image (matrix of numbers, one per pixel). The advantage of the CCD consists in generating images in a digital form, which can be viewed instantly, manipulated, measured and analyzed.

To use the CCD in astronomy as low light level detector, one needs to understand first same basic concepts that helps us realize why we do certain steps in data reduction.

The first concept is quantum efficiency (QE). The detection of a CCD is photon by photon, but not all the photons that falls on it are detected. The QE represent the photons that fall on the CCD and are also detected. This efficiency can be calculated by using the equation:

$$QE = \frac{Nb.\ \ of\ \ detected\ \ photons\ \ on\ \ pixel\ \ per\ \ second}{Nb.\ \ of\ \ incident\ \ photons\ \ on\ \ pixel\ \ per\ \ second} \tag{3.41}$$

The next concept is the count. The pixel value do not contain only the number of photons that hit, but some electrical errors as well. A part of this count represents the electrical compensation, namely bias (see below), and another part is the dark current (see below). After the extraction of the components specified previously, the signal is related to the number of electrons released by photons. But even so, only a part of the photons that hit the detector release electrons. The photons number will be the product between the number of electrons and the QE. Also for several technical reasons, the output value is related to the number of electrons by a divisive number, namely gain. Finally the number of photons detected is related to the output number (DN):

$$Nb.\ \ of\ \ photons = \frac{Nb.\ \ of\ \ electrons}{QE} = \frac{gain * DN}{QE} \tag{3.42}$$

An important concept is the integration time (or exposure time ). The CCD

is an integrating device and the signal is build up in time. This can be controlled mechanically or electrically.

Another concept is the read noise. Every CDD has sophisticated amplifications. This process generates electronic noise in every image. The electronic noise is not dependent on exposure time. The same values are identical for short or long exposure time (modern CDD have a typical read noise of 5 to 20 electrons per pixel per read out).

Next, one discuses the corrections that need to be done for every image. Those corrections help us eliminate the errors specified previously, and in astronomy are known as Bias frame, Dark frame and Flat frame.

### Bias frame

The Bias frame represents the reading differences of each pixel. These frames are taken without the light reaching the detector and with a very small exposure time (as close as 0, depends on the CCD). This bias signal shows the electronic noise of the CCD and the systematic errors. To get rid of these errors and to avoid getting aberrations into the images, is needed a MasterBias frame, which is created by combining the Bias frames (see Fig. 3.5a).

### Dark frame

The temperature plays an important role for CCD. Because of the non-zero temperature, same electrons have enough energy to reach the pixels without being activated by photons. The more the temperature increases, the more the noise, and the lower the temperature, the clearer the images will be (a 6 degree Celsius decrease reduces the noise with a sqrt factor of 2). In this case the subtraction of this frame (Dark frame) helps eliminate them. The Dark frames represent the chip noise and temperature dependence. These frames extract the electronic noise that is created during exposures from the camera electronics. In order to extract the dark frames from the images, it must be taken into account the exposure time of the images (the image and the dark frame must have the same exposure time). If the exposure time is not the same, more noise will be put into the final image. In order to obtain those frames, is needed to set the same exposure time and the light to not reach the detector (see Fig. 3.5b).

### Flat frame

These frames represents the optical imperfections of the telescope and the CCD camera. Usually the detector is not homogeneously illuminated. The dust particles on the telescope's lens (lenses, mirrors, etc.) and the CCD leads to the shading of certain areas of the detector. Another problem is pixel's efficiency, which is not the same for all of them. All these problems can be solved by using Flat frame. After

the flat frames have been taken, it is no longer allowed to move the CCD camera. If one moves the CCD camera, the frames taken are no longer good, and the procedure must be started from the beginning (see Fig. 3.5c).

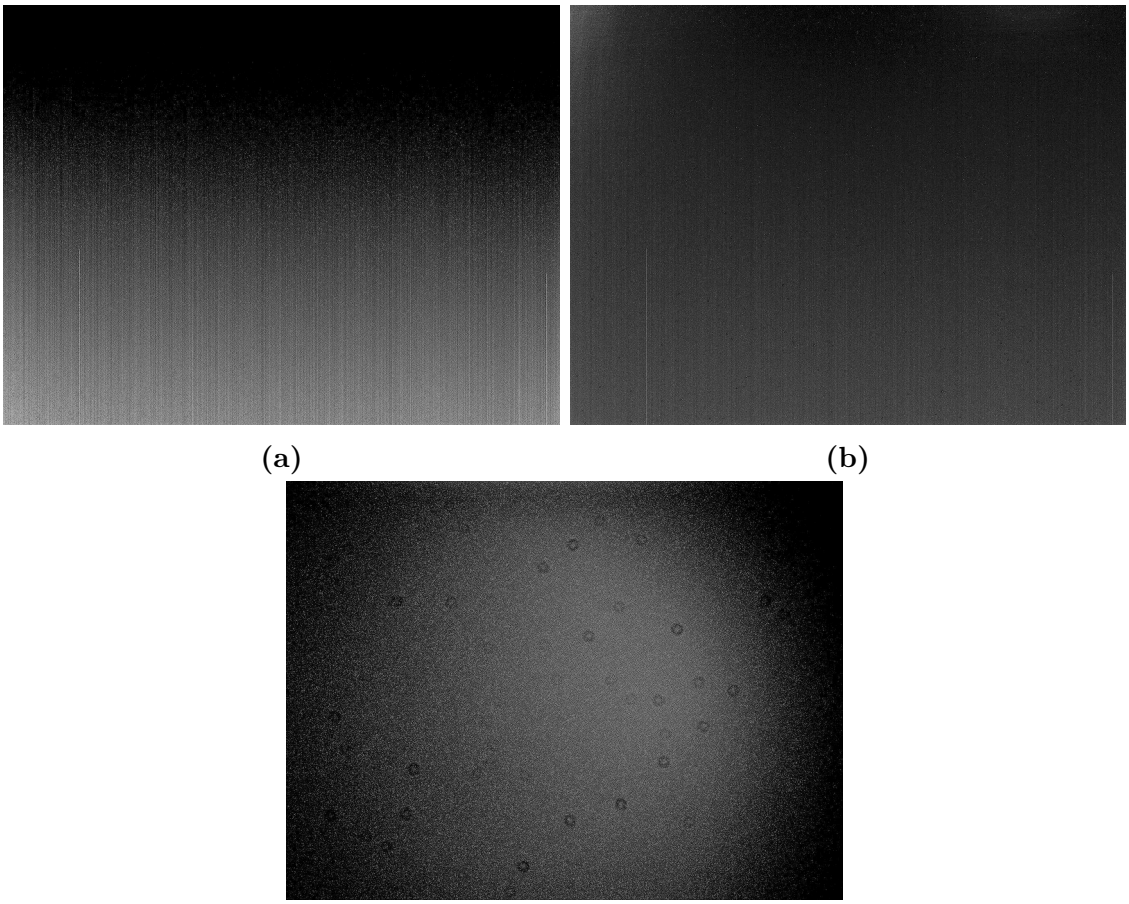

**(a)** **(b)**

**(c)**

**Figure 3.5:** Calibration images. 3.5a). An example of bias frame. 3.5b). An example of dark frame. 3.5c). An example of flat frame.

### Image reduction

In order to obtain a clean image one needs to eliminate the bias, dark and flat frames from the image. To have as little noise as possible, one has to compose these frames and create the so called master frames (as specified at bias frame). The equations for obtaining the clean image are:

$$Dark_f = MasterDark - MasterBias \tag{3.43}$$

$$Flat_f = \frac{MasterFlat - MasterDark - MasterBias}{Avrage \quad Pixels \quad Value} \tag{3.44}$$

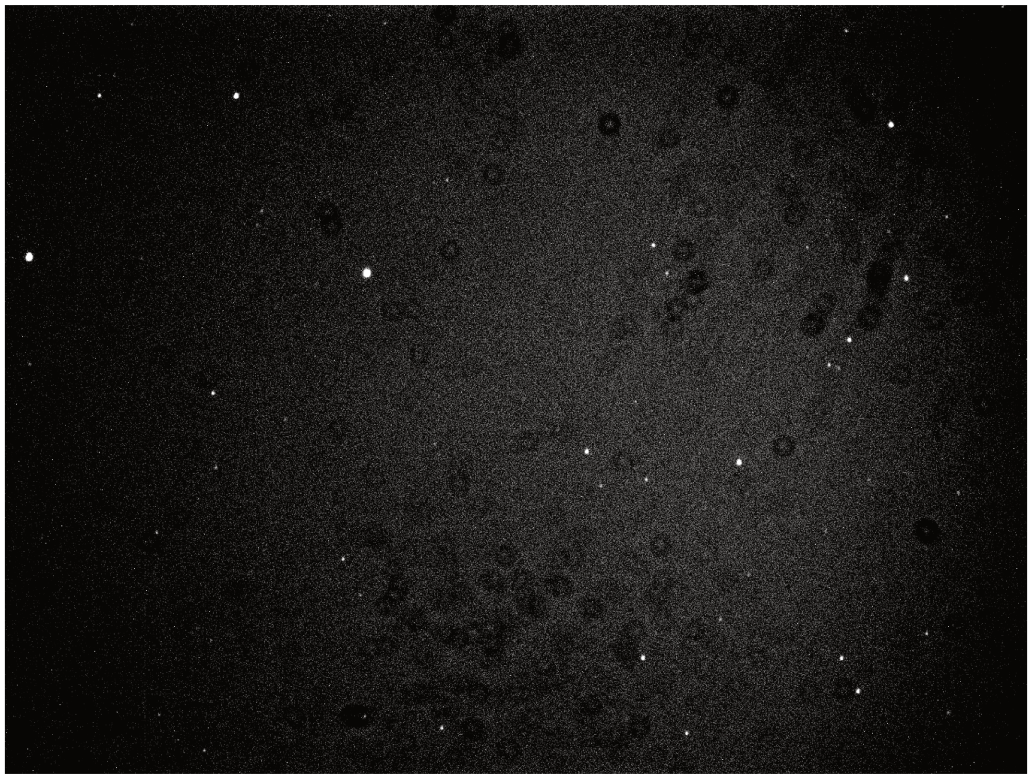

**(a)** The image without the reduction.

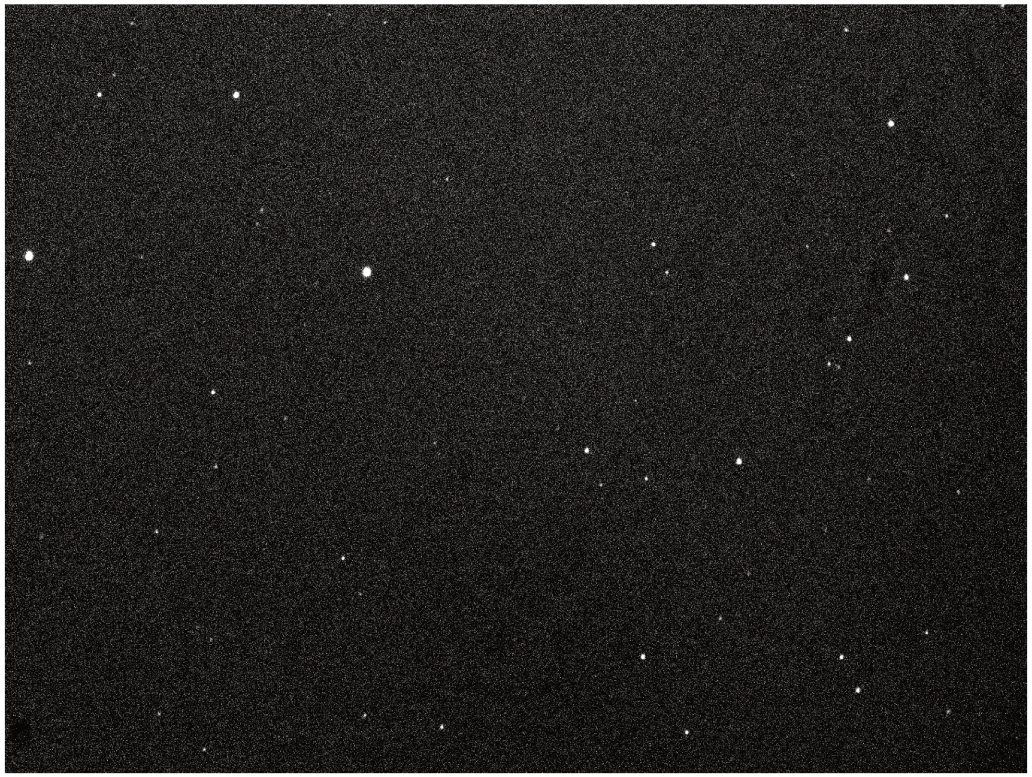

**(b)** The image with the reduction.

**Figure 3.6:** Improvement of an image after corrections (before and after). In the first image it is presented the initial one and in the second the corrected one.

$$Image_f = \frac{ImageFrame - MasterBias - Dark_f}{Flat_f} \tag{3.45}$$

An example of how much the clean image is improve is shown in Fig. 3.6.

## 3.3 Large telescopes

In order to observe as many objects as possible, I applied for observation time on large telescopes. The applications can be made two times per year, in competition with astronomers around the world for observation time. It needs to contain a scientific case (the part where the scientific motivation for the proposal is justified), a technical case (the part justifying the technical requirements such as why one needs that specific telescope, source magnitudes, estimates of the exposure times, etc.), and an object list (containing the targets, magnitudes, observation time per target, coordinates, etc.). These applications were sent to two large telescopes, namely NASA Infrared Telescope Facility(IRTF) in Mauna Kea, USA and Pic du Midi observatory from Pyrenees mountains, France.

The first observatory is Pic Du Midi from Pyrenees mountains, France, located at 2 870 m of altitude. The telescope used from this facility was T1M 1.05 m and an iKon-L Andor CCD camera with a 2k X 2k E2V chip (pixel scale 0.22 "/pix) and SDSS filters (Vaduvescu et al. 2013). It was used the 2x2 binning mode in order to avoid the oversampling of images. The seeing was not constant during the run with FWHM between 1.2 and 2 arcsec.

The second observatory was Infra-Red Telescope Facility (IRTF). This telescope has 3 m and is located on Mauna Kea, Hawaii at approximate 4 200 m altitude. This telescope is equipped with SpeX/Moris system with the 0.8 x 15" slit, in the low resolution mode for covering the spectral interval 0.8 - 2.5 $\mu$m.

### 3.3.1 Colors and reflectance extraction

The asteroids colors are used to determine some characteristics of asteroid's surface and for a first order estimation of its taxonomic type (Fulchignoni et al. 2000). The commonly used systems of filters are Johnson-Cousins U, B, V, R and I (see Bessell 1979; Cousins 1974; Johnson & Morgan 1953) and Sloan Digital Sky Survey (SDSS) u, g, r, i and z (York et al. 2000).

The filter used in the run where SDSS $u = 0.354$ nm, $g = 0.477$ nm, $r = 0.623$ nm, $i = 0.763$ nm and $z = 0.913$. The targets were not detected in $u$ and $z$ filters.

For each asteroid were computed the reflectance colors $g - r$, $g - i$ and $\log reflectance$. The computation method was taken from EAR-A-I0035-5-SDSSTAX-V1.1 database

The reflectance color (C) is:

$$C = (M_1 - M_2) - C_S \tag{3.46}$$

where $M_1$ and $M_2$ are the magnitudes of the object in the two filters and $C_S$ is the color of the Sun ($g-r = 0.45 \pm 0.02$ and $g-i = 0.55 \pm 0.03$) obtained from Ivezić et al. (2001).

The reflectance color error ($\delta_{Color}$) is:

$$\delta_C = \sqrt{\delta_{M_1}^2 + \delta_{M_2}^2 + \delta_{C_S}^2} \tag{3.47}$$

where $\delta_{M_1}$ and $\delta_{M_2}$ are the standard deviations for each filter and $\delta_{C_S}$ is the standard deviations of solar color.

Reflectance $R_C$ is:

$$\log R_C = 0.4C + \log(Rref) \tag{3.48}$$

derived from Pogson equation, used in Carvano et al. (2010) for computing the $\log reflectances$. I used this $\log reflectance$ because I compared the results with the data from database to associate the objects to a taxonomic class.

The error $\delta_{R_C}$ of $R_C$ was obtained by:

$$\delta_{R_C} = 0.4\delta_C \tag{3.49}$$

### 3.3.2 Lightcurve

The lightcurve is the primary method used to determine rotational properties of an asteroid. From the rotation period one can determine if an object has a ruble-pile or monolithic structure (Pravec et al. 2006). From several lightcurves obtained at several oppositions, the absolute magnitude, the shape, and pole of the object could be obtained.

In a single night it can be observed an entire lightcurve or a fragment of it, depending on the objects rotation period. To obtain an entire lightcurve from fragments, they must be cumulated, and the result is called a composite lightcurve.

In general, an asteroid lightcurve has two minims and two maxims, and the variation between them it is called amplitude. The amplitude of the asteroids can range from hundredths of magnitude to a magnitude with few exceptions. This variation is caused by the asteroid irregular shape. During its rotation around the axis, it reflects a different amount of light due to the surface that is illuminated by the Sun. The larger the surface, the greater the amount of reflected light, and the lower the illuminated surface, the less reflected light (see Fig. 3.7).

The composite lightcurves were obtained using the following procedure:

(1) The apparent magnitude $M_a$ of the asteroid was obtained using three reference stars by:

$$M_a = \left(M_{ia} - \frac{\sum M_{is}}{3}\right) + \frac{\sum M_{rs}}{3} \tag{3.50}$$

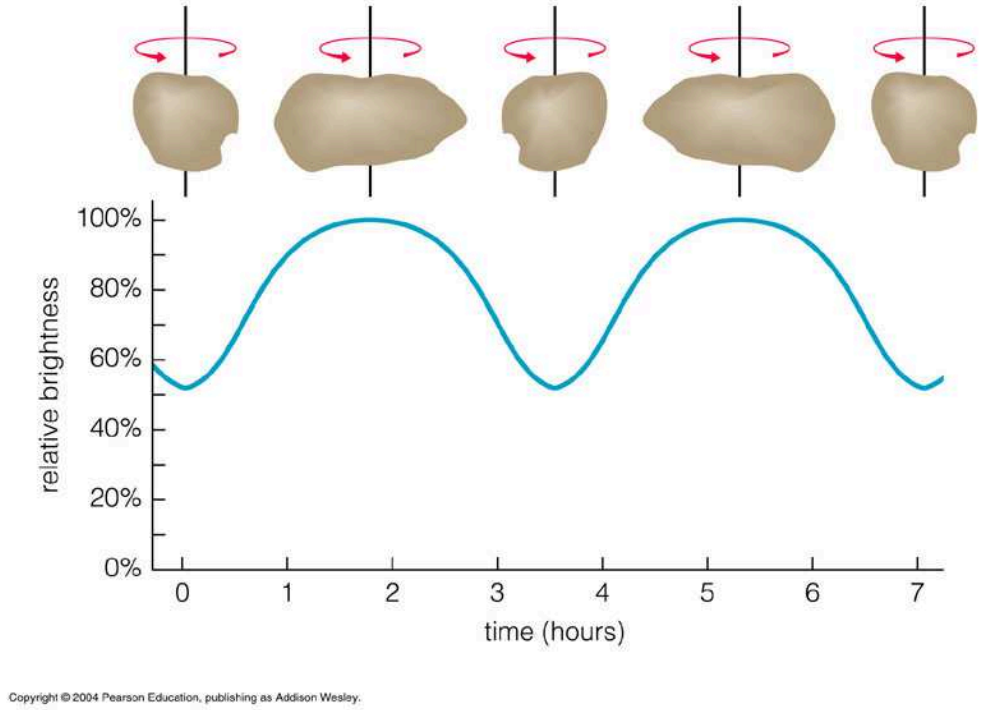




**Figure 3.7:** The way a lightcurve looks like and the reason why.

where $M_{ia}$ and $M_{is}$ are the instrumental magnitude of the asteroid and reference stars, and $M_{rs}$ is the magnitude of the reference stars from SDSS catalog.

(2) Reduced magnitude $M_R$ of the asteroid, magnitude at distance of 1 a.u. from Sun and Earth is:

$$M_R = M_a - 5\log(r * d) \tag{3.51}$$

where $r$ and $d$ are the heliocentric and geocentric distances of the asteroid.

(3) To obtain the composite lightcurve, the influence of the phase angle from the reduced magnitude needs to be removed (i.e. the absolute magnitude). Considering a linear relationship between the reduced magnitude and the phase angle (Fig. 4.35), the absolute magnitude can be obtained by using the following equation:

$$M_{SC} = M_a - l * PA \tag{3.52}$$

where $l$ is the linear plot slope and $PA$ is the phase angle.

(4) Rotational period and composite lightcurve. To obtain the rotation period I used a method for non-equidistant time series data, namely the Lomb-Scargle periodogram (Scargle 1982). This method estimates the period with a sinusoidal fit function (see Fig. 4.36). Finally, all data is normalized to a single rotation period.

# Chapter 4

# Results

From my analysis, considering the selected thresholds (see Section 2.3), evolution and Lyapunov time (see Section 2.4), I obtained 1 445 asteroids that can be associated with 39 meteor showers (see Figs. 4.1 and 4.2), 1 813 associations in total.

I divided these asteroids into three categories (see Subsection 2.5), high, medium and low probability of appurtenance to a meteor shower. This division was made based on the associated metrics: high probability for asteroids associated by all metrics, medium probability for asteroids associated by two metrics and low probability for asteroids associated by one metric. The low probability category was ignored in this statistic.

I obtained 73 asteroids associated with high probability, 499 asteroids associated with medium probability and the rest (1 241 asteroids) were associated with low probability. Also, from my sample, I found multiple occurrences for several asteroids (i.e., 2003UV11, 2004TG10, 2007UL12, 2010TU149, 2011TC4, etc.).

From Figures 4.1 and 4.2 one can see that at the regions between $2 < a < 2.5$, $5 < e < 6$ and $0 < i < 10$ there is a very high density of associations. In a more thorough search I found that approximately 53% of the entire sample is associated with two meteor showers, COR and HVI. In this study I used a global threshold for each metric, and in the case of those two meteor showers, the threshold values used seem to be too permissive (in these cases lower threshold values are needed).

Based on the above considerations, I decided to consider only the asteroids with high probability for these meteor showers. Also, because the main purpose of this study was finding asteroids which can be associated with meteor showers, I ignored all objects that are associated with low probability (but they will not be ignored from the selecting targets for observations).

Therefore, in this case remained 73 associations with high probability and 223 associations with medium probability, corresponding to 28 meteor showers. All the remaining objects are presented in Table 4.1.

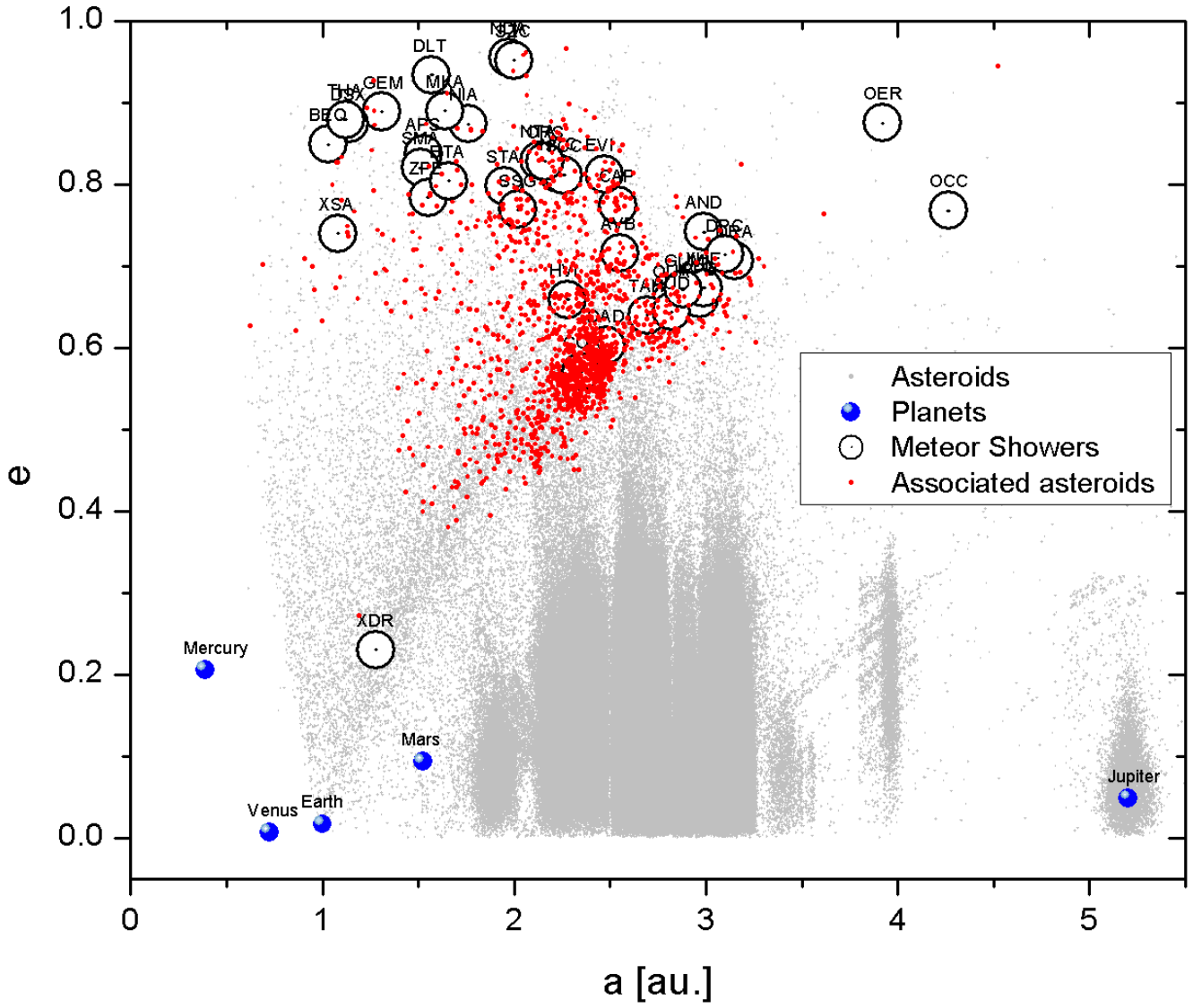


**Figure 4.1:** The positions according to semi–major axis vs. eccentricity for all associated asteroids position in the Solar System. All asteroids are represented by grey points, the planets by blue dots, the meteor showers by black circles and the associations by red squares.

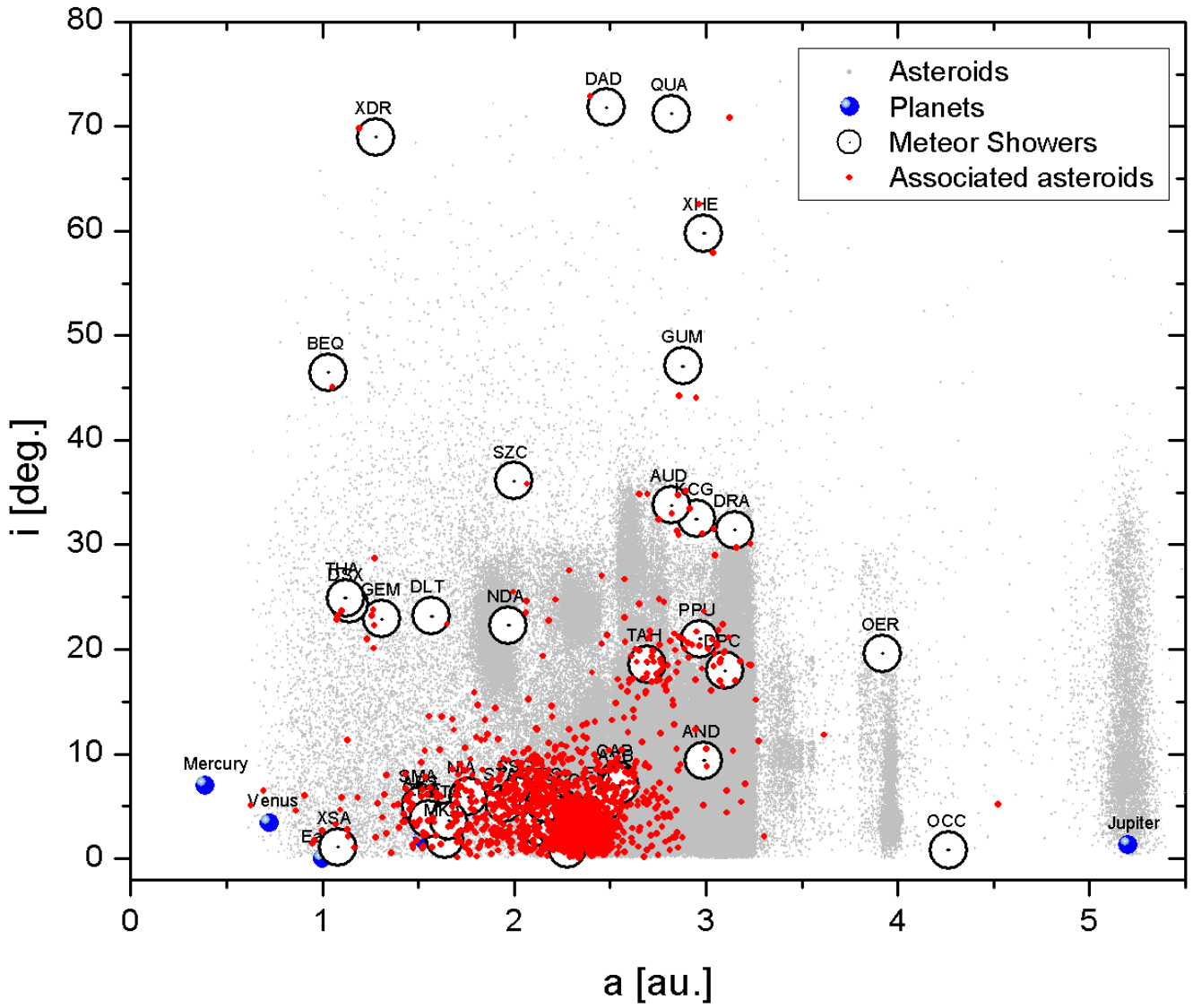


**Figure 4.2:** The positions according to semi–major axis vs. inclination for all associated asteroids position in the Solar System. All asteroids are represented by grey points, the planets by blue dots, the meteor showers by black circles and the associations by red squares.

**Table 4.1:** Set of 28 meteor showers and their associated asteroids (73 associations with high probability and 223 associations with medium probability). The asteroids in bold are associated to several meteor showers and those underlined are the asteroids found with physical data (taxonomy, albedo or rotation period). Parent Body column is the associated parent body from IAU Meteor Data Center as of 25 June 2016. Corvids (COR) and h Virginids (HVI) are on the last two lines and only high probability associations are presented.

| Cod | Name | High Probability | Medium Probability | Parent Body |
|---|---|---|---|---|
| AND | Andromedids | 0 | 1995FF, (152770)1999RR28, (494658)2000UG11, (267729)2003FC5, 2003UQ25, 2004GB2, 2009ST103, 2009TA1, 2009WJ1, 2010TN167, 2010TV54, 2012FG, 2012TT231, 2012VB5, 2016FC14, 2016TW18, 2016UP36, 2016VQ, 2017FL101, 2017SB33, 2017UE5, 2017UL7, 2017UM1 | 3D/Biela |
| APS | Daytime April Piscids | 0 | (438105)2005GO22, **2012KA4**, 2013HT25 | 2005 NZ6 |
| AUD | August Draconids | 0 | 2002GJ8, **2016NO16**, **2017NW5** | - |
| BTA | Daytime $\beta$ Taurids | 0 | **(503941)2003UV11**, **2004TG10**, **2007UL12**, **2010TU149**, **2011TC4**, 2011TX8, **2012UR158**, **2014NK52**, **2015TX24**, 2015VH66, **2016TP18** | 2P/Encke, 2004TG10 |
| CAP | $\alpha$ Capricornids | 2008BO16, 2015DA54 | 1995CS, 2001EC, 2002CB26, 2002NW, 2011CG50, 2012BL14, 2012BQ123, 2012CC29, 2014OO6, 2015CE1, 2015CP, 2015DE54, 2015NJ3, 2016BN14, 2016BP14, 2016BV14, 2016CL137, 2016CW264, 2017MB1, 2017QT1 | 169P/NEAT |

**Table 4.1:** continued.

| Cod | Name | High Probability | Medium Probability | Parent Body |
|---|---|---|---|---|
| DLT | Daytime $\lambda$ Taurids | 0 | 2017SK10 | - |
| DPC | December $\phi$ Cassiopeiids | 0 | 2017UE45 | 3D/Biela |
| DSX | Daytime Sextantids | 0 | (155140)2005UD | (155140)2005UD |
| EVI | $\eta$ Virginids | 2003FB5, 2006UF17 | (455176)1999VF22, (483423)2000DO1, 2001FB90, 2002CN15, 2007EJ88, 2008CA22, 2008VL14, 2010CF55, 2010TN55, 2010VF, 2015ER, 2015FD35, 2015TC144, 2016ES155, 2016EV28 | D/1766 G1 |
| GEM | Geminids | (3200)Phaethon | 0 | (3200)Phaethon |
| KCG | $\kappa$ Cygnids | 0 | **2016NO16**, **2017NW5** | - |
| NCC | Northern $\delta$ Cancrids | (85182)1991AQ, 2006BF56 | 2008WZ94, 2013YL2, 2015PU228, 2017YO4, 2018AK12 | (85182)1991AQ |
| NIA | Northern $\iota$ Aquariids | 0 | 2006PF1, **2012KA4**, **2015PM307** | - |
| NTA | Northern Taurids | **2004TG10**, **2010TU149**, **2012UR158**, **2014NK52** | 2001UX4, **(503941)2003UV11**, **2007UL12**, 2010VN139, **2011TC4**, **2016TP18**, 2016VK | 2P/Encke, 2004TG10 |

**Table 4.1:** continued.

| Cod | Name | High Probability | Medium Probability | Parent Body |
|---|---|---|---|---|
| OCC | October Capricornids | 0 | (4179)Toutatis, 2002RC117, 2005RA, 2005RJ, 2005TD49, 2005XN27, (509191)2006OC5, 2006XA3, 2007WW3, 2008SH148, 2008XU2, 2009ST171, 2010RB12, 2011OL51, 2011YY62, 2012XM134, 2013WX44, 2013XT21, 2014XE32, 2014XL6, 2015TL143, 2016PN38, 2016RZ40, 2016TV93, 2016WN48, 2017VC13, 2017VM2, 2017YC6 | D/1978 R1 |
| OER | $o$ Eridanids | 0 | 2015KK | - |
| ORS | Southern $\chi$ Orionids | 0 | (2101)Adonis, **2007UL12**, 2013CT36 | 2010LU108, 2002XM35 |
| PPU | $\pi$ Puppids | 2011TA4 | 1997UZ10, (417634)2006XG1, 2008RT, 2008XQ2, 2010UY6, 2014SM142, 2014WN202, 2015VR65, 2016TJ18, 2017UW7, 2017XC2 | 26P/Grigg-Skjellerup |
| SCC | Southern $\delta$ Cancrids | 2017YO4 | (480822)1998YM4, 2010XC11 | 2001YB5 |
| SMA | Southern Daytime May Arietids | 2001QJ96 | **2012KA4**, **2015PM307**, 2016LW9, 2017QN18 | - |
| SSG | Southern $\mu$ Sagittariids | 2011BM45, 2012BJ14, **2016CM246** | 1998LE, 1999LW1, 2002AU5, 2007YP56, 2010CR5, 2011BW10, 2011BY18, 2011CT4, 2012BU61, 2013AB65, 2015BA513, 2015BL311, 2015MN11, 2016CA136, 2016NG22, 2018BT6 | - |

**Table 4.1:** continued.

| Cod | Name | High Probability | Medium Probability | Parent Body |
|---|---|---|---|---|
| STA | Southern Taurids | **2007UL12**, 2012ES10, **2016CM246** | **(503941)2003UV11**, 2005TB15, 2007RU17, **2010TU149**, **2011TC4**, 2013GL8, **2015TX24**, 2017UM44 | 2P/Encke |
| TAH | $\tau$ Herculids | 0 | (3671)Dionysus, (455299)2002EL6, 2003LW1, 2004HC39, 2005JJ91, 2006HQ30, 2009FU4, 2010GH65, (436671)2011SV71, 2013JT17, 2014OY1, 2016HN3 | 73P/Schwassmann-Wachmann 3 |
| XSA | Daytime $\xi$ Sagittariids | 0 | (325102)2008EY5, 2015FQ117 | - |
| ZPE | Daytime $\zeta$ Perseids | (162195)1999RK45 | 2007TC14 | 2P/Encke |
| AVB | $\alpha$ Virginids | 2002FU5, 2017FU64 | 1997GD32, 1998SH2, (446791)1998SJ70, 2001TA2, 2002GM5, 2004SA20, 2004VY14, 2005RW3, 2005TE, 2006JO, 2007GU1, 2009HS44, 2009SB15, 2010FL, 2010GE35, 2011EF17, 2011GP65, 2011HP4, 2011TJ, 2012FQ62, 2012JU, 2012LJ, 2012TT5, 2014HD198, 2014HK197, **2014HN199**, 2014HT178, **2014HT197**, **2014HU2**, 2014MC6, 2014XD32, 2015FQ, 2015GJ13, 2016JD18, 2016JS5, **2016RO40**, 2016SF, 2017JA, 2017SP12 | 1998SH2 |

**Table 4.1:** continued.

| Cod | Name | High Probability Medium Probability | Parent Body |
|---|---|---|---|
| COR | Corvids | 1996MQ, (162058)1997AE12, 1999RK33, 2002PX39, 2003RE2, 2004LA10, 2004MC, 2004NU7, 2004RW10, 2005MR1, 2005OF3, 2007LW19, 2008LB, 2009QG2, 2009SX17, 2011QE38, 2012KX41, 2012KZ41, 2012LT, 2013PW31, 2013RN21, 2013RU9, 2014HE197, **2014HT197**, **2014JH15**, 2014KH39, 2014OM207, 2016LE10, 2016LZ8, 2016MS, 2016PD40, 2016PE8, 2016QY1, 2017KQ27, 2017MA3, 2017QB17, 2017SA, 2017SG33 | (374038)2004HW |
| HVI | h Virginids | 2001SZ269, 2007RS146, 2009SD15, 2010RL43, 2010RZ11, 2010TD, 2010TP55, 2012KZ41, **2014HN199**, **2014HU2**, **2014JH15**, **2016RO40** | - |

## 4.1 Dynamical view

From my sample, as expected, all associated asteroids belong to NEAs population (see Fig. 4.3a). This result is proof that my program is working correctly. Also, 82% of associated asteroids have Apollo type orbits (thus passing Earth orbit) and 7% are classified as potential hazardous asteroids (PHA) (see Fig. 4.3b).

It may be taken into account the Tisserand parameter with respect to Jupiter $T_J$. If the $T_J$ is bigger than 3, then it has an asteroidal orbit, if the object has a $T_J$ between 2 and 3, then the object has commentary like orbit and if the object has a $T_J$ smaller than 2, then that object belongs to the minor planet group of damocloids. From my sample I found that 15.3% of the asteroids are on commentary orbits, 84.3% are on asteroidal orbits and 0.4% belongs to damocloids.

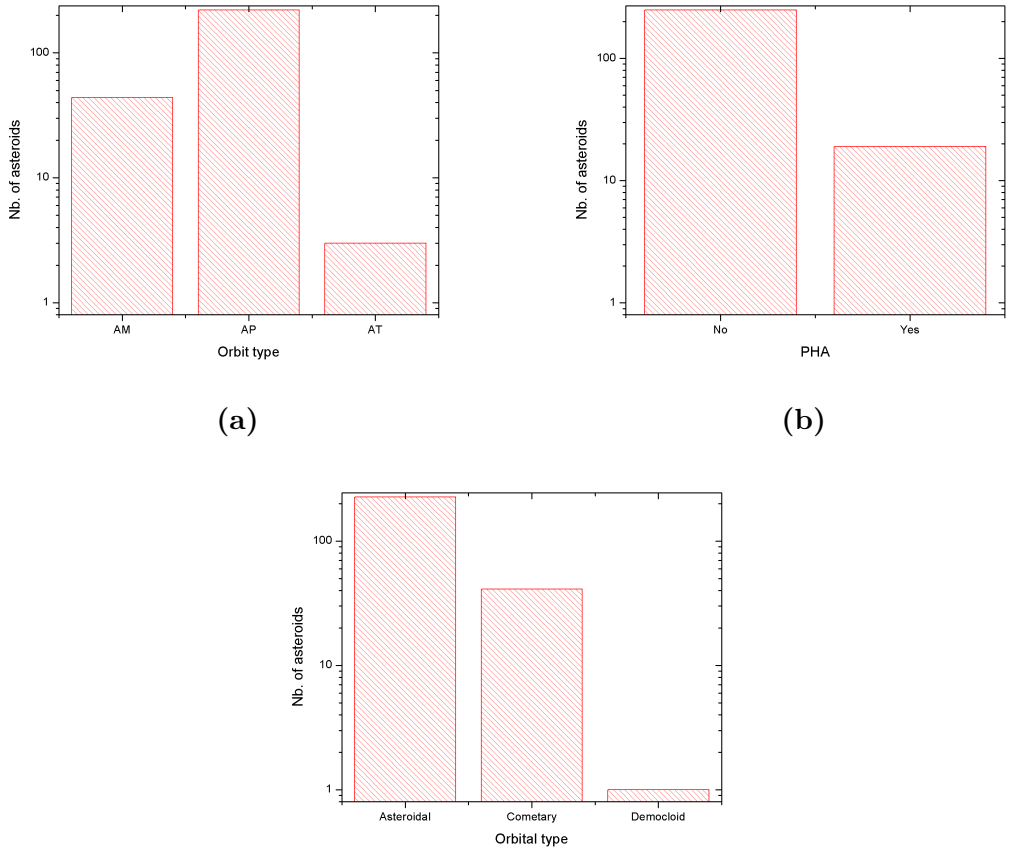


**Figure 4.3:** Dynamical view. 4.3a: All associated asteroids orbital type. 4.3b: The asteroids categorized as potentially hazardous object. 4.3c: The orbital type according to Tisserand parameter.

I compared my associated asteroids results for every meteor shower with known associated parent bodies from IAU Meteor Data Center(the Parent Body column in Table. 4.1). Knowing the parent bodies of the meteor showers I concluded:

1. (3200)Phaethon is associated with Geminids (GEM) meteor shower (Whipple

1983). In the simulation I obtained the same result with high probability.

2. (155140)2005UD is associated with Daytime Sextantids (DSX) meteor shower (Ohtsuka et al. 2005). In my case this asteroid was associated to the same meteor shower with medium probability.

3. (85182)1991AQ (?) is associated with Northern $\delta$ Cancrids (NCC)in the IAU Meteor Data Center. I obtained the same result with high probability.

4. 1998SH2 (?) is associated with $\alpha$ Virginids (AVB) shower in the IAU Meteor Data Center. This asteroid was classified with medium probability into my analysis for the same meteor shower.

5. 2001YB5 (?) is associated with Southern $\delta$ Cancrids (SCC) (Meng et al. 2004). I obtained low probability (the metric $D_{SH}$).

6. (374038)2004HW was associated with Corvids (COR) meteor shower in the IAU Meteor Data Center. My clustering analysis confirms this association has medium probability.

7. 2005NZ6 (?) is associated with Daytime April Piscids (APS) in the IAU Meteor Data Center. This association has low probability (the metric of $D_{SH}$).

8. 2010LU108 is associated with Southern $\chi$ Orionids (ORS) meteor shower in the IAU Meteor Data Center. This association has low probability (the metric of $D_{SH}$).

9. 2004TG10 is associated with Daytime $\beta$ Taurids (BTA) and Northern Taurids (Jenniskens 2006). In my analysis the asteroid 2004TG10 was associated at medium probability with Daytime $\beta$ Taurids (BTA) and with high probability to Northern Taurids (NTA).

10. 2010TU149 was first associated by Rudawska et al. (2012b) to Taurid complex. In my analysis the asteroid 2010TU149 was associated at high probability to Northern Taurids and at medium probability to Southern Taurids and Daytime $\beta$ Taurids.

### 4.1.1 Results of other similar studies

Rudawska et al. (2012a) found five major meteoroid streams associated to eight asteroids. Asteroid 2005UW6 was associated with Taurid Complex. In this study I found that this object is more akin to the Northern Taurids by only one metric. I obtained negative results for the association of 1997US2 and 2001XX103 claimed by Rudawska et al. (2012a).

Micheli (2013) associated asteroid 2007RU17 to Taurid Complex and observed the object by detecting its coma. The observations gave negative results. However he pointed out that the asteroid is part of Taurid Complex. In this study, this asteroid was associated with medium probability to Southern Taurids.

Another clustering study performed by Šegon et al. (2014) associated 43 asteroids with inclination over 15° with meteor showers using D–criteria metrics. In my calculations, I found only two common asteroids, namely (3200)Phaethon and 2009ST103. Another nine associations were found in my database but they are classified with low probability.

Żołądek et al. (2016) studied the enhanced activity of the Southern Taurids detected on 31 October 2015 using D–criteria metrics and found three asteroids associated with fireballs, namely 2015TX24, 2005UR, and 2015TF50. In this study, the asteroid 2015TX24 was associated with medium probability to both Southern Taurids and Daytime $\beta$ Taurids while 2005UR was identified as potential parent body by only one metric. Asteroid 2015TF50 was not found between my candidates.

## 4.2 Physical view

A systematic search for physical parameters of objects in Table 4.1 was performed using the databases specified in Section 2.2. From my sample of NEAs, 13 asteroids have spectra in the visible and near–infrared, 15 asteroids have an associated taxonomic class, and 28 asteroids have an albedo (Figs. 4.4 and 4.5).

As specified in Section 1.2 the asteroid surfaces have specific reflective properties and with the help of visible and near–IR spectra it can be identified the chemical and mineralogical properties of asteroid surfaces. Form my samples, only 5.6% have spectral data and for a global image of compositional properties which could be derived from reflectance spectra, more spectral data is needed.

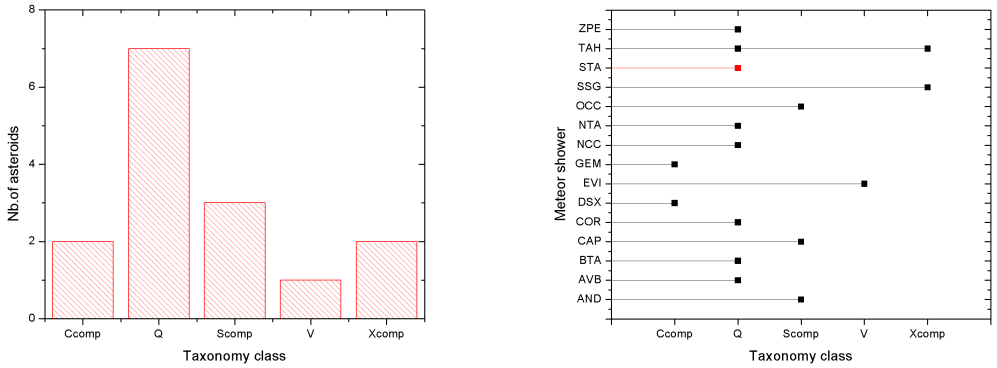


**(a)** **(b)**

**Figure 4.4:** The taxonomic classes of my sample. 4.4a: The number for asteroids with a taxonomic class. 4.4b: The taxonomic class associated to each meteor shower. In graphs, the black squares represent one object and the red squares represent two objects.

In Fig. 4.4a are plotted, the associated asteroids with taxonomic classes. This plot shows that my sample is largely dominated by objects of the S–group (Q-type and Scomp). The Q–types (DeMeo et al. 2009b) presence is associated with

a resurfacing of S–type asteroids during their close approach of the Earth (Binzel et al. 2010).

By comparing my results with the statistic of all NEAs one observes a discrepancy between Q and S–types. In the statistic of all NEAs the most predominant taxonomic classes are S–type, followed by Q–type, while in my sample the situation is opposite. However, if one takes into account that the Q–type are fresh surface S-type asteroids, my result is not surprising.

Also, comparing with other classes, it is known that the objects that experience partial or total melting, such as S-type, V-type, Q-type etc., are more predominant in the inner Solar System, while the primitive ones, such as C-type, are more common in the other Solar System (Gradie & Tedesco 1982). Taking into account these consideration, it is normal that my sample is predominant by the S-group, considering that all associations belong to NEAs.

In Fig. 4.4b is presented the taxonomic classes of associated asteroids found with taxonomic class vs. meteor showers. If the parent body of a meteor shower belongs to a certain taxonomic type, the meteoroid stream needs to have the same taxonomic class. Therefore I can speculate that two meteoroid streams have C–type taxonomic class, seven have Q–type, three S–type, one V–type, one X–type and TAH with Q or/and X–type.

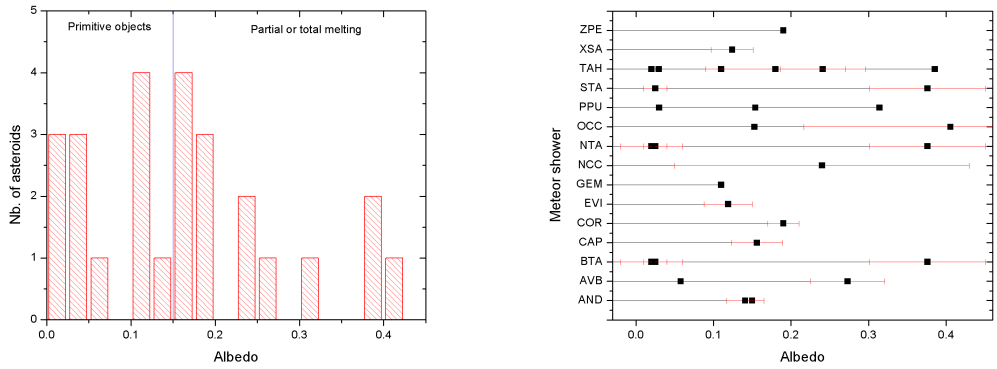


**(a)** **(b)**

**Figure 4.5:** The albedo found from my sample. 4.5a: The number of asteroids with albedo. 4.5b: The correspondence between the albedo and the meteor shower. For 12 objects, I lack the error bar.

In Fig. 4.5a are presented the asteroids with known albedo. As specified in Section 1.2 one can use the albedo to assume the surface composition of asteroids (primitive objects such as C, D, B or G have albedo smaller the 0.15 and objects which experienced partial or total melting such as V, O, A, or X have a larger albedo then 0.15).

Only 10% of asteroids from my sample have albedo recorded in the EARN database. In the asteroids sample we can find an approximate balance between high and low albedo, considering the value $\rho_v = 0.15$ (12 objects exhibits albedos lower

than this value, while 14 objects have values of albedo larger than 0.15).

In Fig. 4.5b one can observe the associated asteroids albedo values found in literature attributed to each meteoroid stream.

### 4.2.1 Rotation period contribution

Pravec et al. (2006) studied the relationship between asteroid dimensions and their rotational periods. They found a limit of this rotational period and they called this parameter spin barrier. The spin barrier was estimated at about 2.2 h. This spin barrier helps us to distinguish between rubble–piles and monolithic NEAs. In the assumption of a rubble–pile structure, if an asteroid is larger than 200 m, it must have a rotational period value larger than the spin barrier one.

For fast–rotating asteroids (Polishook et al. 2016), to overcome their own centrifugal force, a monolithic structure is required. In the case of a fast–rotator, the probability of producing fragments or meteoroids is fairly low.

Asteroids with rubble—pile structures, over 200 m, need to have a small rotation rate because their structure is maintained by their own (low!) self–gravity, or the cohesive forces of bonded aggregates (Richardson et al. 2009).

In the context of these findings, it seems realistic to investigate in detail the asteroids of my sample which could have a rubble–pile structure. Binary asteroids as well as slow–rotators seem to be more appropriate as objects that can be easily desegregates, thus producing meteoroids.

I found 17 asteroids from my sample with rotational periods. The histogram of associated asteroids with known rotational periods is presented in Fig. 4.6.

In my data I found two fast–rotating asteroid. First is 2007LW19 that has a rotational period of 0.10169 ± 0.00014 h (Kwiatkowski et al. 2010a) and diameter[1] between 60–134 m. The second is 2007RS146 that has a rotational period of 0.03209 ± 0.00004 h (Kwiatkowski et al. 2010a) and diameter (computed the same as 2007LW19 diameter) between 65 and 147 m.

Most likely these asteroids have monolithic structures, therefore I can only speculate on their ability of producing meteoroids. Their orbits are classified as unstable (see Fig. 4.7a and 4.7b). Both the associations with Corvids(COR) and h Virginids(HVI) might be also under debate.

[1]diameter range derived from magnitude and assumed albedo for C and S–type - 0.04 and 0.20 respectively

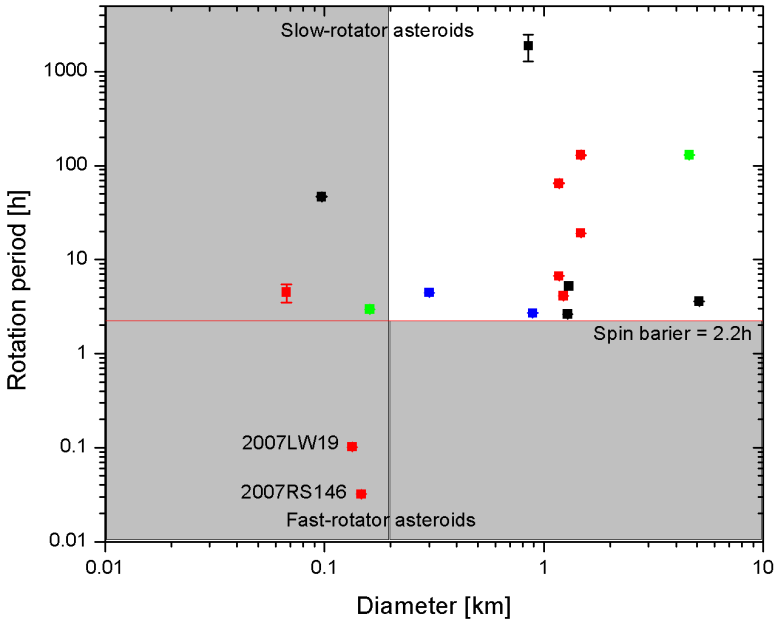


**Figure 4.6:** Rotational periods of associated asteroids from my sample found in the literature. The value of 2.2 h represents the spin barrier for an asteroid larger than 200 m Pravec et al. (2006). In this graph, the white rectangle presents my objects of interest, the blue dots are the binary asteroids, the green dots are the tumbling asteroids and the red dots are the asteroids with derived diameter from H and from the assumed albedo. In the case of the asteroids with derived diameter, it was taken the largest dimension, whereas for the binary asteroids was taken the primary rotation.

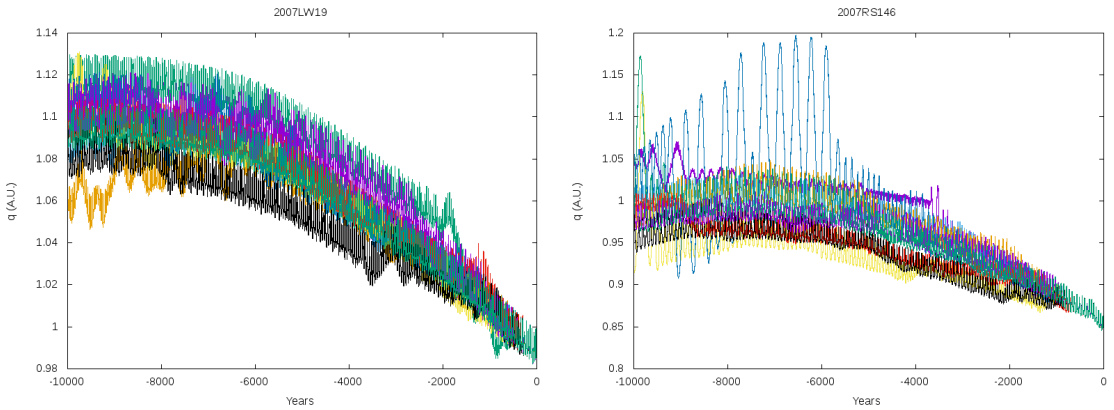


**(a)** $T_L = 56$ years **(b)** $T_L = 49$ years.

**Figure 4.7:** Perihelion evolution of asteroids 2007LW19 (4.7a) and 2007RS146 (4.7b).

### 4.2.2 Meteor showers and my associations

I will make a short description of meteor showers and the related asteroids based on physical data.

Meteor showers are characterized using geocentric the entry speed ($V_g$) taken from Jenniskens et al. (2016a), the zenithal hourly rate (ZHR) and the maximum activity date from the International Meteor Organization (IMO) website[2].

The asteroids spectral data were reviewed using the M4AST tool. If the visible part was available the spectra were normalized to 0.55 $\mu$m. Only for the NIR part, the normalization is performed at 1.25 $\mu$m (if not specified). In few cases we normalized to 1 $\mu$m to show the band similarities. All the results are shown in Table C.1.

**Andromedids (AND).** This meteor shower has a $V_g = 18.2$ km/s. In my search I found three asteroids with physical data associated with this meteor shower. (267729)2003FC5 taxonomic class was determined as S–type (Thomas et al. 2014). Using the bridge between M4AST routines and SMASS–MIT UH–IRTF (MINUS database[3]) I found one spectrum for this asteroid. Only a part of the spectrum of (267729)2003FC5 is reliable (from 0.8 to 1.5 $\mu$m). The feature around 1 $\mu$m is matched by the K–type (Fig. 4.8a).

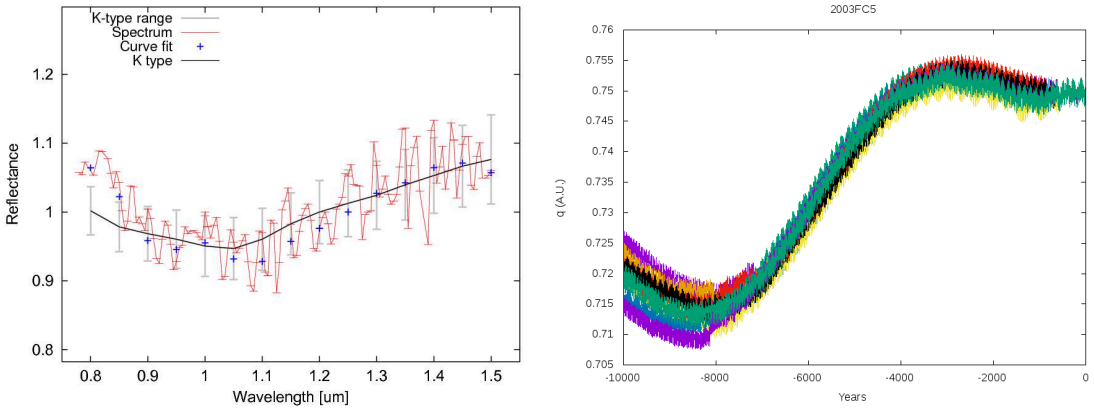


**(a)** $a267729.sp98$ **(b)** $T_L = 119$ years

**Figure 4.8:** Spectra classification with Bus–DeMeo taxonomy using M4AST (4.8a) and the perihelion evolution (4.8b) of asteroid (267729)2003FC5.

2009ST103 has a known albedo 0.141 *pm* 0.024 (Mainzer et al. 2016). For 2000UG11 an assumed albedo 0.15 is associated (Binzel et al. 2002).

From radar observations (Margot et al. 2002) concludes that 2000UG11 is a binary object. More generally, the formation of binary objects (the increase in spin rate due to YORP effect, followed by mass–loss and ended with a satellite in a close orbit) require a rubble–pile or gravitational aggregate structure (Scheeres

[2] http://www.imo.net/files/meteor-shower/cal2018.pdf
[3] http:smass.mit.edu/minus.html

2007; Walsh et al. 2012). 2000UG11 is a good candidate as parent body for this shower.

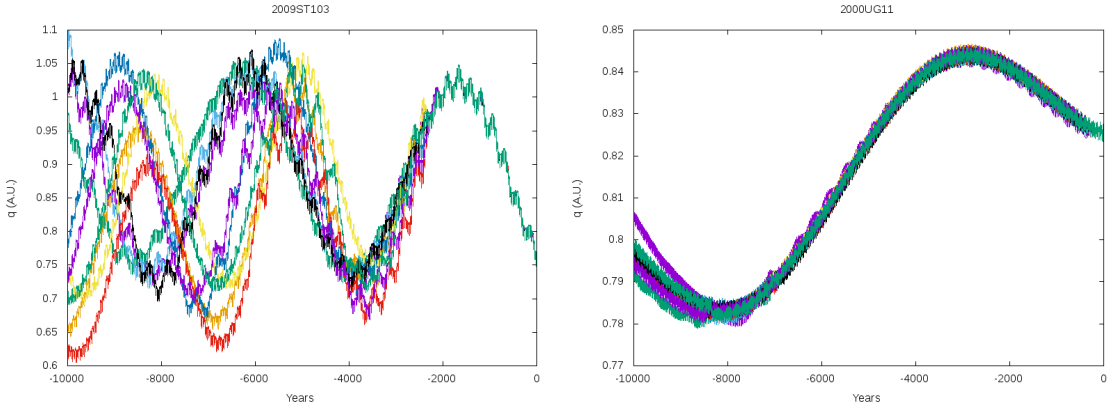


**(a)** $T_L = 389$ years **(b)** $T_L = 85$ years.

**Figure 4.9:** Perihelion evolution of asteroids 2009ST103 (4.9a) and 2000UG11 (4.9b).

From orbital evolution one can see that asteroids 2003FC5 and 2009ST103 have stable orbits ($T_L = 119$ respectively 389, see Fig. 4.9a and 4.8b), while 2000UG11 has unstable orbit ($T_L = 85$ years, see Fig. 4.9b).

$\alpha$ **Capricornids (CAP).** This meteor shower has a $V_g = 23$ km/s and a ZHR = 5 for the maximum of 30th of July. I found three asteroids with physical data, namely 2001EC which is a Sq–type taxonomic class (Binzel et al. 2004), 2002NW which has an albedo of $0.156 \pm 0.033$ (Mainzer et al. 2016) and 2017MB1 which has a rotation period of $6.69 \pm 0.01$ (Warner 2018).

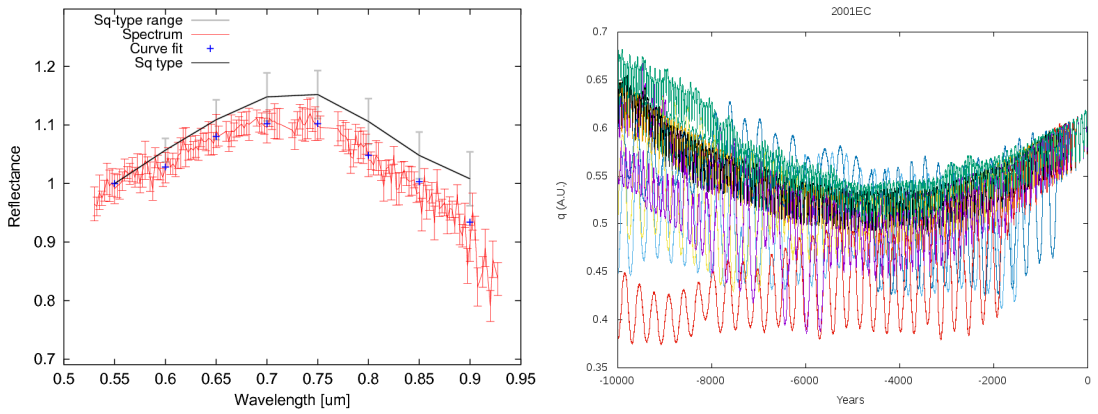


**(a)** $au2001EC.8$ **(b)** $T_L = 34$ years

**Figure 4.10:** Spectra classification with Bus–DeMeo taxonomy using M4AST (4.10a) and the perihelion evolution (4.10b) of asteroid 2001EC.

Using the bridge between M4AST routines and SMASS–MIT UH–IRTF I found one spectrum for the asteroid. Only a part of the spectrum of 2001EC is reliable (from 0.55 to 0.9 $\mu$m). I found the same taxonomic class (spectrum published in Binzel et al. (2004)) as specified in literature (Fig. 4.10a).

From investigation backward in time all asteroids were found with unstable orbit: 2001EC with $T_L = 34$ years (Fig. 4.10b) and 2002NW with $T_L = 41$ years (Fig. 4.11a).

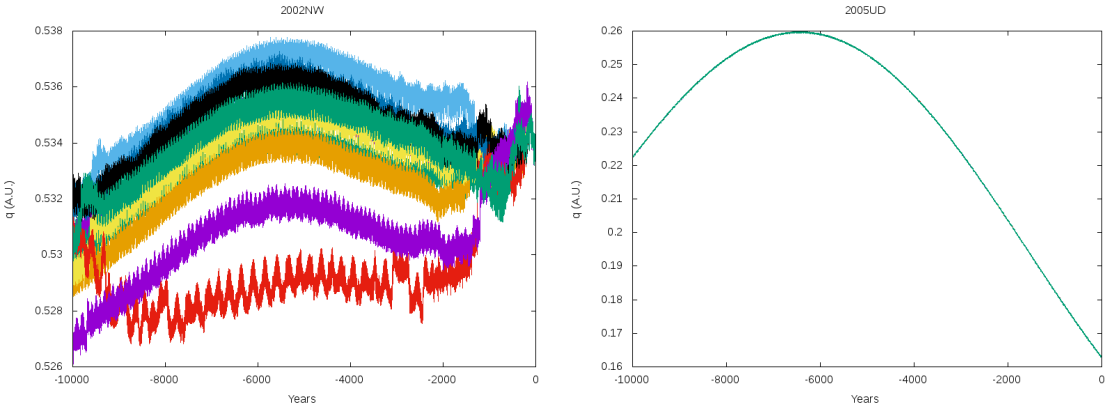


**(a)** $T_L = 41$ years **(b)** $T_L = 478$ years.

**Figure 4.11:** Perihelion ($q$) evolution of asteroids 2002NW (4.11a) and 2005UD (4.11b).

**Daytime Sextantids (DSX).** This shower has $V_g = 32.9$ km/s and a ZHR = 5 for the maximum of 27th of September. I found only one asteroid with physical data, namely 2005UD.

I associated this asteroid with medium probability to DSX. The $V_g = 32.9$ km/s is quite similar to the one of DSX (Jenniskens et al. 2016a). Ohtsuka et al. (2005) classified this object as a C–type asteroid.

Several authors concluded that 2005UD could be a fragment from the asteroid (3200)Phaethon (Ohtsuka et al. 2006; Jewitt & Hsieh 2006; Kinoshita et al. 2007; Jones et al. 2016).

The numerical simulations for 2005UD show that this asteroid has stable orbit ($T_L = 478$ years, see Fig. 4.11b).

**$\eta$ Virginids (EVI).** This meteor shower has a $V_g = 26.6$ km/s. In my search I found two asteroids with physical data.

2000DO1 was classified as V–type based on spectral data obtained from visible and near–infrared observations up to 1.6 $\mu$m (Binzel et al. 2004). For the asteroid 2010CF55 only an albedo of $0.119 \pm 0.031$ was found (Mainzer et al. 2014).

The available spectrum of 2000DO1 covers the wavelengths between 0.5 and 1.6. The curve matching methods from M4AST indicates a Q–type (mean squared error 0.0077). However, the band at 1 $\mu$m is not matched by this type. This band is typically for a V–type (Fig. 4.12a) Thus, I conclude a V–type classification, although the mean square error is higher (0.016) and its orbital evolution shows unstable orbit(Fig. 4.12b).

The orbital evolution of 2010CF55 shows also an unstable orbit ($T_L = 65$

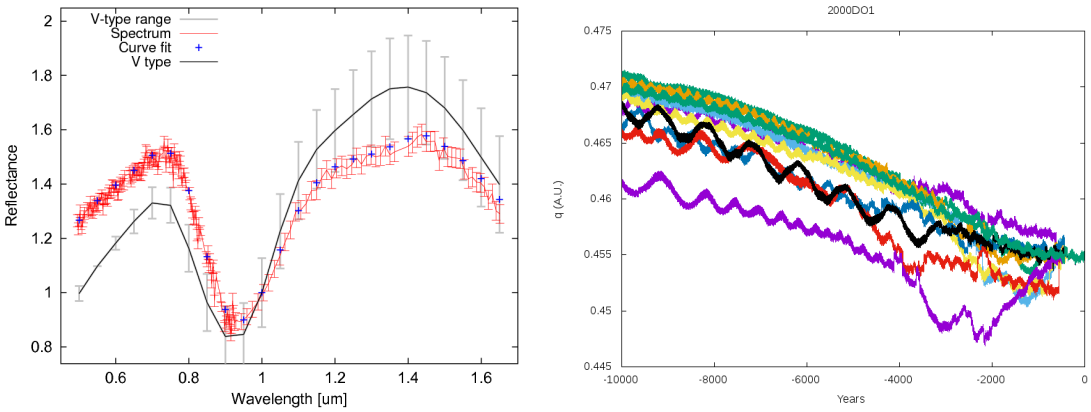


**(a)** $(au2000DO1visir8.visir)$ (1 $\mu$m) **(b)** $T_L = 38$ years

**Figure 4.12:** Spectra classification with Bus–DeMeo taxonomy using M4AST (4.12a) and the perihelion evolution (4.12b) of asteroids 2000DO1.

years, see Figs. 4.13).

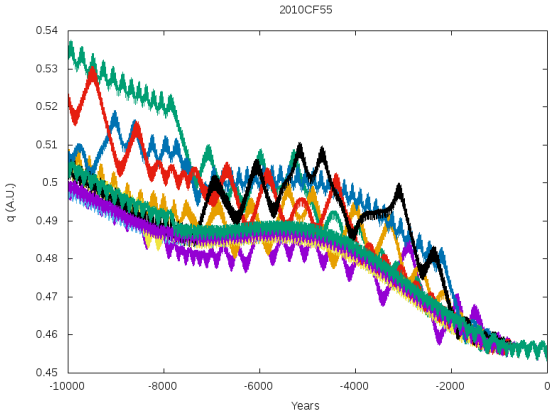


**Figure 4.13:** Perihelion evolution of asteroid 2010CF55, $T_L = 65$ years

**Geminids (GEM).** This meteor shower has a $V_g = 33.8$ km/s and a ZHR of 120–130 (Rendtel 2004) for the maximum of 14th of December. Its parent body (3200)Phaethon has a $V_g = 33.9$ km/s, quite similar to this meteor shower (Jenniskens et al. 2016a). Phaeton was taxonomically classified as a B–type or F–type (Licandro et al. 2007; Fornasier et al. 2006; Binzel et al. 2004).

This asteroid was intensively studied. Even if the parent body of Geminids stream is an asteroid, its structure model agrees with the commentary scenario of its origin, which leads to the conclusion that (3200)Phaethon could be an extinct comet (Ryabova 2007). In 2009 and 2012 it exhibits anomalous brightening around its perihelion, which has been interpreted as the ejection of dust particles (Li & Jewitt 2013; Jewitt & Li 2010). Ryabova (2012) modeled this dust ejection and the evolution of the meteoroid swarm and conclude that the approach of the swarm to the Earth will be in 2014, 2017, 2018 and 2020. Statistics made between 2009 and 2015 do not confirm an increase in Geminids activity (Miskotte 2016). An important discovery about this asteroid was a tail detection (Jewitt et al. 2013). Other studies show that (3200)Phaethon has similar orbit with asteroid 2005UD (Ohtsuka et al.

2006; Jewitt & Hsieh 2006; Kinoshita et al. 2007; Jones et al. 2016), which suggests that (3200)Phaethon and 2005UD might have common origin. This asteroid has a stable orbit ($T_L$ = 226 years, see Fig. 2.5a).

**$\delta$ Cancrid Complex.** This complex contains Northern $\delta$ Cancrids (NCC) and Southern $\delta$ Cancrids (SCC). The NCC meteor shower has an estimated value of geocentric entry speed of $V_g$ = 27.2 km/s. I found two asteroids associated. (85182)1991AQ is associated with high probability (i.e. all three metrics found this object under the threshold) to NCC. Based on ECAS filters (Zellner et al. 1985) this asteroid was classified as Q–type by Wisniewski et al. (1997). NEOWISE estimation of its albedo is 0.242 ± 0.194 (Mainzer et al. 2016). And the asteroid 2013YL2 that is associated with medium probability to NCC. And asteroid 2013YL2 that has a rotation period of 2.97 ± 0.01 h (Warner 2014a)

Both asteroids were found with unstable orbit, (85182)1991AQ with an $T_L$ = 94 years, see Fig. 4.14a and 2013YL2 with an $T_L$ = 45 years, see Fig. 4.14b.

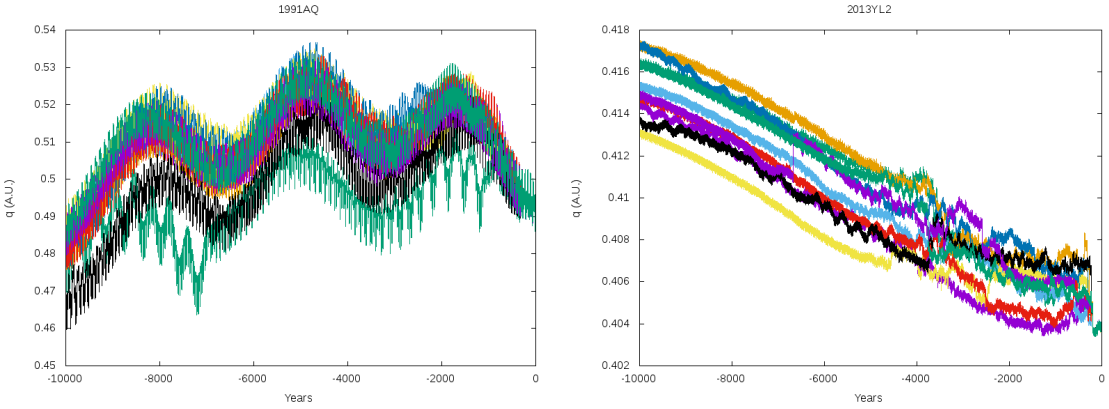


**(a)** $T_L$ = 94 years **(b)** $T_L$ = 45 years

**Figure 4.14:** Perihelion evolution of asteroids (85182)1991AQ (4.14a) and 2013YL2 (4.14b).

**October Capricornids (OCC).** This shower has a $V_g$ = 10 km/s. (4179)Toutatis and 2016PN38 are the only associated asteroids from my sample which has physical data.

The asteroid 2016PN38 has an albedo 0.1528 of (Masiero et al. 2018). (4179)Toutatis was classified as S, Sk, or Sq (Davies et al. 2007; Binzel et al. 2004; DeMeo et al. 2014). Its albedo was estimated around 0.13 (Lupishko et al. 1995). This asteroid was observed in detail from the ground in both optical and radar wavelength and from space by ChangE–2 spacecraft (Zheng et al. 2016). From space the boulders, grooves, and craters observed at the surface led to the conclusion that this asteroid is a rubble–pile asteroid (Zhu et al. 2014). Its irregular shape, long rotation period, and the complex rotation (not simple principal–axis rotation) imply a tumbling asteroid (Harris 1994).

(4179)Toutatis rotates with a precession period of 7.38 days and a spin of 5.38 days (Mueller et al. 2002). These values are derived from photometric observations in agreement to the ones derived from radar measurements (Ostro et al.

1999). Considering that (4179)Toutatis has a rubble–pile structure and its rotation is more complex than a simple principal–axis, this asteroid makes a good candidate for parent body.

Six unpublished spectra of (4179)Toutatis (see Fig 4.15) are found in the MINUS database. I computed the taxonomy and I found the Sq, Q, or Sr taxonomic types for these spectra.

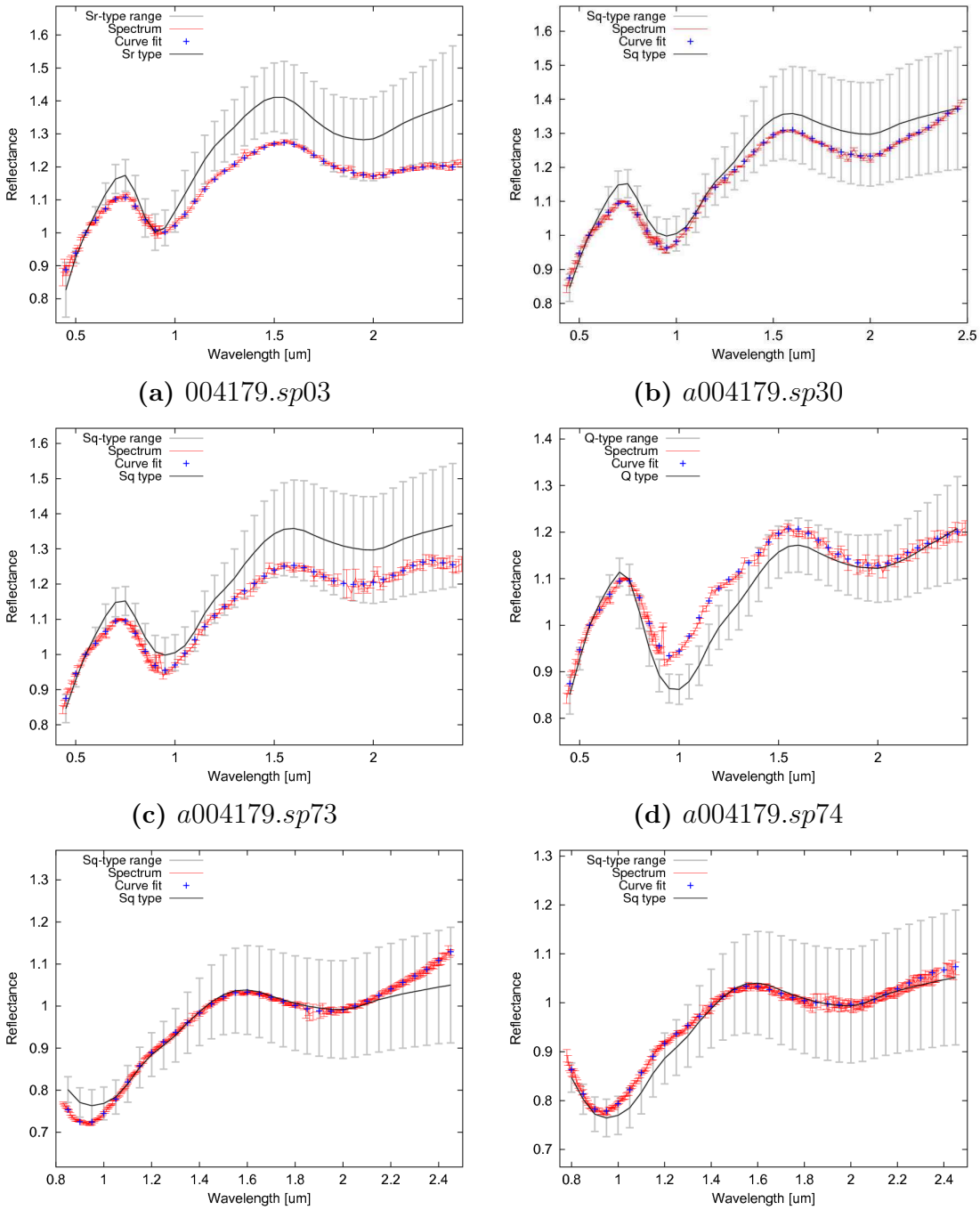


**(a)** 004179.*sp*03 **(b)** *a*004179.*sp*30

**(c)** *a*004179.*sp*73 **(d)** *a*004179.*sp*74

**(e)** *a*004179.*sp*115*n*1 **(f)** *a*004179.*sp*116

**Figure 4.15:** Spectra classification with Bus–DeMeo taxonomy using M4AST of (4179)Toutatis asteroid.

Neither the observation of ChangE–2, nor ground based observations allowed me to observe dust meteoroids or commentary activity around this object.

The orbital evolution of those objects shows unstable orbits: (4179)Toutatis with $T_L = 59$ years, Fig. 4.16a and 2016PN38 with $T_L = 54$ years, Fig. 4.16b

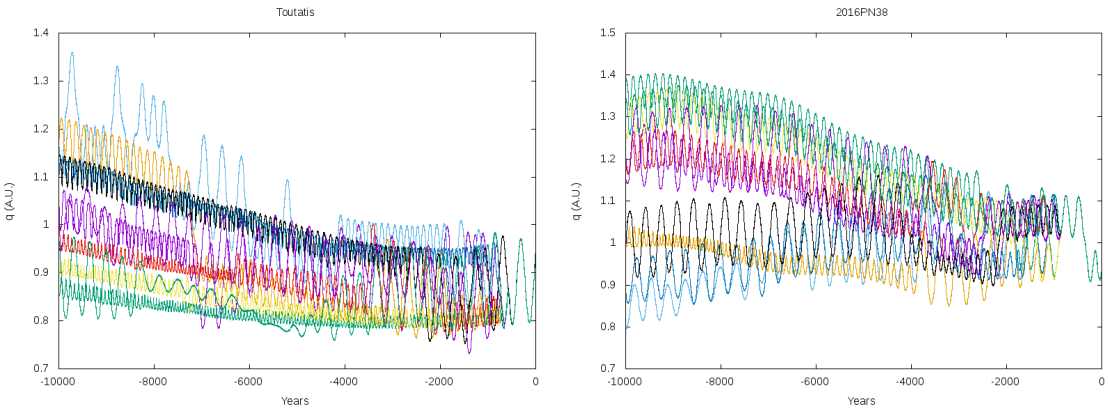


**(a)** $T_L = 59$ years **(b)** $T_L = 54$ years

**Figure 4.16:** Perihelion evolution of asteroids (4179)Toutatis (4.16a) and 2016PN38 (4.16b).

**Taurid Complex (TC).** The Taurid complex was intensively investigated (Steel et al. 1991; Babadzhanov et al. 2008c; Popescu et al. 2014; Tubiana et al. 2015). TC is a complex of several showers. The most important are Northern Taurids (NTA) and Southern Taurids (STA). NTA has a $V_g = 28$ km/s and a ZHR = 5 in 12 November, while STA has a $V_g = 26.6$ km/s and a ZHR = 5 in 10 October. Several asteroids were suggested as parent body of this complex, together with the comet P/Enke.

For this complex I found six asteroids with physical data.

The asteroid 2004TG10 is associated with two meteor showers NTA and BTA respectively (see Table 4.1). This asteroid has a $V_g = 30.1$ km/s slightly larger than the one of TC. Its albedo is around 0.02 ± 0.04 (Nugent et al. 2015). The object 2010TU149 is associated with three meteor showers (see Table 4.1)and its $V_g = 27.7$ km/s. Its albedo is around 0.025 ± 0.015 h (Mainzer et al. 2016). And 2012UR158 is associated with NTA and BTA meteor showers (see Table 4.1) and its albedo is around 0.0234 (Masiero et al. 2018). The albedo of these three NEAs is an indicator of very dark surface commonly D, C, B, F–type objects.

2003UV11 was associated with three meteor showers (see Table 4.1). Its taxonomic class was determined as Q–type (DeMeo et al. 2014) while its albedo is 0.376 ± 0.075 (Mainzer et al. 2016). The asteroid 2007RU17 was associated with medium probability to Southern Taurids (STA). A Q–type taxonomic class determined based on spectroscopic data (DeMeo et al. 2014). And, finally, 2013GL8 associated with STA meteor shower was found with a rotation period of 64.6 ± 0.5 h (Warner 2017).

I found three unpublished spectra from MINUS database, two for asteroid

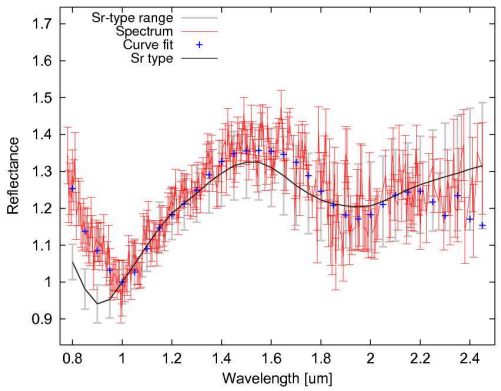


**(a)** $au2003UV11.sp94$ (1 $\mu$m)

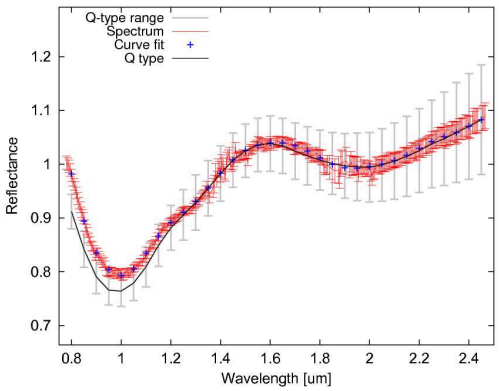


**(b)** $au2003UV11.sp95$

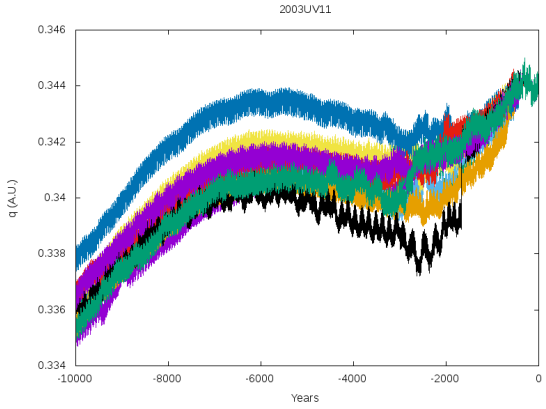


**(c)** $T_L = 86$ years

**Figure 4.17:** Spectra classification with Bus–DeMeo taxonomy using M4AST (4.17a and 4.17b) and the perihelion evolution (4.17c) of asteroids 2003UV11.

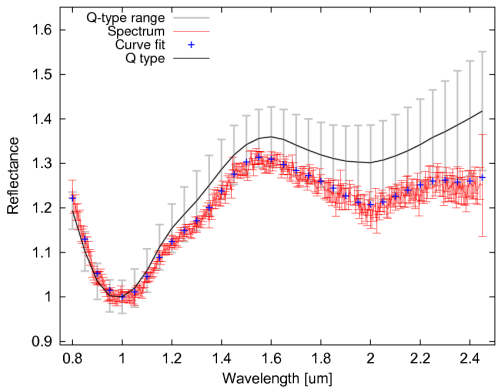


**(a)** $au2007RU17.sp94$ (1 $\mu$m)

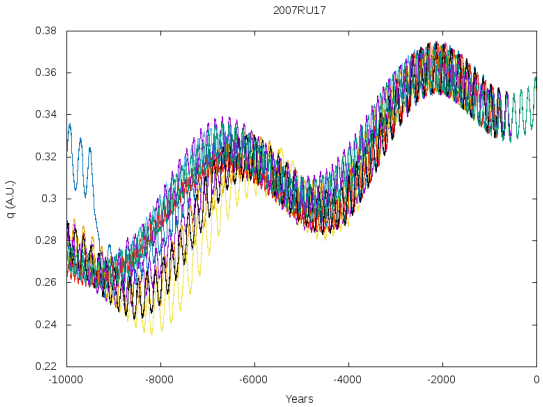


**(b)** $T_L = 50$ years

**Figure 4.18:** Spectra classification with Bus–DeMeo taxonomy using M4AST (4.18a) and the perihelion evolution (4.18b) of asteroids 2007RU17.

2003UV11 and one for 2007RU17. By using M4AST curve matching methods for $au2003UV11.sp94$ spectrum I found as relevant result the Sr–type (see Fig. 4.17a). This type fits well the 2 $\mu$m bands and the maximum at 1.5 $\mu$m. However, the band at 1 $\mu$m it is matched by the Q–type. With the same settings 2007RU17 it

is matched by the Q–type (see Fig. 4.18a). Also their orbital evolution shows that both have unstable orbits (see Figs. 4.17c and 4.18b).

As for the dynamical evolution for the rest of the asteroids, two of them were classified as unstable orbits (2004TG10 $T_L = 75$ years, Fig. 4.19a and 2010TU149 $T_L = 59$ years, Fig. 4.19b and other two have stable orbits (2012UR158 $T_L = 358$ years, Fig. 4.19c and 2013GL8 $T_L = 543$ years, Fig. 4.19d).

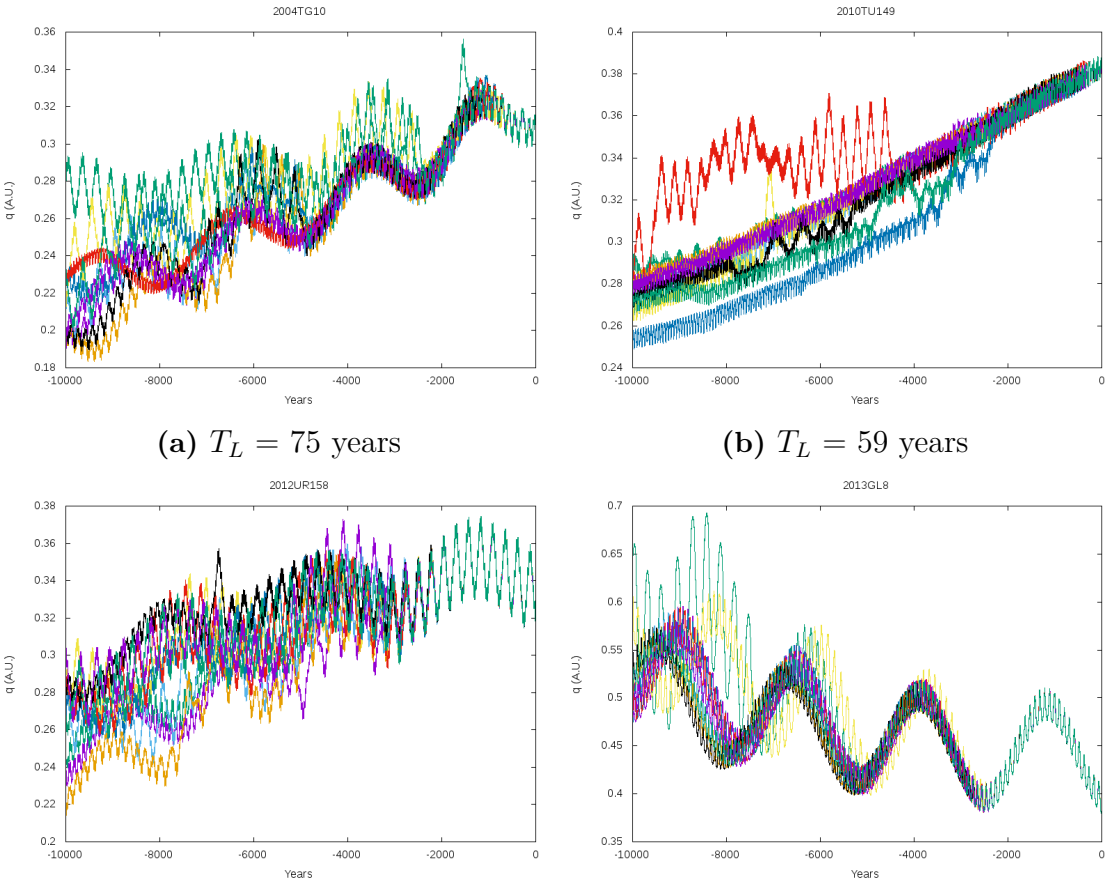


**(a)** $T_L = 75$ years **(b)** $T_L = 59$ years

**(c)** $T_L = 358$ years **(d)** $T_L = 543$ years

**Figure 4.19:** Perihelion evolution of asteroids 2004TG10 (4.19a), 2010TU149 (4.19b), 2012UR158 (4.19c) and 2013GL8 (4.19d).

$\tau$ **Herculids (TAH).** This meteor shower has a $V_g = 15$ km/s. I found seven asteroids in my sample for which there are physical parameters available.

(3671)Dionysus was associated to TAH with medium probability. It is classified as Cb or X (Bus & Binzel 2002b; Binzel et al. 2004; Thomas et al. 2014) and its albedo is 0.18 ± 0.09 (Harris & Lagerros 2002). I investigated the unpublished spectrum from the MINUS database. The spectrum of this asteroid has a poor SNR (signal to noise ratio). The feature around 1 $\mu$m seems to be a data reduction artifact. The C–complex types match this spectrum (e.g., Ch , Fig. 4.20a)

In 1997 (3671)Dionysus passed between 17 million kilometers from the Earth. This close approach was observed and the photometry showed four events (May 1997 and 2–9 June 1997) which confirmed that Dionysus is a binary object

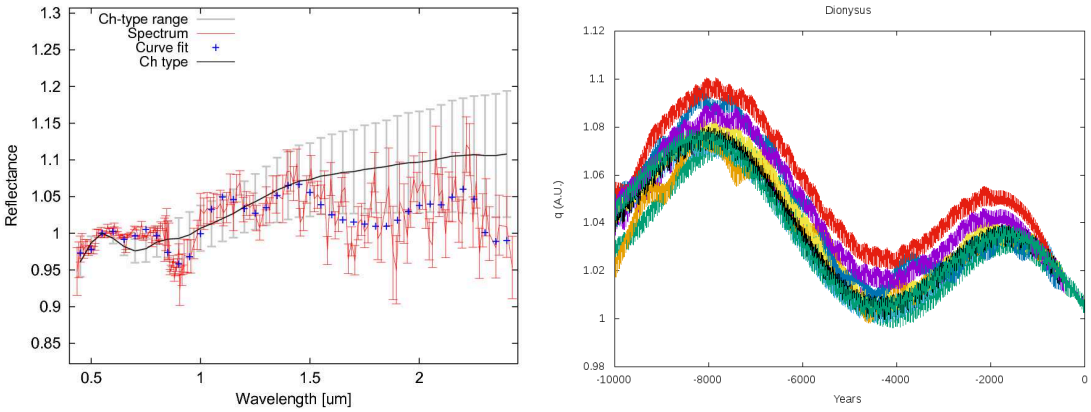


**(a)** $a003671.sp91$ **(b)** $T_L = 52$ years

**Figure 4.20:** Spectra classification with Bus–DeMeo taxonomy using M4AST (4.20a) and the perihelion evolution (4.20b) of asteroid (3671)Dionysus.

(Mottola et al. 1997). The synodical periods of primary and the system allow my to infer that this object could be a complex rubble–pile structure.

2006HQ30 is a Sq or Q object (DeMeo et al. 2014). Its taxonomic class indicates that this object is more akin to ordinary chondrites composition. For this asteroid I found one unpublished spectra in MINUS database. From M4AST curve matching methods with band at 1 $\mu$m it is matched by the Q–type (Fig. 4.21a).

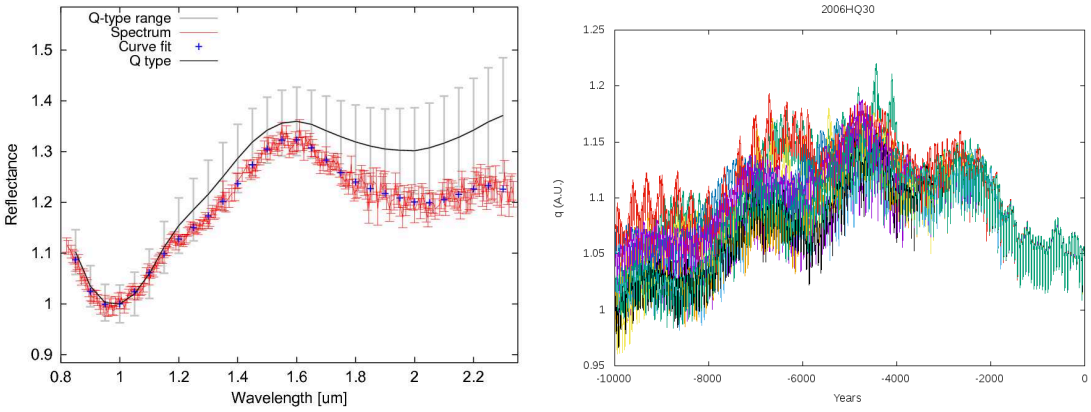


**(a)** $(au2006HQ30.sp51)$ (1 $\mu$m) **(b)** $T_L = 443$ years

**Figure 4.21:** Spectra classification with Bus–DeMeo taxonomy using M4AST (4.21a) and the perihelion evolution (4.21b) of asteroid 2006HQ30.

For the other five asteroids I found they have only an estimated albedo. Three of them have low albedo, akin to primitive objects, 2011SV71 – 0.02 ± 0.1 (Nugent et al. 2016), 2016HN3 – 0.0294 (Masiero et al. 2018) and 2014OY1 – 0.11 ± 0.09 (Nugent et al. 2015) and two have established high albedo, 2002EL6 – 0.3855 (Masiero et al. 2018) and 2010GH65 – 0.241 ± 0.055 (Mainzer et al. 2011).

From the numerical integration I conclude that (3671)Dionysus, 2002EL6, 2014OY1 and 2016HN3 have unstable orbits (see Figs. 4.20b, 4.22a, 4.22d and 4.22e), while for 2006HQ30, 2010GH65 and 2011SV71 orbits are stable (see

Figs. 4.21b, 4.22b and 4.22c).

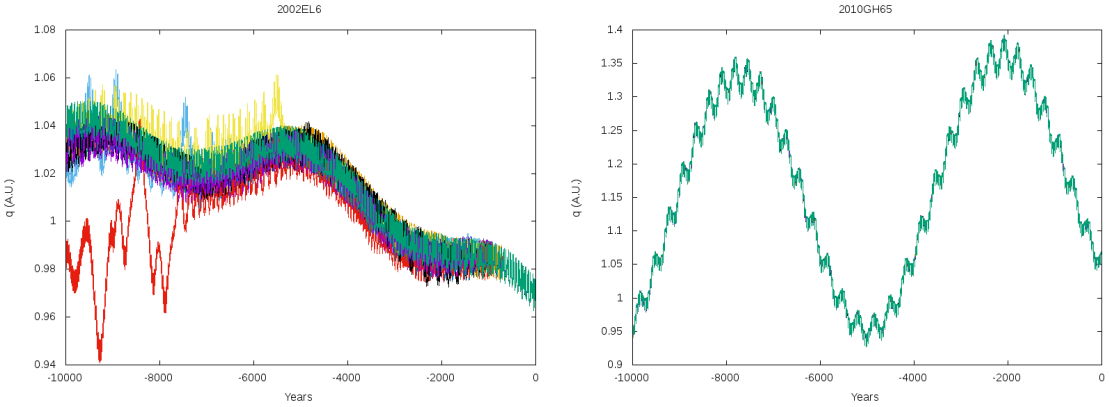


**(a)** $T_L = 60$ years




**(b)** $T_L = 2\,299$ years

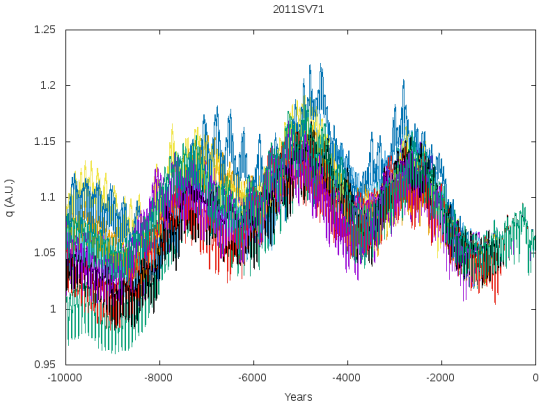


**(c)** $T_L = 120$ years

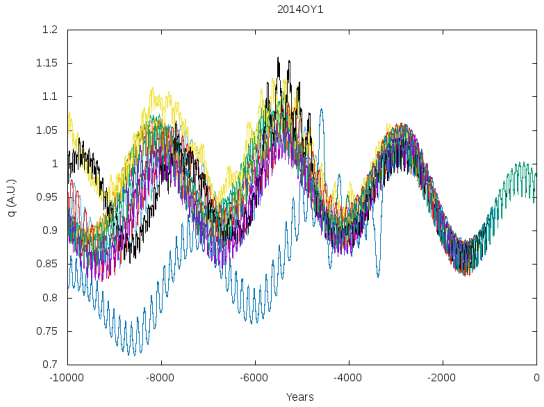


**(d)** $T_L = 72$ years

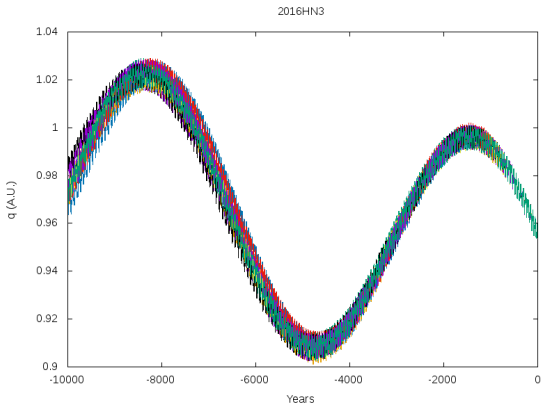


**(e)** $T_L = 86$ years

**Figure 4.22:** Perihelion evolution of asteroids 2002EL6 (4.22a), 2010GH65 (4.22b), 2011SV71 (4.22c), 2014OY1 (4.22d), and 2016HN3 (4.22e).

**Daytime $\xi$ Sagittariids (XSA).** This shower has a $V_g = 24.4$ km/s. (325102)2008EY5 is the only object of my sample with an albedo of $0.124 \pm 0.027$ (Mainzer et al. 2011). Its orbit is unstable ($T_L = 84$ years, see Fig. 4.23a).

**Daytime $\zeta$ Perseids (ZPE).** This meteor shower has a $V_g = 26.4$ km/s. The associated asteroid 1999RK45 has a Q–type taxonomic class (Tubiana et al.

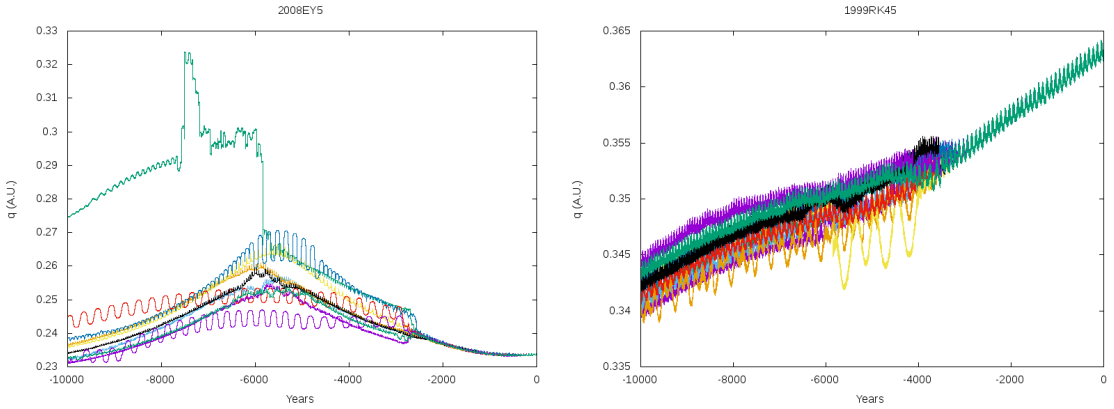


**(a)** Perihelion ($q$) evolution of asteroid 2008EY5, $T_L = 84$ years.

**(b)** Perihelion ($q$) evolution of asteroid 1999RK45, $T_L = 465$ years.

**Figure 4.23:** Perihelion ($q$) evolution of asteroids 2008EY5 (4.23a) and 1999RK45 (4.23b).

2015) and its albedo is around 0.19 (Trilling et al. 2010). From orbital evolution I obtained a stable orbit ($T_L = 465$ years, see Fig. 4.23b).

$\alpha$ **Virginids (AVB).** This meteor shower has a $V_g = 18.8$ km/s. I found four asteroids with physical data. From those asteroids, (446791)1998SJ70 is a Q–type asteroid (DeMeo et al. 2014), 2010FL and 1998SH2 with albedo 0.271 ± 0.048 (Mainzer et al. 2016) respectively 0.0578 (Masiero et al. 2018) and 2007GU1 that has a rotation period of 4.5 ± 1 h (Kwiatkowski et al. 2010b).

I found one unpublished spectrum in MINUS database for (446791)1998SJ70. By using M4AST curve matching methods I found as relevant result the S–type. However, the best matched is Q–type with band at 1 $\mu$m (see Fig. 4.24a). Also, its orbit was classified as unstable (Fig. 4.24b)

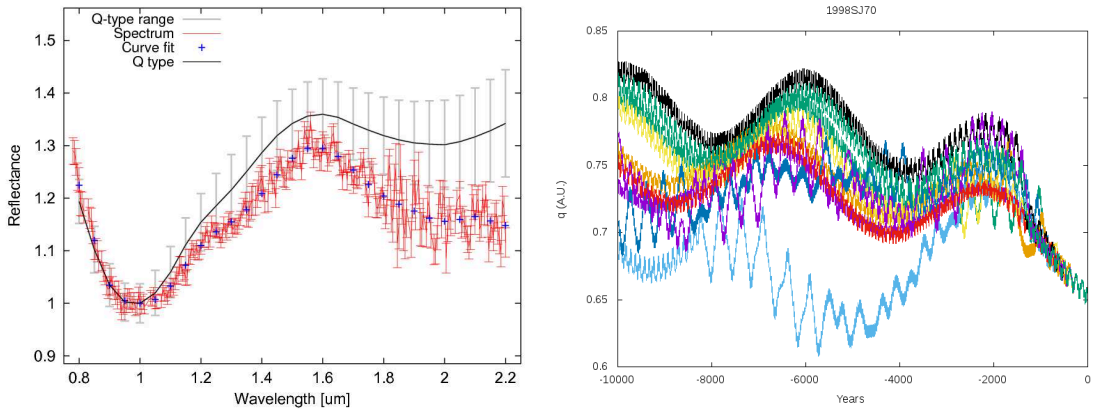


**(a)** ($au1998SJ70.sp74$) (1 $\mu$m)

**(b)** $T_L = 44$ years

**Figure 4.24:** Spectra classification with Bus–DeMeo taxonomy using M4AST (4.24a) and the perihelion evolution (4.24b) of asteroid 1998SJ70.

From the orbital evolution, I found that asteroids 1998SH2, 2007GU1, 2010FL have stable orbits (see Fig. 4.25a, 4.25b and 4.25c).

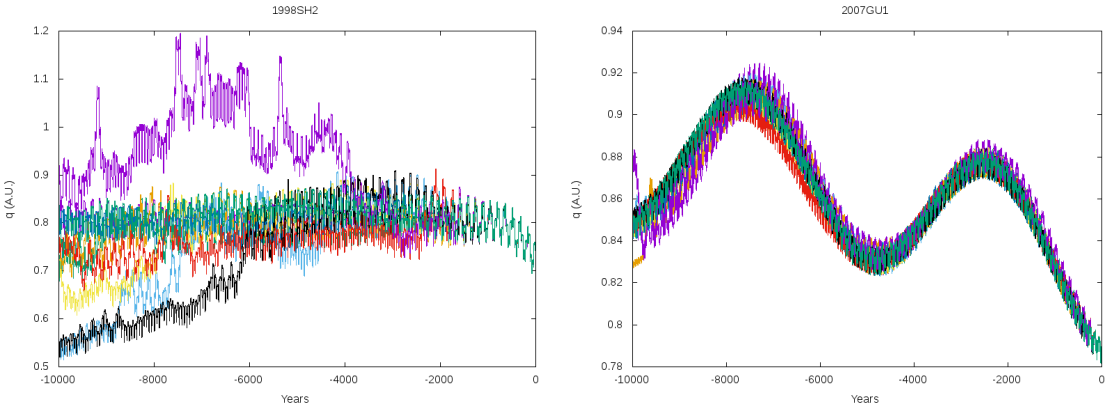


**(a)** $T_L = 172$ years **(b)** $T_L = 224$ years

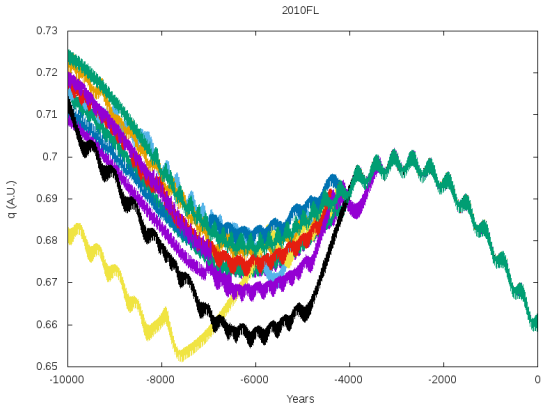


**(c)** $T_L = 324$ years

**Figure 4.25:** Perihelion evolution of asteroids 1998SH2 (4.25a), 2007GU1 (4.25b), and 2010FL (4.25c).

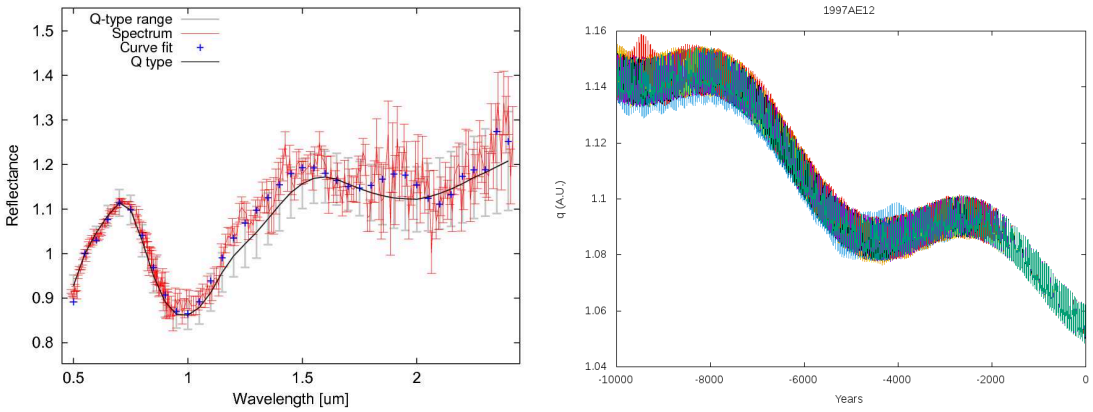


**(a)** ($au1997AE12.sp26$) (1 $\mu$m) **(b)** $T_L = 137$ years

**Figure 4.26:** Spectra classification with Bus–DeMeo taxonomy using M4AST (4.26a) and the perihelion evolution (4.26b) of asteroid 1997AE12.

**Corvids(COR).** This meteor shower has a $V_g = 8.7$ km/s. I found one asteroid with physical data, namely (162058)1997AE12. Its taxonomic class is Q–type (DeMeo et al. 2014) and its albedo is $0.19 \pm 0.02$ (Nugent et al. 2015). I found one unpublished spectrum in MINUS database for this asteroid. By using M4AST

curve matching methods I found the best fit to Q–type (see Fig. 4.26a).Also, its orbit was classified as stable ($T_L = 172$ years, see Fig. 4.26b).

**Daytime April Piscids (APS)** This meteor shower has a $V_g = 29.2$ km/s. For this meteor shower I found one asteroid with rotation period. The asteroid's name is 2005GO22 and has a rotation period of 4.103 ± 0.005 h (Warner 2016b). From the orbital evolution I concluded this asteroid has unstable orbit ($T_L = 35$ years, see Fig. 4.27)

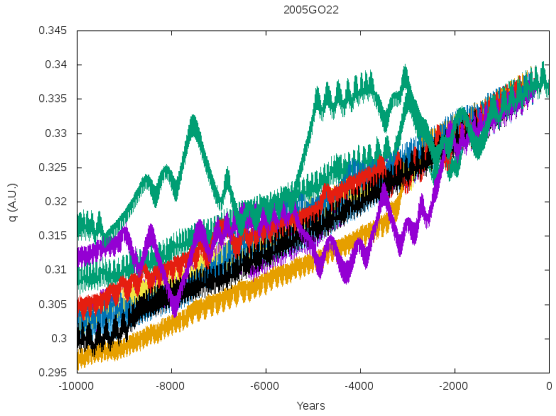


**Figure 4.27:** Perihelion ($q$) evolution of asteroid 2005GO22, $T_L = 35$ years.

$\pi$ **Puppids (PPU)** This meteor shower has a $V_g = 15$ km/s. I found three asteroids having an established albedo: 2006XG1 with an albedo of 0.403± 0.2 (Mainzer et al. 2016), 2010UY6 with an albedo of 0.03 (Mainzer et al. 2012). and 2016TJ18 with an albedo of 0.3141 (Masiero et al. 2018).

Also, the orbital evolution classified the asteroid 2006XG1 with unstable orbit (Fig. 4.28c) and the asteroids 2010UY6 and 2016TJ18 with stable orbit (Fig. 4.28a and 4.28b).

**Southern $\mu$ Sagittariids(SSG)** This meteor shower has a $V_g = 25.7$ km/s. The asteroid 2002AU5 is associated to this meteor shower and was found with X-type taxonomic class (Binzel et al. 2004). This asteroid has a stable orbit as well (Fig. 4.29b).

I found one spectrum in MINUS database for 2002AU5 (specter published in Binzel et al. (2004)). By using M4AST curve matching methods I found best matched the X–type(Fig. 4.29a).

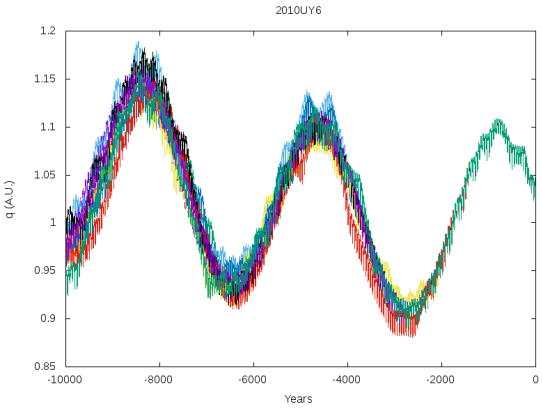


**(a)** $T_L = 219$ years

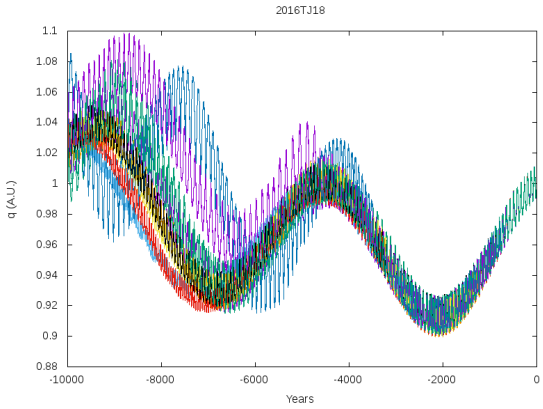


**(b)** $T_L = 100$ years

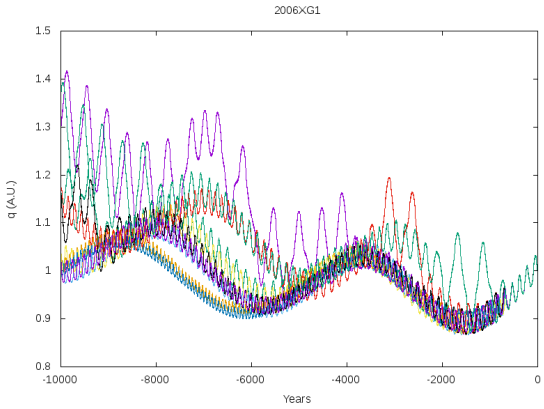


**(c)** $T_L = 64$ years

**Figure 4.28:** Perihelion evolution of asteroids 2010UY6 (4.28a), 2016TJ18 (4.28b), and 2006XG1 (4.28c).

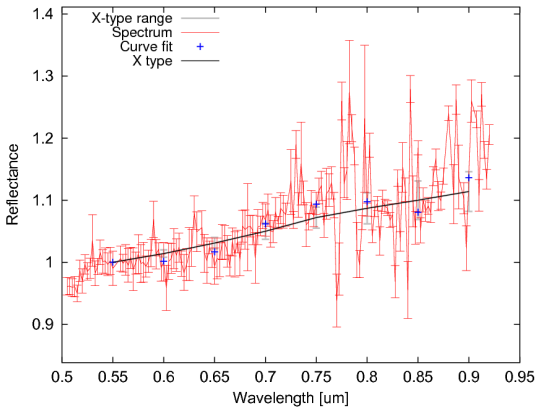


**(a)** ($au1998SJ70.sp74$) (1 $\mu$m)

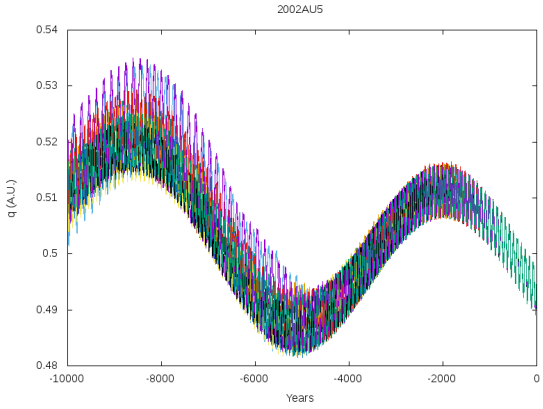


**(b)** $T_L = 137$ years

**Figure 4.29:** Spectra classification with Bus–DeMeo taxonomy using M4AST (4.29a) and the perihelion evolution (4.29b) of asteroid 2002AU5.

## 4.3 Fallen meteors - Meteor Showers - Asteroids association

Another interesting study is the association of asteroids and fall meteorites[4]. Some of the results were published in (Dumitru et al. 2017).

Popescu et al. (2014) studied the spectral properties of asteroids associated with TC. They found that five of their objects ((2201)Oljato,(4183)Cuno, (4486)Mithra, (5143)Heracles, and (6063)Jason) are S–type, with a spectrum similar with ordinary chondrites of petrologic type 6 (evolved surface). The spectrum of Farmington meteorite associated with TC, is similar with same of these asteroids spectra. Only (269690)1996RG3 is a C–type object which could be associated to a primitive–commentary origin.

Birlan et al. (2015) associated HED meteorites with V–type PHA asteroids. Their result consists of two V–type PHA asteroids, (1981)Midas and 1997GL3, that can be associated with HED meteorites.

I made a search for fall meteorites in the Meteoritical Bulletin Database. In my search, I found 362 fall meteorites over a period of 150 years, from which 114 of them occur during the maximum activity of the 28 meteor showers associated with asteroids based on databases presented in Section 2.2.

Fig. 4.30 shows the five categories of fall meteorites (Weisberg et al. 2006). We only used the maximum activity period, because the probability of a meteor falling from a particular stream is highest then.

From the total number of fall meteors associated 78% are ordinary chondrite meteorites (associated with all meteor showers), 7% are iron meteorites (associated with eight meteor showers), 5.26% are carbonaceous chondrite meteorites (associated with seven meteor showers), 7.9% achondrites meteorites (associated with eight), and 1.75% stony-iron meteorites (associated with AVB and SMA).

In a tentative approach I associated the fall meteorites with my associated asteroids that have physical data. The association between asteroid taxonomic class and meteoritic types is taken from Burbine (2016). The spectra comparison was made with M4AST tool, Relab database. This association is only a link from the fallen date of meteorites and maximum activity of the meteor shower, and it takes into consideration the fallen location of meteorites and radiants of meteor showers.

I note that hundreds of thousands of meteors are recorded annually, but only about 30% of them are associated to meteor showers (Jenniskens et al. 2016b). Thus, we can only speculate on the origin of meteorites to meteor showers and their possible asteroid parent bodies.

[4]fall meteorites - are those which were seen to fall form the sky and which were pursued and located successfully. This meteorites could be distinguished to the one found on the ground and related to any sighting.

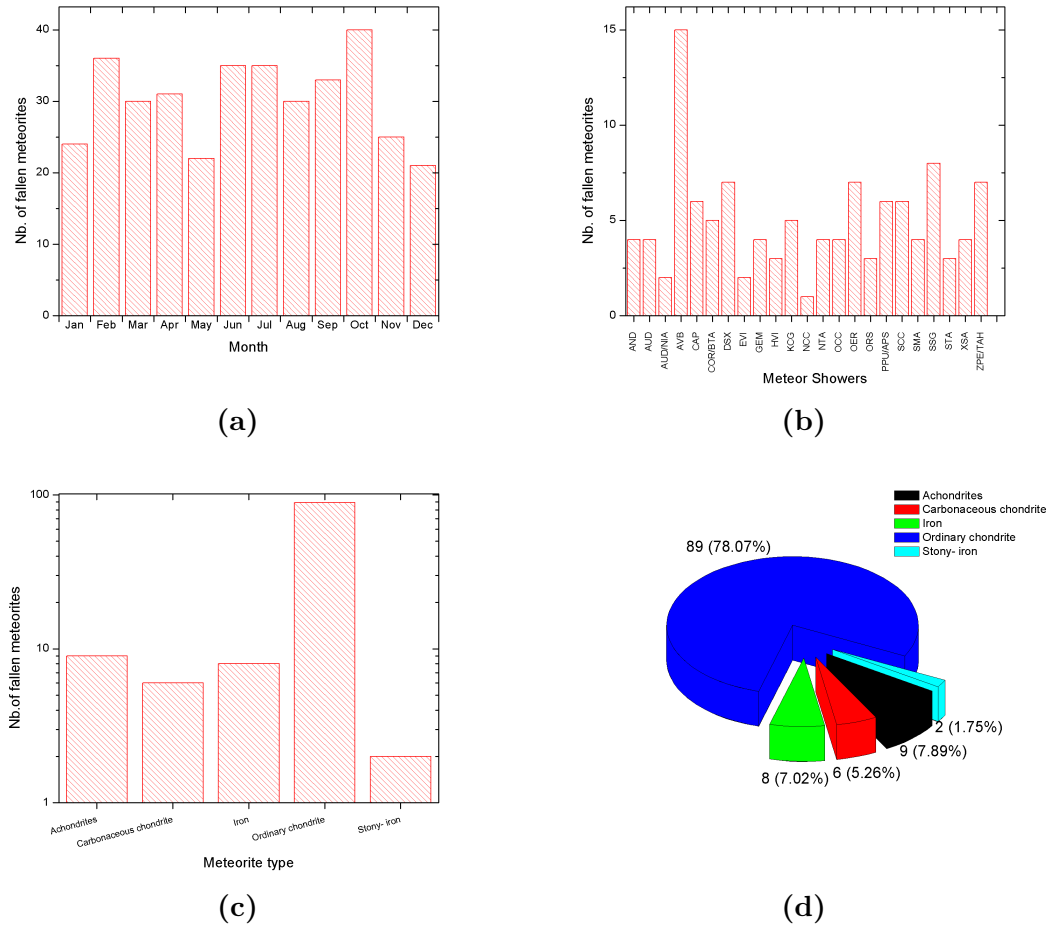


**Figure 4.30:** Number of fallen asteroids per month (4.30a) and per meteor shower(4.30b) over 150 years. The type of fallen meteorites are presented in 4.30c and 4.30d. Plotted are the 114 fall meteorites landing on Earth associated with maximum activity of meteor showers from my sample, except 4.30a where I plotted all found fallen meteors.

In total, I obtained 11 asteroids that can be associated with 57 fall meteorites (see Table 4.2).

**Table 4.2:** 57 fall meteorites that can be associated with 11 asteroids. This association is only a link from the fallen date of meteorites and maximum activity of the meteor shower. The asteroids associated to the the meteor shower are only the asteroids with physical data, considering the fallen location of meteorite and radiant of meteor shower. In table will note: Ordinary chondrite with OC, Achondrites with AC, Carbonaceous chondrites with CC.

| Shower | Asteroid | Taxonomy | Fall Meteor | Class | Meteor Ref. |
|---|---|---|---|---|---|
| | (446791)1998SJ70 | Q | Glanerbrug | OC | - |
| | | | Berduc | OC | - |
| | | | Wethersfield (1971) | OC | - |
| | | | Jesenice | OC | - |
| | | | Pétèlkolé | OC | - |

**Table 4.2:** continued.

| Shower | Asteroid | Taxonomy | Fall Meteor | Class | Meteor Ref. |
|---|---|---|---|---|---|
| | | | Muzaffarpur | Iron | - |
| AVB | | | Schenectady | OC | - |
| | | | Xinglongquan | OC | - |
| | | | Mason Gully | OC | - |
| | | | Mifflin | OC | - |
| | | | Suizhou | OC | - |
| | | | Uzcudun | OC | - |
| | | | Aioun el Atrouss | AC | - |
| | | | Success | OC | - |
| | 2001EC | Sq | Sidi Ali Ou Azza | OC | - |
| | | | Kokubunji | OC | - |
| CAP | | | Moshampa | OC | - |
| | | | Wuan | OC | - |
| | | | Jodiya | OC | - |
| | | | Maigatari-Danduma | OC | - |
| COR | (162058)1997AE12 | Q | Ningqiang | CC | - |
| | | | Saint-Séverin | OC | - |
| and | and | | Famenin | OC | - |
| | | | Serra Pelada | AC | - |
| BTA | 2003UV11 | Q | Ibitira | AC | - |
| EVI | 2000DO1 | V | Gyokukei | OC | - |
| | | | Quija | OC | - |
| | (3200)Phaethon | F,B | Vissannapeta | AC | - |
| GEM | | | Dunbogan | OC | - |
| | | | Nuevo Mercurio | OC | - |
| | | | Mreïra | OC | - |
| | 2003UV11 | Q | Komar Gaon | OC | - |
| NTA | | | Kamargaon | OC | - |
| | | | Juromenha | Iron | - |
| | | | Salzwedel | OC | - |
| | (4179)Toutatis | S,Sk,Sq | Ningbo | Iron | - |
| OCC | | | Tathlith | OC | - |
| | | | Marilia | OC | - |
| | | | Berthoud | AC | - |
| | 2002AU5 | X | Varre-Sai | OC | - |
| | | | Madiun | OC | - |
| | | | Aomori | OC | - |
| SSG | | | Piplia Kalan | AC | - |
| | | | Kunya-Urgench | OC | - |
| | | | Guangrao | OC | - |
| | | | Uchkuduk | OC | - |
| | | | Bunburra Rockhole | AC | - |
| | 2007RU17 | Q | Ishinga | OC | - |
| STA | and | | Peekskill | OC | - |
| | 2003UV11 | Q | Dwaleni | OC | - |

**Table 4.2:** continued.

| Shower | Asteroid | Taxonomy | Fall Meteor | Class | Meteor Ref. |
|---|---|---|---|---|---|
| | | | Tsukuba | OC | - |
| | 2006HQ30 | Sq,Q | Indian Butte | OC | - |
| | | | Ste. Marguerite | OC | - |
| TAH | and | | Hökmark | OC | - |
| | | | Lanxi | OC | - |
| | 3671)Dionysus | Cb,X | Kunashak | OC | - |
| | | | Sheyang | OC | - |

(1) Clarke (1974); (2) Garvie (2012); (3) Russell et al. (2003); (4) Graham (1987); (5) web[a]; (6) Fleischer et al. (1970); (7) Telus et al. (2016); (8) Krinov (1961); (9) Graham (1989); (10) Russell et al. (2005); (11) Weisberg et al. (2008); (12) Chennaoui Aoudjehane et al. (2016);(13) Graham (1988); (14) Krinov (1958); (15) Wlotzka (1993); (16) Clarke (1971);(17) Krinov (1970); (18) Wlotzka (1995); (19) Graham (1984); (20) web[b]; (21) Graham (1986);(22) Graham (1982);

[a] http://www.lpi.usra.edu/meteor/metbull.php?code=62494
[b] http://www.lpi.usra.edu/meteor/metbull.php?code=63102

For $\alpha$ Virginids (AVB) I found 14 fallen meteorites (12 OC and, one AC and one Iron) and one asteroid with spectral data, (446791)1998SJ70, which can be compared with the spectra of the fallen meteorites. (446791)1998SJ70 is an Q-type asteroid (Burbine 2016) that it can be associated with OC-type meteorites. After the spectra comparison with RELAB, I found that (446791)1998SJ70 can be associated with two meteorites, Wethersfield (1971) and Schenectady (Fig. 4.31). Both meteorites are OC-type.

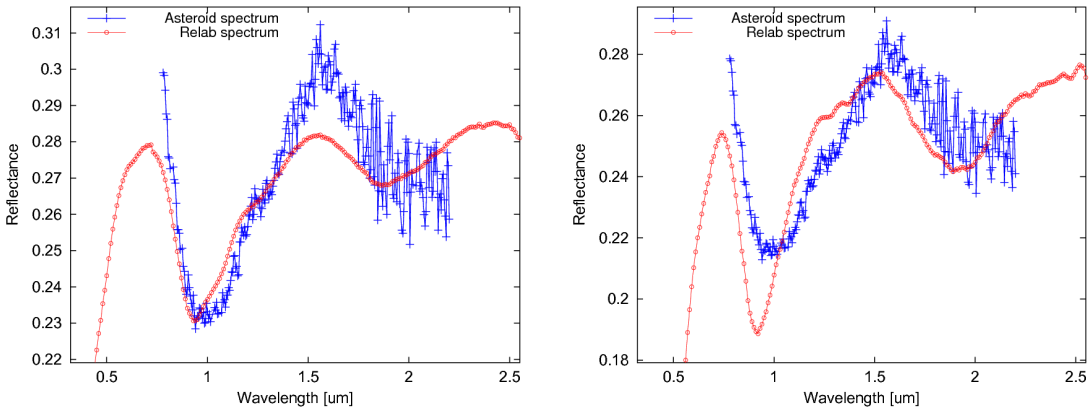


**(a)** $C1TB144$ **(b)** $C1TB83$

**Figure 4.31:** Spectra comparison between meteorites and asteroids associated to meteor showers. Both asteroid and meteorite spectra were normalized to 1.25 $\mu$m. 4.31a: (446791)1998SJ70 (au1998SJ70.sp74) compared with Wethersfield (1971) meteorite. 4.31b: (446791)1998SJ70 (au1998SJ70.sp74) compared with Schenectady meteorite.

The October Capricornids (OCC) was associated with four meteorites (two OC-type, one AC-type and one iron) that can be compared with (4179)Toutatis, an

asteroid with the taxonomic type S, Sk or Sq-type. Also, this asteroid needs to have a similarity with an OC-type meteorite. The RELAB shows that this asteroid has similarities with the Marilia, an OC-type meteorite (Fig. 4.32).

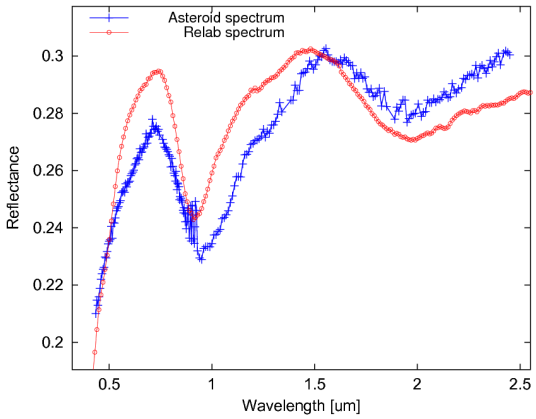


**Figure 4.32:** Spectra comparison between Marilia meteorite ($C1TB78$) and asteroid (4179)Toutatis ($a004179.sp74$) associated to OCC meteor showers. Asteroid and meteorite spectra were normalized to 1.25 $\mu$m.

Other three OC-type meteorites were associated with Southern Taurids (STA) meteor shower. For this shower there are two asteroids that have spectra data (2003UV11 and 2007RU17). Both asteroids have a Q-type taxonomic class and need to have similarities with OC-type meteorites. The comparison from RELAB shows that those asteroids have similarities with Dwaleni, an OC-type meteorite (Fig. 4.33).

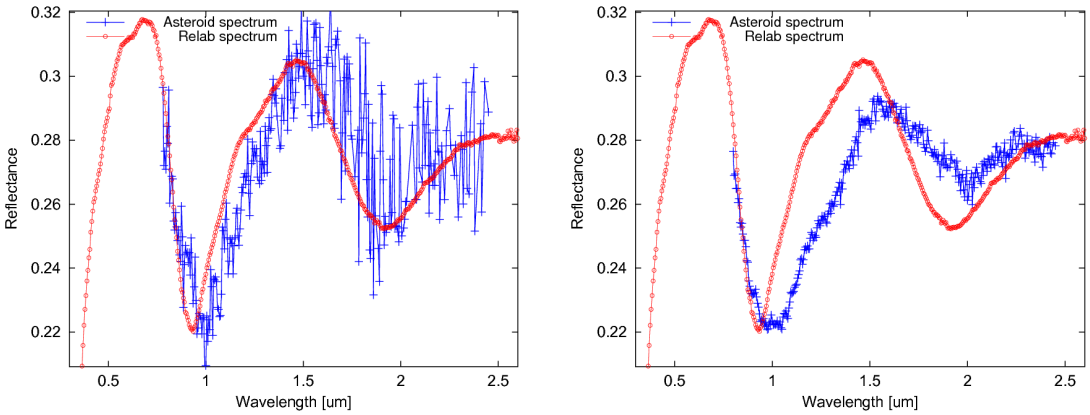


**(a)** $CLMB03$ **(b)** $CLMB03$

**Figure 4.33:** Spectra comparison between meteorites and asteroids associated to meteor showers. Both asteroid and meteorite spectra were normalized to 1.25 $\mu$m. 4.33a: 2003UV11 ($au2003UV11.sp94$) compared with Dwaleni meteorite. 4.33b: 2007RU17 ($au2007RU17.sp94$) compared with Dwaleni meteorite.

For $\tau$ Herculids (TAH) I associated seven meteorites (all OC-type) that can be compared with two asteroids (2006HQ30 and (3671)Dionysus). Here, the asteroid 2006HQ30 has a taxonomic class of Sq or Q-type, similar to OC-type meteorites and the (3671)Dionysus that is a Cb or X-type asteroid, and needs to have

similarities with CC-type or AC-type meteorites. As expected, the RELAB shows that (3671)Dionysus do not have similarities with the associated meteorites and 2006HQ30 has similarities with Kunashak, an OC-type meteorite (Fig. 4.34).

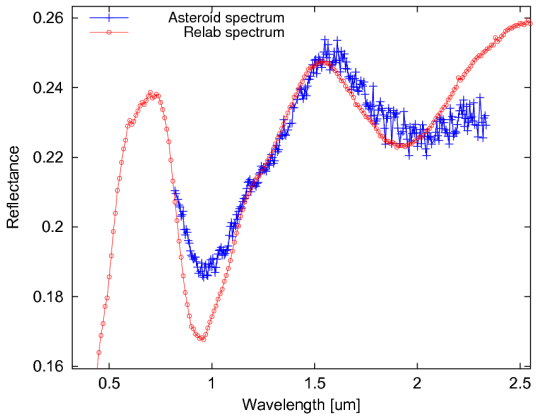


**Figure 4.34:** Spectra comparison between Kunashak meteorite ($C1TB139$) and asteroid 2006HQ30 ($au2006HQ30.sp51$) associated to TAH meteor showers. Asteroid and meteorite spectra were normalized to 1.25 $\mu$m.

As for the meteor showers $\alpha$ Capricornids (CAP), Corvids (COR), Daytime $\beta$ Taurids (BTA), $\eta$ Virginids (EVI), Geminids (GEM), Northern Taurids (NTA) and Southern $\mu$ Sagittariids (SSG) I have not found any similarities between the associated asteroids and meteorites.

In the case of meteor showers EVI (V-type asteroid), GEM (F or B-type asteroid) and SSG (X-type asteroid) the result was expected considering that most of the associated meteorites are OC-type. But I was puzzled in the case of CAP, COR, BTA and NTA, which have three Q-type associated asteroids and 12 OC-type associated meteorites and no similarity was found.

In summary, I found five asteroids that have similarities with five meteorites. The results are presented in Table B.1. At a first inspection, I observed a discrepancy between asteroid and meteorite spectra (in particular, around 1 $\mu$m abortion band), for all spectra comparison. This may be due to the space-weathering mechanisms (Brunetto et al. 2006; Pieters et al. 2000).

## 4.4 Associated asteroids observed

My observations were obtained at Pic du Midi observatory from Pyrenees mountains, France located at 2 870 m altitude. The observations were made in April 6-7, 2016 and January 17-18, 2018 using the T1M 1.05 m telescope, an iKon-L Andor CCD camera with a 2k X 2k E2V chip (pixel scale 0.22 "/pix) and SDSS filters (Vaduvescu et al. 2013). It was used the 2x2 binning mode in order to avoid the oversampling of images. The seeing was not constant during the run with FWHM between 1.2 and 2 arcsec.

The observed targets were (363599) 2004 FG11, (85953) 1999 FK21 and (259221) 2003 BA21, previously associated with Daytime $\zeta$ Perseids (ZPE), Daytime $\xi$ Sagittariids (XSA) and, respectively with two meteor showers, Daytime Sextantids (DSX) and November $\theta$ Aurigids (THA) (Dumitru et al. 2018, 2017).

### 4.4.1 Asteroid (363599) 2004 FG11

In 2004-March-23 it has been discovered by LINEAR. Its a Near Earth Asteroid (NEA) from Appolo population. It has a taxonomic class of V-type (Hicks et al. 2010; Somers et al. 2010). The albedo is 0.306 $\pm$ 0.050 and its diameter is equal to 0.152 $\pm$ 0.003 km (Mainzer et al. 2014).

This asteroid is reported as a binary asteroid, with the principal rotation smaller than 4 h and for the binary system 20 h, by means of radar observations (Taylor et al. 2012). After two years another computation for binary system period was made and a period of 22 $\pm$ 0.5 h has found (Warner 2014b)

### 4.4.2 Asteroid (259221) 2003 BA21

It has been discovered in 27-January-2003 by LINEAR. This asteroid is a NEA from Apollo population. It has a large eccentricity and its perihelion is interior to the Mercury orbit.

Its taxonomic class was set to S-type (Binzel et al. 2004), albedo of 0.32 and diameter of 0.59 km based on the near Earth Asteroids thermal model (NEATM) proposed by Harris in 1998 (see Delbó et al. 2003, and references herein). Its rotational period was estimated to 17.62 $\pm$ 0.05 (Warner 2016a).

Also, was reported by Skiff in 2011 as a tumbling asteroid, but after some verification it turned out that the asteroid do not have strong signs of tumbling. More data sets are needed for a definitive solution (see Warner 2016a, and ref.).

### 4.4.3 Asteroid (85953) 1999 FK21

**(85953) 1999 FK21** has been discovered in 1999-March-24 by LINEAR. This asteroid is a Near Earth Asteroid (NEA) from the Athens population.

## 4.5 Results from observations

### 4.5.1 Asteroid (363599) 2004 FG11 lightcurve

Firstly, I computed the absolute magnitude of the asteroid and I extracted the phase angle dependence from the data using Eq. 3.52 (Fig. 4.35)

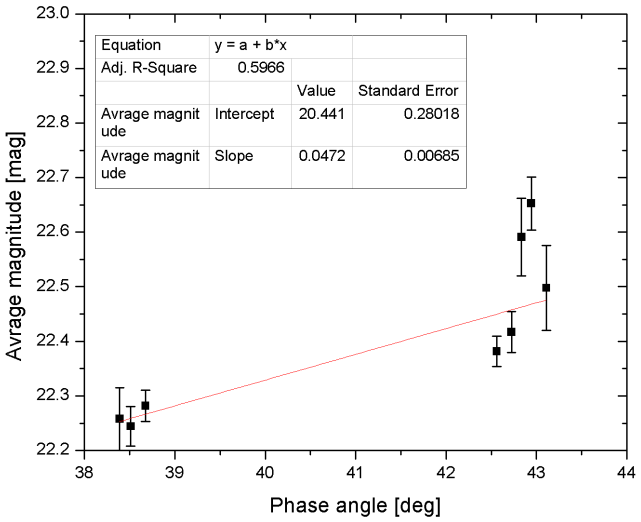


**Figure 4.35:** The representation of reduced magnitude versus phase angle.

I obtained an absolute magnitude of 20.441 ± 0.28 in r filter ( corresponding to a V filter transformation 20.7 ± 0.4). For the Lomb-Scargle analysis I used the NASA Exoplanet Archive Periodogram Service[5].

The most probable period inferred from my observations of (363599) 2004 FG11 is of 0.2926 ± 0.0004 days (7.021 ± 0.001 h). This solution does not agree with the one from the literature where the estimation of rotational period is shorter than 4 h and the period of the binary system is 22 ± 0.5 h.

In order to check if my data fits one the rotation period from literature, I packed the lightcurve data using the period inferred from the peak closest to a 4h period (blue arrow in Fig. 4.36). These two lightcurves are presented in Fig. 4.37. The amplitude of the lightcurve is around (0.35 ± 0.7) mag. Even if the visual inspection favors the 7 hours period, the period of 4 hours could not be completely excluded.

The period of the binary system was investigated using the data previously published by Warner (2014b). For this, I manually set the period of the binary system to 22 h and I made a direct comparison of the results, are presented in Fig. 4.38. My data overlap with the same region of the rotational period as the one from the literature.

[5]https://exoplanetarchive.ipac.caltech.edu

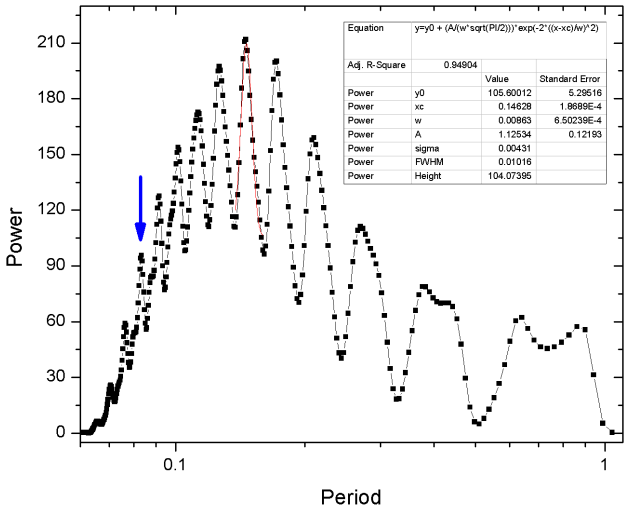


**Figure 4.36:** Periodogram for (363599) 2004 FG11). The blue arrow represents the closest peak to the 4 h rotational period of primary (available from literature).

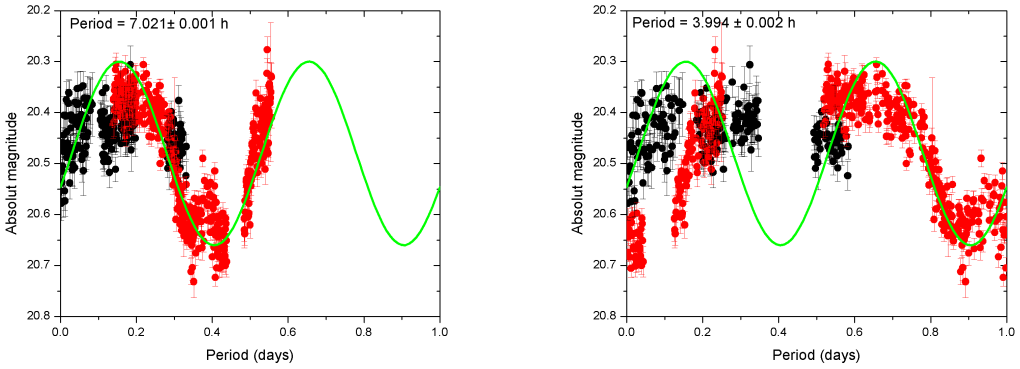


**(a)** **(b)**

**Figure 4.37:** (363599) 2004 FG11 compose lightcurve. The black and red colors represent the nights when data were taken (black - 2016 April 06 and red - 2016 April 07). 4.37a: The lightcurve with a period of 7.021 ± 0.001 h. 4.37b: The lightcurve with a period of 3.994 ± 0.002 h

The result of my comparison is presented in Fig. 4.38 and I noticed the good agreement between my data and those of the literature.

From this test alone one can not draw a definitive conclusion. My data agrees well with the known period of the binary system, but I have not found the 4 h period of the primary. More observational data is needed for refining the rotational parameters of this binary system.

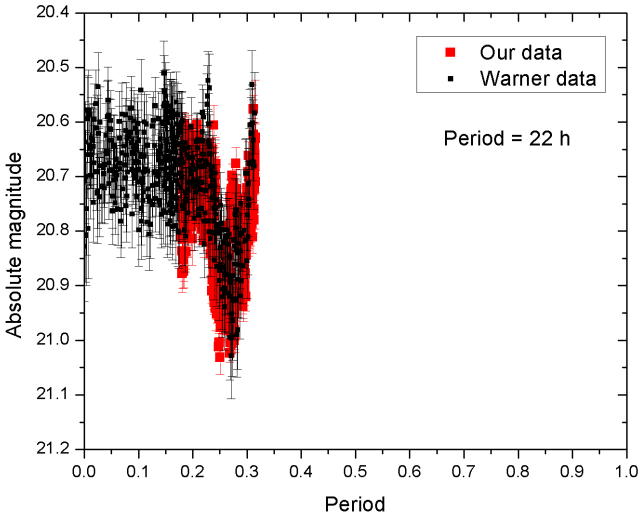


**Figure 4.38:** A comparison between my data and B. Warner data.

### 4.5.2 Asteroid (259221) 2003 BA21 lightcurve

In Fig. 4.39 is presented the periodogram of this asteroid.

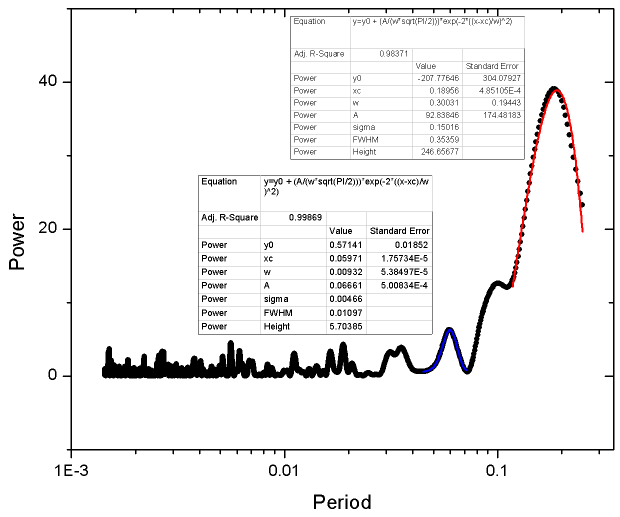


**Figure 4.39:** Periodogram for (259221) 2003 BA21.

The most probable period from my observations of (259221) 2003 BA21 is at 0.379 ± 0.001 days (9.09 ± 0.02 h). I also checked the lightcurve for the next most probable period, that I found at 0.11942 ± 0.00002 days (2.866 ± 0.001 h). The obtained lightcurves for those two periods are presented in Fig. 4.40.

From the visual inspection I privileged the period at 9.09 ± 0.02 h, the period of 2.866 ± 0.001 h being too noisy. For a robust conclusion I had to investigate

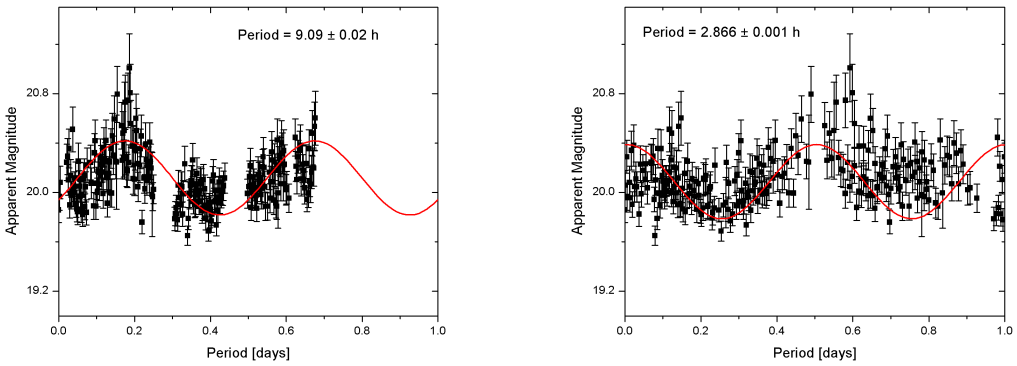


**(a)** **(b)**

**Figure 4.40:** (259221) 2003 BA21 lightcurve. 4.40a: The most probable lightcurve with a period of 9.09 ± 0.02 h. 4.37b: The next probable lightcurve with a period of 2.866 ± 0.001 h

**Table 4.3:** Colors and the corresponding spectral reflectances according to the SDSS system.

| Name | g-r | $\sigma_{g-r}$ | $R_r$ | $\sigma_{R_r}$ | g-i | $\sigma_{g-i}$ | $R_i$ | $\sigma_{R_i}$ |
|---|---|---|---|---|---|---|---|---|
| 1999 FK21 | 0.0911 | 0.1454 | 1.0364 | 0.0581 | 0.0703 | 0.1600 | 1.0281 | 0.0640 |
| 2004 FG11 | 0.1909 | 0.0826 | 1.0764 | 0.0331 | 0.1927 | 0.1024 | 1.0771 | 0.0409 |

observational data which stretched over several nights.

### 4.5.3 Colors and reflectances of asteroids (363599) 2004 FG11 and 85953) 1999 FK21

For each asteroid I computed the colors $g-r$ and $g-i$ and reflectances (Table 4.3) with the method presented in section 3.3.1.

In the next step I compared this values with SDSS-based asteroid Taxonomy[6] database. I selected the most representative taxonomic classes (DeMeo et al. 2009b): V, X-types and C-complex, S-groups (composed by A, L, S and Q-type). For each of them an ellipse borders the area of reflectances in the ($R_r$, $R_i$) diagram. The values inferred for my objects are also displayed (Fig. 4.41)

The (363599) 2004 FG11 asteroid, classified as a V type, may be associated with all the representative classes, but is most akin to a V-type, or S-group and less likely to be a C or X-type.

The (85953) 1999 FK21 asteroid, classified as S-type, belongs most likely to a X or C taxonomic group (Fig. 4.41).

[6]https://sbn.psi.edu/pds/resource/sdsstax.html

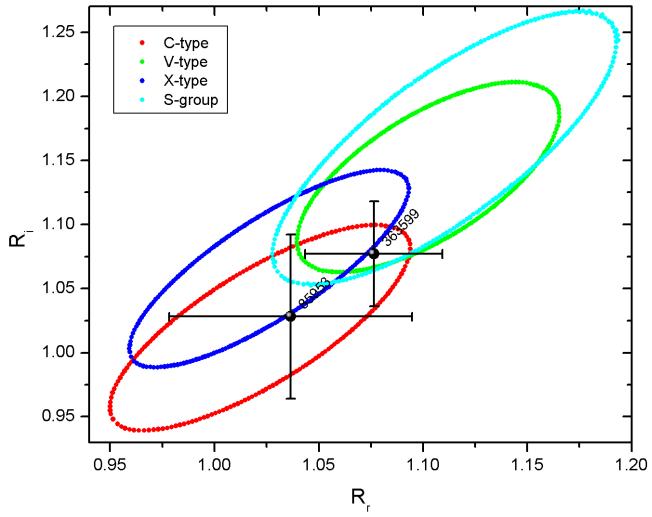


**Figure 4.41:** Asteroids taxonomic classes association. The S-group contains taxonomic classes A, L, S and Q-type. The taxonomic classes are based on the SDSS-based Asteroid Taxonomy database.

# Chapter 5

# Conclusions and perspectives

The main objective of this study is to determinate the asteroids that can produce or feed the meteor showers using a global process. The outcome of such a global process is useful for the fundamental science on Solar System evolution and also for mitigation or space awareness.

In this study, I used three D–Criteria metrics ($D_{ACS}$, $D_{SH}$ and $D_H$), a new threshold selection method and I computed the Lyapunov time for all the associated objects. I also classified the associated objects after the associated metrics.

My result sample consists of 296 asteroids that can be associated to 28 meteor showers.

From the dynamical parameters perspective, all the associated objects belong to Near Earth Asteroids population. By using the Tisserand parameter, I concluded that from the entire sample of associations 15.3% of the asteroids are on commentary orbits, 84.3% are on asteroidal orbits and 0.4% belong to damocloids. Also, 82% of my sample have Apollo orbits and 7% are classified as potential hazardous asteroids.

Comparing my associations results with the already known parent bodies I obtained the same results for: (3200)Phaethon and Geminids (GEM), 2005UD and Daytime Sextantids (DSX), (85182)1991AQ and Northen $\delta$ Cancrids (NCC), 1998SH2 and $\alpha$ Virginids (AVB), 2004TG10, 2010TU149 and Northern Taurids (NTA).

From the physical data perspective, I analyzed the objects in my sample in terms of their potential to produce meteoroids. In these analyses were used only the objects found in literature with data. As a result, about 10% of objects from my sample have data: 15 asteroids have taxonomic class, 28 asteroids have albedo and 17 asteroids with known rotation period.

Thus, the fast-rotator asteroids 2007LW19 and 2007RS146 might have a monolithic structure and is unlikely to produce meteoroids. At the opposite end of the scale, slow–rotators and tumbling asteroids are more akin to be rubble–pile

objects, thus weak gravitational instabilities or non-gravitational forces could easily detach meteoroids from these bodies. I noticed here the binary asteroid 2000UG11 associated with AND, and the tumbling asteroid (4179)Toutatis (rubble-pile body) associated with OCC.

Regarding the association attempt between fall meteors, meteor showers and associated asteroids with spectra, I managed to associate 57 meteorites with 11 associated asteroids with physical data. The best spectra similarities were obtained between: (4179)Toutatis and Marilia, 2003UV11, 2007RU17 and Dwaleni, 2006HQ30 and Kunashak, (446791)1998SJ70 and Schenectady, Wethersfield(1971). All the associated meteorites are ordinary chondrites and were associated to asteroids with taxonomic class S and Q-type.

Some of the results presented above were published in Dumitru et al. (2017).

From the observational program perspective, that aims obtaining lightcurves and colors for my asteroids sample which do not have data, I observed 3 asteroids. The obtained data are: two lightcurvers for asteroids (363599)2004FC11 and (259221)2003BA21 and colors for asteroids (363599)2004FC11 and (85953)1999FK21. All data were obtained by using a telescope of 1 m from Pic du Midi observatory.

For (363599) 2004 FG11 I obtained a primary rotation period of 7.021 $\pm$ 0.001 h and a lightcurve compatible with the known binary system period of 22 h and for (259221)2003BA21 I obtained a rotation period of 9.09 $\pm$ 0.02 h.

Using colors obtained in the run and a comparison with SDSS database I can confirm a V-type class for (363599) 2004 FG11. (85953) 1999 FK is more akin to a C or X types than the S-type.

Also, those results were published in Dumitru et al. (2018).

In the future, I will continue this research and I will try to improve it. The future goals are the following:

1. The search and test of other D-Criteria metrics.

2. The improvement of the threshold selection method.

3. Obtaining physical data for my associated asteroids.

4. Extending the study of asteroids and meteorites association.

5. Extending the current study after obtaining more data.

6. Search links between comets–primitive asteroids–meteor showers–carbonaceous meteorites and main belt objects–stony asteroids–meteor showers–ordinary chondrites meteorites.

7. Confirmation of parent bodies from my association.

An important role in the associations between asteroids and meteor showers is the method used. In this study I use three D-Criteria metrics based on shape and size. In the future I intend to test other metrics, based on orbital dynamics, and compare between them.

Another important role in this study was the threshold. This part has given us a big headache. Even in my case, the method for threshold selection was very permissive in some cases. This part requires some improvements in order to satisfy all cases. In the future, I will try to obtain a threshold for every meteor shower or for each population of asteroids.

In this study I hit a large lack of physical data for my sample. In the future, the goal would be to continue with the observational programs in order to obtain physical data for my sample of asteroids and many more. The physical data that will be obtained are lightcurves, rotation periods, colors, spectra, etc. After getting more data we will be able to improve this study and find more parent bodies.

In my study the associations between asteroids and meteorites, I only found links between S-type asteroids and OC-type meteorites. These results are due to the lack of asteroids spectral data. In the future, this part of the study needs to be remade on a larger period and more associated asteroids with spectral data. It will be interesting to see if can be found other types of asteroids, such as primitive ones, that can be associated with meteorites found on the ground.

Also, an interesting approach, will be to see if there is a link between comets–asteroids–meteor showers–meteorites or main belt–asteroids–meteor showers–meteorites. This idea takes into account that NEAs originate from comets and main belt. The goal of this approach is to see if the majority of asteroids with primitive structure can be linked with comets and the stony asteroids can be linked with the main belt objects.

# Bibliography


Abedin, A., Wiegert, P., Pokorný, P., & Brown, P. 2017, Icarus, 281, 417

Alvarez, L. W., Alvarez, W., Asaro, F., & Michel, H. V. 1980, Science, 208, 1095

Asher, D. J., Clube, S. V. M., & Steel, D. I. 1993, MNRAS, 264, 93

Babadzhanov, P. B. 1996, Earth Moon and Planets, 72, 305

Babadzhanov, P. B. 2003, A&A, 397, 319

Babadzhanov, P. B. & Obrubov, I. V. 1983, in Asteroids, Comets, and Meteors, ed. C.-I. Lagerkvist & H. Rickman, 411–417

Babadzhanov, P. B., Williams, I. P., & Kokhirova, G. I. 2008a, MNRAS, 386, 2271

Babadzhanov, P. B., Williams, I. P., & Kokhirova, G. I. 2008b, A&A, 479, 249

Babadzhanov, P. B., Williams, I. P., & Kokhirova, G. I. 2008c, MNRAS, 386, 1436

Babadzhanov, P. B., Williams, I. P., & Kokhirova, G. I. 2009, A&A, 507, 1067

Barucci, M. A., Capria, M. T., Coradini, A., & Fulchignoni, M. 1987, Icarus, 72, 304

Bessell, M. S. 1979, PASP, 91, 589

Binzel, R. P., Lupishko, D., di Martino, M., Whiteley, R. J., & Hahn, G. J. 2002, Physical Properties of Near-Earth Objects, ed. W. F. Bottke, Jr., A. Cellino, P. Paolicchi, & R. P. Binzel, 255–271

Binzel, R. P., Morbidelli, A., Merouane, S., et al. 2010, Nature, 463, 331

Binzel, R. P., Rivkin, A. S., Stuart, J. S., et al. 2004, Icarus, 170, 259

Birlan, M., Fulchignoni, M., & Barucci, M. A. 1996, Icarus, 124, 352

Birlan, M., Popescu, M., Irimiea, L., & Binzel, R. 2016, in AAS/Division for Planetary Sciences Meeting Abstracts, Vol. 48, AAS/Division for Planetary Sciences Meeting Abstracts, 325.17

Birlan, M., Popescu, M., Nedelcu, D. A., et al. 2015, A&A, 581, A3

Bischoff, A. & Geiger, T. 1995, Meteoritics, 30, 113

Brown, P., Weryk, R. J., Wong, D. K., & Jones, J. 2008, Icarus, 195, 317

Brown, P., Wong, D. K., Weryk, R. J., & Wiegert, P. 2010, Icarus, 207, 66

Brunetto, R., Vernazza, P., Marchi, S., et al. 2006, Icarus, 184, 327

Burbine, T. H. 2016, in Lunar and Planetary Science Conference, Vol. 47, Lunar and Planetary Science Conference, 2425

Bus, S. J. & Binzel, R. P. 2002a, Icarus, 158, 146

Bus, S. J. & Binzel, R. P. 2002b, Icarus, 158, 106

Carvano, J. M., Hasselmann, P. H., Lazzaro, D., & Mothé-Diniz, T. 2010, A&A, 510, A43

Chapman, C. R., Morrison, D., & Zellner, B. 1975, Icarus, 25, 104

Chennaoui Aoudjehane, H., Agee, C. B., Aaranson, A., & Bouragaa, A. 2016, LPI Contributions, 1921, 6120

Chesley, S. R. & Milani, A. 1999, in AAS/Division for Planetary Sciences Meeting Abstracts, Vol. 31, AAS/Division for Planetary Sciences Meeting Abstracts #31, 28.06

Clarke, Jr., R. S. 1971, Meteoritics, 6

Clarke, Jr., R. S. 1974, Meteoritics, 9

Clube, S. V. M. & Napier, W. M. 1984, MNRAS, 211, 953

Combi, M. R., Harris, W. M., & Smyth, W. H. 2004, Gas dynamics and kinetics in the cometary coma: theory and observations, ed. M. C. Festou, H. U. Keller, & H. A. Weaver, 523–552

Connors, M., Wiegert, P., & Veillet, C. 2011, Nature, 475, 481

Cousins, A. W. J. 1974, MNRAS, 166, 711

Cunningham, C. J. & Hughes, D. W. 1988, S&T, 76, 366

Davies, J. K., Harris, A. W., Rivkin, A. S., et al. 2007, Icarus, 186, 111

de la Fuente Marcos, C. & de la Fuente Marcos, R. 2013, MNRAS, 432, L31

de la Fuente Marcos, C. & de la Fuente Marcos, R. 2014, MNRAS, 439, 2970

de la Fuente Marcos, C. & de la Fuente Marcos, R. 2017, MNRAS, 467, 1561

Delbó, M., Harris, A. W., Binzel, R. P., Pravec, P., & Davies, J. K. 2003, Icarus, 166, 116

DeMeo, F., Binzel, R. P., Slivan, S. M., & Bus, S. J. 2009a, NASA Planetary Data System, 114

DeMeo, F. E., Binzel, R. P., & Lockhart, M. 2014, Icarus, 227, 112

DeMeo, F. E., Binzel, R. P., Slivan, S. M., & Bus, S. J. 2009b, Icarus, 202, 160

Denning, W. F. 1907, MNRAS, 67, 566

Drummond, J. D. 1981, Icarus, 45, 545

Drummond, J. D. 1982, Icarus, 49, 143

Dumitru, B. A., Birlan, M., Popescu, M., & Nedelcu, D. A. 2017, A&A, 607, A5

Dumitru, B. A., Birlan, M., Sonka, A., Colas, R., & Nedelcu, D. A. 2018, Astron. Nachr., 1

Farinella, P., Foschini, L., Froeschlé, C., et al. 2001, A&A, 377, 1081

Farinella, P., Gonczi, R., Froeschle, C., & Froeschle, C. 1992, in Asteroids, Comets, Meteors 1991, ed. A. W. Harris & E. Bowell

Fleischer, R. L., Lifshin, E., Price, P. B., et al. 1970, Icarus, 12, 402

Fornasier, S., Belskaya, I. N., Shkuratov, Y. G., et al. 2006, A&A, 455, 371

Fox, K., Williams, I. P., & Hughes, D. W. 1984, MNRAS, 208, 11P

Fulchignoni, M., Birlan, M., & Antonietta Barucci, M. 2000, Icarus, 146, 204

Garvie, L. A. J. 2012, Meteoritics and Planetary Science, 47, 1887

Gnos, E., Hofmann, B. A., Al-Kathiri, A., et al. 2004, Science, 305, 657

Gradie, J. & Tedesco, E. 1982, Science, 216, 1405

Graham, A. L. 1982, Meteoritics, 17

Graham, A. L. 1984, Meteoritics, 19

Graham, A. L. 1986, Meteoritics, 21

Graham, A. L. 1987, Meteoritics, 22

Graham, A. L. 1988, Meteoritics, 23

Graham, A. L. 1989, Meteoritics, 24, 57

Graner, F. & Dubrulle, B. 1994, A&A, 282, 262

Grazier, K., Newman, W., Hyman, J., & Sharp, P. 2005, 46

Greenberg, J. M. 1998, A&A, 330, 375

Gupta, G. & Sahijpal, S. 2010, Journal of Geophysical Research (Planets), 115, E08001

Gustafson, B. A. S. 1989, A&A, 225, 533

Harris, A. W. 1994, Icarus, 107, 209

Harris, A. W. & Lagerros, J. S. V. 2002, Asteroids in the Thermal Infrared, ed. W. F. Bottke, Jr., A. Cellino, P. Paolicchi, & R. P. Binzel, 205–218

Hicks, M., Lawrence, K., & Benner, L. 2010, The Astronomer's Telegram, 2571

Hildebrand, A. R., Penfield, G. T., Kring, D. A., et al. 1991, Geology, 19, 867

Hoffmeister, C. 1937, Die meteore, ihre kosmischen und irdischen beziehungen, von dr. C. Hoffmeister ... MIT 25 abbildungen im text und 4 tafeln.

Ivezić, Ž., Tabachnik, S., Rafikov, R., et al. 2001, AJ, 122, 2749

Jenniskens, P. 1994, A&A, 287, 990

Jenniskens, P. 2004, AJ, 127, 3018

Jenniskens, P. 2006, Meteor Showers and their Parent Comets

Jenniskens, P. 2008, Icarus, 194, 13

Jenniskens, P., Nénon, Q., Albers, J., et al. 2016a, Icarus, 266, 331

Jenniskens, P., Nénon, Q., Gural, P. S., et al. 2016b, Icarus, 266, 355

Jenniskens, P., Nénon, Q., Gural, P. S., et al. 2016c, Icarus, 266, 384

Jewitt, D. 2012, AJ, 143, 66

Jewitt, D. & Hsieh, H. 2006, AJ, 132, 1624

Jewitt, D., Hsieh, H., & Agarwal, J. 2015, The Active Asteroids, ed. P. Michel, F. E. DeMeo, & W. F. Bottke, 221–241

Jewitt, D. & Li, J. 2010, AJ, 140, 1519

Jewitt, D., Li, J., & Agarwal, J. 2013, ApJ, 771, L36

Johnson, H. L. & Morgan, W. W. 1953, ApJ, 117, 313

Jones, J., Poole, L. M. G., & Webster, A. R. 2016, MNRAS, 455, 3424

Jopek, T. J. 1993, Icarus, 106, 603

Jopek, T. J. & Bronikowska, M. 2017, Planet. Space Sci., 143, 43

Jopek, T. J. & Jenniskens, P. M. 2011, in Meteoroids: The Smallest Solar System Bodies, ed. W. J. Cooke, D. E. Moser, B. F. Hardin, & D. Janches, 7–13

Jopek, T. J. & Kaňuchová, Z. 2014, Meteoroids 2013, 353

Jopek, T. J., Rudawska, R., & Bartczak, P. 2008, Earth Moon and Planets, 102, 73

Jopek, T. J., Valsecchi, G. B., & Froeschlé, C. 2004, Earth Moon and Planets, 95, 5

Jopek, T. J. & Williams, I. P. 2013, MNRAS, 430, 2377

Kinoshita, D., Ohtsuka, K., Sekiguchi, T., et al. 2007, A&A, 466, 1153

Krinov, E. L. 1958, Meteoritical Bulletin Archive

Krinov, E. L. 1961, Meteoritical Bulletin Archive

Krinov, E. L. 1970, Meteoritics, 5

Kronk, G. W. 1988, Meteor showers. A descriptive catalog

Kronk, G. W. 2014, Meteor Showers

Kulik, L. A. 1938, Leaflet of the Astronomical Society of the Pacific, 3, 78

Kwiatkowski, T., Buckley, D. A. H., O'Donoghue, D., et al. 2010a, A&A, 509, A94

Kwiatkowski, T., Polinska, M., Loaring, N., et al. 2010b, A&A, 511, A49

Lang, K. R. 2011, The Cambridge Guide to the Solar System

Lazzaro, D., Angeli, C. A., Carvano, J. M., et al. 2004, Icarus, 172, 179

Lee, E. A., Astakhov, S. A., & Farrelly, D. 2007, MNRAS, 379, 229

Levin, B. I. 1956, Fizicheskaia teoriia meteorov.

Li, J. & Jewitt, D. 2013, AJ, 145, 154

Licandro, J., Campins, H., Mothé-Diniz, T., Pinilla-Alonso, N., & de León, J. 2007, A&A, 461, 751

Lindblad, B. A. 1971a, Smithsonian Contributions to Astrophysics, 12, 14

Lindblad, B. A. 1971b, Smithsonian Contributions to Astrophysics, 12, 1

Lovell, A. C. B. 1954, Meteor astronomy.

Lowry, S., Fitzsimmons, A., Lamy, P., & Weissman, P. 2008, Kuiper Belt Objects in the Planetary Region: The Jupiter-Family Comets, ed. M. A. Barucci, H. Boehnhardt, D. P. Cruikshank, A. Morbidelli, & R. Dotson, 397–410

Lupishko, D. F., Vasilyev, S. V., Efimov, J. S., & Shakhovskoj, N. M. 1995, Icarus, 113, 200

Mainzer, A., Bauer, J., Grav, T., et al. 2014, ApJ, 784, 110

Mainzer, A., Grav, T., Bauer, J., et al. 2011, ApJ, 743, 156

Mainzer, A., Grav, T., Masiero, J., et al. 2012, ApJ, 760, L12

Mainzer, A. K., Bauer, J. M., Cutri, R. M., et al. 2016, NASA Planetary Data System, 247

Margot, J. L., Nolan, M. C., Benner, L. A. M., et al. 2002, Science, 296, 1445

Masiero, J. R., Nugent, C., Mainzer, A. K., et al. 2018, The Astronomical Journal, 154, 168

Mathar, R. J. 2015, PACS, 95

Meng, H., Zhu, J., Gong, X., et al. 2004, Icarus, 169, 385

Micheli, M. 2013, PhD thesis, University of Hawai'i at Manoa

Miskotte, K. 2016, eMeteorNews, 1, 52

Mottola, S., Hahn, G., Pravec, P., & Sarounova, L. 1997, IAU Circ., 6680

Mueller, B. E. A., Samarasinha, N. H., & Belton, M. J. S. 2002, Icarus, 158, 305

Muinonen, K., Belskaya, I. N., Cellino, A., et al. 2010, Icarus, 209, 542

Nedelcu, D. A., Birlan, M., Popescu, M., Bădescu, O., & Pricopi, D. 2014, A&A, 567, L7

Nedelcu, D. A., Birlan, M., Souchay, J., et al. 2010, A&A, 509, A27

North, G. 1997, Journal of the British Astronomical Association, 107, 82

Norton, O. R. & Chitwood, L. A. 2008, Field Guide to Meteors and Meteorites

Nugent, C. R., Mainzer, A., Bauer, J., et al. 2016, AJ, 152, 63

Nugent, C. R., Mainzer, A., Masiero, J., et al. 2015, ApJ, 814, 117

Ohtsuka, K., Sekiguchi, T., Kinoshita, D., & Watanabe, J. 2005, Central Bureau Electronic Telegrams, 283

Ohtsuka, K., Sekiguchi, T., Kinoshita, D., et al. 2006, A&A, 450, L25

Olivier, C. P. 1925, Meteors

Olmsted, D. 1834, American Journal of Science, 25, 354

Olmsted, D. 1835, American Journal of Science, 27, 419

Olmsted, D. 1836, American Journal of Science, 30, 373

Olsson-Steel, D. 1988, Icarus, 75, 64

Ostro, S. J., Hudson, R. S., Rosema, K. D., et al. 1999, Icarus, 137, 122

Peters, C. F. W. 1867, Astronomische Nachrichten, 68, 287

Pierazzo, E., Hahmann, A. N., & Sloan, L. C. 2003, Astrobiology, 3, 99

Pieters, C. M., Taylor, L. A., Noble, S. K., et al. 2000, Meteoritics and Planetary Science, 35, 1101

Polishook, D., Moskovitz, N., Binzel, R. P., et al. 2016, Icarus, 267, 243

Popescu, M., Birlan, M., & Nedelcu, D. A. 2012, A&A, 544, A130

Popescu, M., Birlan, M., Nedelcu, D. A., Vaubaillon, J., & Cristescu, C. P. 2014, A&A, 572, A106

Popova, O. P., Jenniskens, P., Emel'yanenko, V., et al. 2013, Science, 342, 1069

Porubčan, V., Kornoš, L., & Williams, I. P. 2006, Contributions of the Astronomical Observatory Skalnate Pleso, 36, 103

Porubčan, V., Williams, I. P., & Kornoš, L. 2004, Earth Moon and Planets, 95, 697

Pravec, P., Scheirich, P., Kušnirák, P., et al. 2006, Icarus, 181, 63

Randall, L. 2015, Dark Matter and the Dinosaurs: The Astounding Interconnectedness of the Universe

Rayner, J. T., Toomey, D. W., Onaka, P. M., et al. 2003, PASP, 115, 362

Reddy, V., Dunn, T. L., Thomas, C. A., Moskovitz, N. A., & Burbine, T. H. 2015, Mineralogy and Surface Composition of Asteroids, ed. P. Michel, F. E. DeMeo, & W. F. Bottke, 43–63

Rendtel, J. 2004, Earth Moon and Planets, 95, 27

Richardson, D. C., Michel, P., Walsh, K. J., & Flynn, K. W. 2009, Planet. Space Sci., 57, 183

Rubin, A. E. & Grossman, J. N. 2010, Meteoritics and Planetary Science, 45, 114

Rudawska, R., Vaubaillon, J., & Atreya, P. 2012a, A&A, 541, A2

Rudawska, R., Vaubaillon, J., & Jenniskens, P. 2012b, in European Planetary Science Congress 2012, EPSC2012–886

Russell, S. S., Zipfel, J., Folco, L., et al. 2003, Meteoritics and Planetary Science, 38, A189

Russell, S. S., Zolensky, M., Righter, K., et al. 2005, Meteoritics and Planetary Science, 40, A201

Ryabova, G. O. 2007, MNRAS, 375, 1371

Ryabova, G. O. 2012, MNRAS, 423, 2254

Ryabova, G. O. 2016, MNRAS, 456, 78

Ryabova, G. O., Pleshanova, A. V., & Konstantinov, V. S. 2008, Solar System Research, 42, 335

Scargle, J. D. 1982, ApJ, 263, 835

Scheeres, D. J. 2007, Icarus, 189, 370

Schiaparelli, G. V. 1867, Astronomische Nachrichten, 68, 331

Sekanina, Z. 1973, Icarus, 18, 253

Sekanina, Z. 1976, Icarus, 27, 265

Shapley, H. 1930, Flights from chaos; a survey of material systems from atoms to galaxies, adapted from lectures at the College of the city of New York, Class of 1872 foundation.

Smit, J. 1980, Nature, 285, 198

Somers, J. M., Hicks, M., Lawrence, K., et al. 2010, in Bulletin of the American Astronomical Society, Vol. 42, AAS/Division for Planetary Sciences Meeting Abstracts #42, 1055

Southworth, R. B. & Hawkins, G. S. 1963, Smithsonian Contributions to Astrophysics, 7, 261

Steel, D. I., Asher, D. J., & Clube, S. V. M. 1991, MNRAS, 251, 632

Tancredi, G. 1998, Celestial Mechanics and Dynamical Astronomy, 70, 181

Tancredi, G., Sánchez, A., & Roig, F. 2001, AJ, 121, 1171

Taylor, P. A., Nolan, M. C., Howell, E. S., et al. 2012, Central Bureau Electronic Telegrams, 3091

Telus, M., Alexander, C. M. O., Hauri, E. H., & Wang, J. 2016, in Lunar and Planetary Science Conference, Vol. 47, Lunar and Planetary Science Conference, 1742

Terentjeva, A. K. 1989, WGN, Journal of the International Meteor Organization, 17, 242

Tholen, D. J. 1989, in Asteroids II, ed. R. P. Binzel, T. Gehrels, & M. S. Matthews, 1139–1150

Thomas, C. A., Emery, J. P., Trilling, D. E., et al. 2014, Icarus, 228, 217

Toon, O. B., Zahnle, K., Morrison, D., Turco, R. P., & Covey, C. 1997, Reviews of Geophysics, 35, 41

Treiman, A. H., Gleason, J. D., & Bogard, D. D. 2000, Planet. Space Sci., 48, 1213

Trilling, D. E., Mueller, M., Hora, J. L., et al. 2010, AJ, 140, 770

Tsirvoulis, G. & Michel, P. 2016, Physical Properties of Near-Earth Asteroids, ed. M. Vasile & E. Minisci, 83–102

Tubiana, C., Snodgrass, C., Michelsen, R., et al. 2015, A&A, 584, A97

Ureche, V. 1982, Astroizi, ed. C. Damina, 250–252

Šegon, D., Gural, P., Andreić, Ž., et al. 2014, Meteoroids 2013

Šegon, D., Vaubaillon, J., Gural, P. S., et al. 2017, A&A, 598, A15

Vaduvescu, O., Birlan, M., Tudorica, A., et al. 2013, Planet. Space Sci., 85, 299

Vaduvescu, O., Macias, A. A., Tudor, V., et al. 2017, Earth Moon and Planets, 120, 41

Valsecchi, G. B., Jopek, T. J., & Froeschle, C. 1999, MNRAS, 304, 743

Vaubaillon, J., Colas, F., & Jorda, L. 2005, A&A, 439, 751

Vernazza, P., Beck, P., Lamy, P., & Guilbert-Lepoutre, A. 2016, Romanian Astronomical Journal, 26, 35

Walsh, K. J., Delbo', M., Mueller, M., Binzel, R. P., & DeMeo, F. E. 2012, ApJ, 748, 104

Warner, B. 2018, Minor Planet Bul., 45

Warner, B. D. 2014a, Minor Planet Bulletin, 41, 113

Warner, B. D. 2014b, Minor Planet Bulletin, 41, 213

Warner, B. D. 2016a, Minor Planet Bulletin, 43, 240

Warner, B. D. 2016b, Minor Planet Bulletin, 43, 66

Warner, B. D. 2017, Minor Planet Bulletin, 44, 223

Weisberg, M. K., McCoy, T. J., & Krot, A. N. 2006, Systematics and Evaluation of Meteorite Classification, ed. D. S. Lauretta & H. Y. McSween, 19–52

Weisberg, M. K., Smith, C., Benedix, G., et al. 2008, Meteoritics and Planetary Science, 43, 1551

Weiss, E. 1868, Astronomische Nachrichten, 72, 81

Weissman, P. R., A'Hearn, M. F., Rickman, H., & McFadden, L. A. 1989, in Asteroids II, ed. R. P. Binzel, T. Gehrels, & M. S. Matthews, 880–920

Whipple, F. L. 1983, IAU Circ., 3881

Williams, I. P. 2011, Astronomy and Geophysics, 52, 2.20

Wisniewski, W. Z., Michałowski, T. M., Harris, A. W., & McMillan, R. S. 1997, Icarus, 126, 395

Wlotzka, F. 1993, Meteoritics, 28

Wlotzka, F. 1995, Meteoritics, 30, 792

York, D. G., Adelman, J., Anderson, Jr., J. E., et al. 2000, AJ, 120, 1579

Zellner, B., Tholen, D. J., & Tedesco, E. F. 1985, Icarus, 61, 355

Zheng, C., Ping, J., & Wang, M. 2016, Icarus, 278, 119

Zhu, M.-H., Fa, W., Ip, W.-H., et al. 2014, Geophys. Res. Lett., 41, 328

Żołądek, P., Olech, A., Wiśniewski, M., et al. 2016, in Proceedings of the International Meteor Conference Egmond, the Netherlands, 2-5 June 2016, ed. A. Roggemans & P. Roggemans, 358–360

# List of Figures

# List of Tables

# Appendix A

# Pseudocode

**Listing A.1:** The structure of an object

```
typedef struct{
        string name;
        double a, e, i, q, peri, node;
        int type;
}
```

**Listing A.2:** The code for D-Criteria of Jopek

```
double eq_I12(object obj1, object obj2){
   return acos(cos(obj1.i*deg2rad)*cos(obj2.i*deg2rad)+
          sin(obj1.i*deg2rad)*sin(obj2.i*deg2rad)*
          cos((obj1.node-obj2.node)*deg2rad));
}

double eq_t12(object obj1, object obj2, double I12 ,

   return (obj1.peri-obj2.peri)*deg2rad +
           sign*2*asin(cos((obj1.i+obj2.i)/2*deg2rad)*
           sin((obj1.node-obj2.node)/2* deg2rad)*
           (1/cos(I12/2)));
}

bool obj_compare_2node(object obj1, object obj2,

    if(I12<0){
       std::cout << "I12 < 0 !!!!"; return false;}
    if((obj1.node-obj2.node>180)&&(cos(I12/2)>0.0))
       {return true;}
    return false;
}

// D-h function
double d_jopek(object obj1, object obj2, float prag)
```

```
{
    double elem1=0.0, elem2=0.0, elem3=0.0, elem4=0.0;
    double elem5=0.0, total=0.0, I12=0.0, t12=0.0;

    elem1=obj1.e-obj2.e;
    elem2=(obj1.q-obj2.q)/(obj1.q+obj2.q);
    I12=eq_I12(obj1, obj2);
    elem3=2*sin(I12/2);
    elem4=(obj1.e + obj2.e)/2;
    if(obj_compare_2node(obj1, obj2, I12)){
        t12=eq_t12(obj1, obj2, I12, -1.);
    }
    else{
        t12=eq_t12(obj1, obj2, I12);
    }
    elem5=2*sin(t12/2);

    total=sqrt(elem1*elem1+elem2*elem2+elem3*elem3+
            (elem4*elem4)*(elem5*elem5));

    if(total>prag){return -999;}
    return total;
}
```

**Listing A.3:** The structure of an pair

```
typedef struct{
    object obj1, obj2;
    double dsh, dacs, dj;
};
```

# Appendix B

# Objects found in SMASS–MIT UH–IRTF and processed with M4AST



**Table B.1:** Spectra found in SMASS–MIT UH–IRTF database and the taxonomic classes associated using M4AST.

| Object | File name | $\lambda_{min}$ | $\lambda_{max}$ | Taxonomy | Figure | Status | Meteorite | Type | Figure |
|---|---|---|---|---|---|---|---|---|---|
| (267729)2003FC5 | $a267729.sp98$ | 0.78 | 2.4 | K | Fig. 4.8a | 1 | | | |
| 2001EC | $au2001EC.8$ | 0.53 | 0.9275 | Sq | Fig. 4.10a | 2 | | | |
| 2000DO1 | $au2000DO1visir8.visir$ | 0.495 | 1.6511 | V | Fig. 4.12a | 2 | | | |
| (4179)Toutatis | $004179/sp03$ | 0.435 | 2.475 | Sr | Fig. 4.15a | 1 | | | |
| | $004179/sp30$ | 0.435 | 2.475 | Sq | Fig. 4.15b | 1 | | | |
| | $004179/sp73$ | 0.435 | 2.475 | Sq | Fig. 4.15c | 1 | | | |
| | $004179/sp74$ | 0.435 | 2.475 | Q | Fig. 4.15d | 1 | Marilia | OC | Fig. 4.32 |
| | $004179/sp115n1$ | 0.435 | 2.475 | Sq | Fig. 4.15e | 1 | | | |
| | $004179/sp116$ | 0.435 | 2.475 | Sq | Fig. 4.15f | 1 | | | |

**Table B.1:** continued.

| Object | File name | $\lambda_{min}$ | $\lambda_{max}$ | Taxonomy | Figure | Status | Meteorite | Type | Figure |
|---|---|---|---|---|---|---|---|---|---|
| 2003UV11 | $au2003UV11.sp94$ | 0.78 | 2.45 | Sr | Fig. 4.17a | 1 | Dwaleni | OC | Fig. 4.33a |
| 2003UV11 | $au2003UV11.sp95$ | 0.78 | 2.465 | Q | Fig. 4.17b | 1 | | | |
| 2007RU17 | $au2007RU17.sp94$ | 0.8 | 2.45 | Q | Fig. 4.18a | 1 | Dwaleni | OC | Fig. 4.33b |
| (3671)Diomysus | $a003671.sp91$ | 0.435 | 2.45 | Ch | Fig. 4.20a | 1 | | | |
| 2006HQ30 | $au2006HQ30.sp51$ | 0.82 | 2.46 | Q | Fig. 4.21a | 1 | Kunashak | OC | Fig. 4.34 |
| (446791)1998SJ70 | $au1998SJ74.sp70$ | 0.78 | 2.45 | Q | Fig. 4.24a | 1 | Wethersfield(1971) | OC | Fig. 4.31a |
| | | | | | | | Schenectady | OC | Fig. 4.31b |
| 2002AU5 | $au2002AU5.8$ | 0.505 | 0.92 | X | Fig. 4.29a | 2 | | | |
| (162058)1997AE12 | $au1997AE12.sp26$ | 0.49 | 2.445 | Q | Fig. 4.26a | 1 | | | |

(1)–unpublished (2)–published (Binzel et al. 2004)

# Appendix C

# Meteor showers data used



**Table C.1:** List of associated meteor showers. In the table are presented all the information used in mt statistic:IAU number and code, name, the geocentric speed ($V_g$), the orbital elements references(regarding the orbital elements), the maximum activity pick (day and mount), the zenithal hourly rate of the meteor shower, the references for those data and the known associated parent body.

| No | Code | Meteor shower | $V_g$ | a[a.u.] | q[a.u.] | e | $\Omega$[deg] | $\omega$[deg] | inc[deg] | Ref. | Activity | ZHR | Ref. | Parent body |
|---|---|---|---|---|---|---|---|---|---|---|---|---|---|---|
| 018 | AND | Andromedids | 18.2 | 2.990 | 0.759 | 0.742 | 243.7 | 222.5 | 9.4 | 1 | 08/11 | 1 | 10 | 3D/Biela |
| 144 | APS | Daytime April Piscids | 29.2 | 1.530 | 0.249 | 0.837 | 49.5 | 26.0 | 4.5 | 4 | 22/04 | L | 10 | 2005 NZ6? |
| 197 | AUD | August Draconids | 21.1 | 2.820 | 1.008 | 0.644 | 188.7 | 142.6 | 33.8 | 1 | 21-25/08 | 1 | 12 | |
| 021 | AVB | $\alpha$ Virginids | 18.8 | 2.550 | 0.744 | 0.716 | 247.9 | 30.0 | 7 | 2 | 7,18/04 | 5 | 13 | 1998 SH2? |
| 173 | BTA | Daytime $\beta$ Taurids | 27.4 | 1.660 | 0.325 | 0.804 | 238.3 | 277.0 | 3.6 | | 28/06 | M | 11 | 2P/Encke |

**Table C.1:** continued.

| No | Code | Meteor shower | $V_g$ | a[a.u.] | q[a.u.] | e | $\Omega$[deg] | $\omega$[deg] | inc[deg] | Ref. | Activity | ZHR | Ref. | Parent body |
|---|---|---|---|---|---|---|---|---|---|---|---|---|---|---|
| 001 | CAP | $\alpha$ Capricornids | 23.0 | 2.540 | 0.578 | 0.774 | 268.9 | 125.4 | 7.5 | 1 | 30/07 | 5 | 10 | 169P/NEAT |
| 063 | COR | Corvids | 8.70 | 2.350 | 0.999 | 0.571 | 193.7 | 91.8 | 2.6 | 1 | 27/06 | | 11 | 2004 HW |
| 325 | DLT | Daytime $\lambda$ Taurids | 36.4 | 1.570 | 0.104 | 0.933 | 210.8 | 1.7 | 23.2 | 3 | | | | |
| 446 | DPC | December $\phi$ Cassiopeiids | 16.5 | 3.100 | 0.896 | 0.714 | 218.7 | 252.1 | 18 | 5 | | | | 3D/Biela |
| 221 | DSX | Daytime Sextantids | 32.9 | 1.140 | 0.147 | 0.874 | 214.3 | 6.4 | 24.3 | 1 | 27/09 | M | 10 | 2005 UD |
| 011 | EVI | $\eta$ Virginids | 26.6 | 2.470 | 0.460 | 0.812 | 281.0 | 355.7 | 5.4 | 1 | 18/03 | 1 | 13 | D/1766 G1 |
| 004 | GEM | Geminids | 33.8 | 1.310 | 0.145 | 0.889 | 324.3 | 261.7 | 22.9 | 1 | 14/12 | 120 | 11 | 3200 Phaethon |
| 343 | HVI | $h$ Virginids | 17.2 | 2.280 | 0.742 | 0.659 | 72.7 | 218.2 | 0.9 | 2 | 01/05 | 1 | 10 | |
| 012 | KCG | $\kappa$ Cygnids | 20.9 | 2.950 | 0.995 | 0.662 | 196.9 | 140.0 | 32.5 | 1 | 17/08 | 3 | 11 | |
| 096 | NCC | Northern $\delta$ Cancrids | 27.2 | 2.230 | 0.410 | 0.814 | 286.6 | 290.0 | 2.7 | | 14/01 | | 11 | 1991 AQ |
| 033 | NIA | Northern $\iota$ Aquariids | 31.3 | 1.760 | 0.234 | 0.874 | 310.5 | 147.8 | 5.9 | 1 | 25/08 | 3 | 11 | |
| 017 | NTA | Northern Taurids | 28.0 | 2.130 | 0.355 | 0.829 | 294.6 | 220.6 | 3 | 1 | 12/11 | 5 | 10 | 2P/Encke, 2004 TG10 |
| 233 | OCC | October Capricornids | -15.3 | 4.264 | 0.987 | 0.768 | 190.8 | 203.8 | 0.8 | 6 | 02/10 | 1 | 14 | D/1978 R1 |
| 338 | OER | $o$ Eridanids | 28.5 | 3.920 | 0.497 | 0.875 | 94.1 | 49.2 | 19.6 | 1 | 22/11 | 1 | 11 | |
| 257 | ORS | Southern $\chi$ Orionids | 27.9 | 2.160 | 0.381 | 0.828 | 111.3 | 64.3 | 5.3 | | 10/12 | 3 | 11 | 2010 LU108, 2002 XM35 |

**Table C.1:** continued.

| No | Code | Meteor shower | $V_g$ | a[a.u.] | q[a.u.] | e | $\Omega$[deg] | $\omega$[deg] | inc[deg] | Ref. | Activity | ZHR | Ref. | Parent body |
|---|---|---|---|---|---|---|---|---|---|---|---|---|---|---|
| 137 | PPU | $\pi$ Puppids | 15.0 | 2.970 | 1.000 | 0.660 | 359.0 | 33.6 | 21 | 7 | 23/04 | var | 11 | 26P/Grigg-Skjellerup |
| 097 | SCC | Southern $\delta$ Cancrids | 27.0 | 2.260 | 0.430 | 0.811 | 105.0 | 109.3 | 4.7 | | 20/01 | 1 | 11 | 2001 YB5 |
| 156 | SMA | Southern Daytime May Arietids | 28.3 | 1.510 | 0.272 | 0.820 | 231.7 | 227.1 | 5.1 | 3 | 16/05 | L | 11 | |
| 069 | SSG | Southern $\mu$ Sagittariids | 25.1 | 2.020 | 0.457 | 0.769 | 104.5 | 266.4 | 6 | 2 | 19/06 | | 15 | |
| 002 | STA | Southern Taurids | 26.6 | 1.950 | 0.353 | 0.798 | 116.6 | 34.4 | 5.3 | 1 | 10/10 | 5 | 10 | 2P/Encke |
| 061 | TAH | $\tau$ Herculids | 15.0 | 2.695 | 0.970 | 0.640 | 204.2 | 72.6 | 18.6 | 8 | 09/06 | 1 | 13 | 73P/Schwassmann-Wachmann 3 |
| 100 | XSA | Daytime $\xi$ Sagittariids | 24.4 | 1.080 | 0.285 | 0.740 | 46.9 | 304.9 | 1.1 | 9 | 09/01 | | 11 | |
| 172 | ZPE | Daytime $\zeta$ Perseids | 26.4 | 1.550 | 0.335 | 0.784 | 58.4 | 75.0 | 3.8 | 3 | 09/06 | H | 10 | 2P/Encke |

(1) (Jenniskens et al. 2016a); (2) (Jenniskens et al. 2016b); (3) (Brown et al. 2008); (4) (Brown et al. 2010); (5) (Jenniskens et al. 2016c); (6) (Terentjeva 1989); (7) (Jenniskens 1994); (8) (Lindblad 1971a); (9) (Sekanina 1976); (10) web[a]; (11) (Kronk 2014); (12) (Denning 1907); (13) web[b]; (14) web[c]; (15) web[d];

[a] https://www.imo.net/files/meteor-shower/cal2018.pdf
[b] http://meteorshowersonline.com/
[c] http://cams.seti.org/maps.html
[d] https://ntrs.nasa.gov/archive/nasa/casi.ntrs.nasa.gov/20170001495.pdf

# Appendix D

# D-parameter and Lyapunov time



**Table D.1:** D–parameter and Lyapunov time for all asteroids–meteor showers associations. The columns are: the asteroid name, the orbital elements used for MPCORB, the Lyapunov time and its error, associated meteor shower and the D–parameter for all metrics.

| Asteroid | a[a.u.] | e | i[deg.] | q[a.u.] | Ω[deg.] | $\omega$[deg.] | $T_L$ | Shower | $D_{acs}$ | $D_{sh}$ | $D_j$ |
|---|---|---|---|---|---|---|---|---|---|---|---|
| (152770)1999RR28 | 1.879 | 0.653 | 7.135 | 0.651 | 284.34 | 178.40 | 48 | AND | | 0.1840 | 0.1676 |
| (155140)2005UD | 1.275 | 0.872 | 28.679 | 0.163 | 207.58 | 19.74 | 478 | DSX | | 0.1521 | 0.1595 |
| (162058)1997AE12 | 2.367 | 0.554 | 4.853 | 1.055 | 60.85 | 304.81 | 172 | COR | 0.0431 | 0.1952 | 0.1889 |
| (162195)1999RK45 | 1.598 | 0.773 | 5.892 | 0.363 | 4.10 | 120.03 | 465 | ZPE | 0.0414 | 0.1502 | 0.1528 |
| (2101)Adonis | 1.874 | 0.765 | 1.326 | 0.441 | 43.48 | 349.62 | 34 | ORS | | 0.1563 | 0.1617 |
| (267729)2003FC5 | 1.916 | 0.609 | 5.826 | 0.749 | 270.65 | 189.24 | 119 | AND | | 0.1794 | 0.1792 |
| (3200)Phaethon | 1.271 | 0.890 | 22.256 | 0.140 | 322.17 | 265.23 | 226 | GEM | 0.0171 | 0.0319 | 0.0362 |
| (325102)2008EY5 | 0.626 | 0.627 | 5.109 | 0.234 | 106.53 | 245.58 | 84 | XSA | | 0.1485 | 0.1708 |
| (3671)Dionysus | 2.199 | 0.541 | 13.533 | 1.009 | 204.24 | 82.08 | 52 | TAH | | 0.1733 | 0.1700 |
| (417634)2006XG1 | 2.458 | 0.596 | 20.492 | 0.994 | 344.13 | 38.48 | 65 | PPU | | 0.1340 | 0.1339 |

**Table D.1:** continued.

| Asteroid | a[a.u.] | e | i[deg.] | q[a.u.] | Ω[deg.] | ω[deg.] | $T_L$ | Shower | $D_{acs}$ | $D_{sh}$ | $D_j$ |
|---|---|---|---|---|---|---|---|---|---|---|---|
| (4179)Toutatis | 2.538 | 0.629 | 0.448 | 0.942 | 278.58 | 124.61 | 59 | OCC | | 0.1804 | 0.1763 |
| (436671)2011SV71 | 2.626 | 0.611 | 13.430 | 1.021 | 190.46 | 80.61 | 120 | TAH | | 0.1319 | 0.1242 |
| (438105)2005GO22 | 1.914 | 0.824 | 1.585 | 0.337 | 18.73 | 62.02 | 35 | APS | | 0.1303 | 0.1778 |
| (446791)1998SJ70 | 2.238 | 0.705 | 7.306 | 0.660 | 246.89 | 21.55 | 44 | AVB | | 0.1453 | 0.1328 |
| (455176)1999VF22 | 1.313 | 0.739 | 3.903 | 0.343 | 271.69 | 3.51 | 39 | EVI | | 0.1423 | 0.1666 |
| (455299)2002EL6 | 2.302 | 0.577 | 9.516 | 0.973 | 186.51 | 84.94 | 60 | TAH | | 0.1874 | 0.1874 |
| (480822)1998YM4 | 1.477 | 0.719 | 3.433 | 0.414 | 344.53 | 341.77 | 89 | SCC | | 0.1830 | 0.1833 |
| (483423)2000DO1 | 1.430 | 0.682 | 3.457 | 0.455 | 302.71 | 335.87 | 38 | EVI | | 0.1394 | 0.1394 |
| (494658)2000UG11 | 1.928 | 0.573 | 8.924 | 0.824 | 240.56 | 224.17 | 85 | AND | | 0.1823 | 0.1752 |
| (503941)2003UV11 | 1.453 | 0.763 | 5.924 | 0.345 | 124.78 | 31.92 | 86 | BTA | | 0.1498 | 0.1514 |
| (503941)2003UV11 | | | | | | | | NTA | | 0.1703 | 0.1706 |
| (503941)2003UV11 | | | | | | | | STA | | 0.0866 | 0.0871 |
| (509191)2006OC5 | 2.400 | 0.653 | 4.747 | 0.834 | 245.73 | 149.19 | 127 | OCC | | 0.2064 | 0.1617 |
| (85182)1991AQ | 2.222 | 0.777 | 3.128 | 0.496 | 242.96 | 339.68 | 94 | NCC | 0.0381 | 0.1324 | 0.1384 |
| 1995CS | 1.939 | 0.774 | 2.596 | 0.439 | 252.82 | 135.15 | 60 | CAP | | 0.1853 | 0.1836 |
| 1995FF | 2.317 | 0.709 | 0.595 | 0.673 | 296.81 | 171.98 | 56 | AND | | 0.1852 | 0.1748 |
| 1996MQ | 2.409 | 0.583 | 3.461 | 1.004 | 29.86 | 262.13 | 75 | COR | 0.0274 | 0.1246 | 0.1245 |
| 1997GD32 | 2.093 | 0.598 | 5.255 | 0.842 | 226.60 | 55.28 | 101 | AVB | | 0.1686 | 0.1507 |
| 1997UZ10 | 2.837 | 0.620 | 12.779 | 1.079 | 359.10 | 38.66 | 301 | PPU | | 0.1791 | 0.1651 |
| 1998LE | 1.518 | 0.700 | 9.174 | 0.456 | 132.94 | 237.55 | 46 | SSG | | 0.1096 | 0.1096 |
| 1998SH2 | 2.744 | 0.714 | 2.403 | 0.785 | 268.32 | 6.46 | 172 | AVB | | 0.1022 | 0.0973 |
| 1999LW1 | 1.438 | 0.682 | 6.672 | 0.457 | 168.54 | 204.61 | 229 | SSG | | 0.1467 | 0.1467 |
| 1999RK33 | 2.498 | 0.583 | 2.840 | 1.042 | 55.75 | 317.71 | 61 | COR | 0.0508 | 0.1058 | 0.0989 |
| 2001EC | 2.579 | 0.773 | 0.592 | 0.586 | 108.58 | 323.02 | 34 | CAP | | 0.1435 | 0.1435 |
| 2001FB90 | 2.467 | 0.777 | 1.883 | 0.549 | 15.15 | 265.62 | 116 | EVI | | 0.1499 | 0.1494 |

**Table D.1:** continued.

| Asteroid | a[a.u.] | e | i[deg.] | q[a.u.] | Ω[deg.] | $\omega$[deg.] | $T_L$ | Shower | $D_{acs}$ | $D_{sh}$ | $D_j$ |
|---|---|---|---|---|---|---|---|---|---|---|---|
| 2001QJ96 | 1.592 | 0.797 | 5.858 | 0.323 | 121.63 | 338.76 | 50 | SMA | 0.0382 | 0.1689 | 0.1823 |
| 2001SZ269 | 2.364 | 0.662 | 2.452 | 0.800 | 191.13 | 98.96 | 54 | HVI | 0.0391 | 0.0784 | 0.0650 |
| 2001TA2 | 1.770 | 0.647 | 3.266 | 0.625 | 227.36 | 50.41 | 48 | AVB | | 0.1551 | 0.1321 |
| 2001UX4 | 1.721 | 0.753 | 8.943 | 0.426 | 333.82 | 182.44 | 71 | NTA | | 0.1593 | 0.1691 |
| 2002AU5 | 2.021 | 0.754 | 9.185 | 0.497 | 21.53 | 354.82 | 137 | SSG | 0.0575 | 0.2042 | |
| 2002CB26 | 1.988 | 0.731 | 6.867 | 0.535 | 266.06 | 139.38 | 160 | CAP | | 0.1603 | 0.1592 |
| 2002CN15 | 1.325 | 0.696 | 6.123 | 0.403 | 332.14 | 298.58 | 205 | EVI | | 0.1783 | 0.1815 |
| 2002FU5 | 2.506 | 0.701 | 4.234 | 0.748 | 156.54 | 111.61 | 89 | AVB | 0.0525 | 0.1823 | 0.1823 |
| 2002GJ8 | 3.234 | 0.681 | 30.109 | 1.031 | 174.42 | 144.87 | 63 | AUD | | 0.1638 | 0.1626 |
| 2002GM5 | 2.113 | 0.695 | 7.280 | 0.645 | 274.51 | 13.47 | 82 | AVB | | 0.1652 | 0.1503 |
| 2002NW | 1.611 | 0.669 | 6.041 | 0.534 | 288.21 | 102.19 | 41 | CAP | | 0.1348 | 0.1334 |
| 2002PX39 | 2.454 | 0.593 | 1.799 | 1.000 | 140.65 | 135.33 | 104 | COR | 0.0432 | 0.1041 | 0.1041 |
| 2002RC117 | 2.443 | 0.633 | 2.502 | 0.896 | 222.01 | 169.88 | 81 | OCC | | 0.1691 | 0.1505 |
| 2003FB5 | 2.521 | 0.797 | 5.514 | 0.511 | 292.21 | 354.70 | 154 | EVI | 0.0226 | 0.1527 | 0.1533 |
| 2003LW1 | 2.119 | 0.508 | 12.361 | 1.043 | 199.02 | 75.05 | 391 | TAH | | 0.1882 | 0.1774 |
| 2003RE2 | 2.467 | 0.540 | 2.493 | 1.134 | 33.17 | 299.27 | 256 | COR | 0.0496 | 0.1805 | 0.1357 |
| 2003UQ25 | 2.540 | 0.681 | 2.130 | 0.811 | 276.79 | 187.23 | 36 | AND | | 0.1596 | 0.1544 |
| 2004GB2 | 2.117 | 0.651 | 12.445 | 0.738 | 254.94 | 209.40 | 329 | AND | | 0.1170 | 0.1160 |
| 2004HC39 | 1.812 | 0.501 | 14.658 | 0.905 | 224.21 | 56.09 | 722 | TAH | | 0.1917 | 0.1837 |
| 2004LA10 | 2.509 | 0.576 | 1.080 | 1.063 | 141.79 | 139.08 | 85 | COR | 0.0594 | 0.0871 | 0.0665 |
| 2004MC | 2.437 | 0.592 | 2.419 | 0.993 | 204.04 | 91.24 | 65 | COR | 0.0361 | 0.1016 | 0.1015 |
| 2004NU7 | 2.233 | 0.545 | 0.896 | 1.017 | 137.89 | 133.47 | 65 | COR | 0.0557 | 0.1455 | 0.1447 |
| 2004RW10 | 2.351 | 0.593 | 3.110 | 0.957 | 71.77 | 206.16 | 30 | COR | 0.0239 | 0.1238 | 0.1184 |
| 2004SA20 | 2.409 | 0.710 | 2.986 | 0.698 | 149.46 | 133.67 | 30 | AVB | | 0.1634 | 0.1600 |
| 2004TG10 | 2.234 | 0.862 | 4.180 | 0.309 | 317.37 | 205.10 | 75 | BTA | | 0.1457 | 0.1471 |

**Table D.1:** continued.

| Asteroid | a[a.u.] | e | i[deg.] | q[a.u.] | Ω[deg.] | ω[deg.] | $T_L$ | Shower | $D_{acs}$ | $D_{sh}$ | $D_j$ |
|---|---|---|---|---|---|---|---|---|---|---|---|
| 2004TG10 | | | | | | | | NTA | 0.0520 | 0.1245 | 0.1350 |
| 2004VY14 | 1.961 | 0.650 | 7.026 | 0.686 | 230.34 | 60.41 | | AVB | | 0.1854 | 0.1807 |
| 2005JJ91 | 2.783 | 0.601 | 24.482 | 1.111 | 206.13 | 66.97 | 1721 | TAH | | 0.1856 | 0.1386 |
| 2005MR1 | 2.363 | 0.553 | 3.292 | 1.056 | 93.64 | 196.29 | 167 | COR | 0.0221 | 0.1099 | 0.0979 |
| 2005OF3 | 2.388 | 0.586 | 3.284 | 0.989 | 94.81 | 174.07 | 145 | COR | 0.0230 | 0.1822 | 0.1819 |
| 2005RA | 2.552 | 0.659 | 4.419 | 0.870 | 80.65 | 321.45 | 92 | OCC | | 0.2034 | 0.1778 |
| 2005RJ | 2.578 | 0.664 | 6.327 | 0.865 | 255.41 | 141.24 | 116 | OCC | | 0.1929 | 0.1634 |
| 2005RW3 | 2.105 | 0.644 | 2.700 | 0.749 | 219.62 | 48.92 | 79 | AVB | | 0.1546 | 0.1545 |
| 2005TB15 | 1.812 | 0.756 | 7.289 | 0.443 | 139.08 | 9.55 | 43 | STA | | 0.1190 | 0.1373 |
| 2005TD49 | 2.679 | 0.628 | 0.121 | 0.997 | 189.72 | 198.59 | 129 | OCC | | 0.1604 | 0.1602 |
| 2005TE | 1.750 | 0.578 | 6.493 | 0.739 | 270.94 | 12.77 | 45 | AVB | | 0.1578 | 0.1577 |
| 2005XN27 | 2.406 | 0.633 | 0.299 | 0.882 | 169.90 | 215.14 | 46 | OCC | | 0.2070 | 0.1871 |
| 2006BF56 | 2.342 | 0.799 | 0.962 | 0.470 | 102.62 | 125.26 | 31 | NCC | 0.0504 | 0.1817 | 0.1846 |
| 2006HQ30 | 2.595 | 0.607 | 12.023 | 1.020 | 180.03 | 85.49 | 403 | TAH | | 0.1904 | 0.1855 |
| 2006JO | 2.377 | 0.667 | 8.200 | 0.791 | 248.32 | 41.07 | 125 | AVB | | 0.1568 | 0.1526 |
| 2006PF1 | 2.194 | 0.877 | 14.533 | 0.270 | 335.11 | 125.36 | 199 | NIA | | 0.1712 | 0.1822 |
| 2006UF17 | 2.467 | 0.810 | 3.721 | 0.469 | 235.68 | 47.72 | 109 | EVI | 0.0294 | 0.1194 | 0.1195 |
| 2006XA3 | 2.364 | 0.624 | 4.990 | 0.888 | 308.61 | 84.75 | 149 | OCC | | 0.1989 | 0.1805 |
| 2007EJ88 | 2.330 | 0.779 | 1.912 | 0.514 | 204.74 | 79.77 | 33 | EVI | | 0.1575 | 0.1580 |
| 2007GU1 | 2.206 | 0.645 | 9.158 | 0.784 | 243.42 | 25.83 | 224 | AVB | | 0.1364 | 0.1331 |
| 2007LW19 | 2.349 | 0.582 | 2.127 | 0.983 | 233.03 | 63.65 | 56 | COR | 0.0135 | 0.1162 | 0.1154 |
| 2007RS146 | 2.366 | 0.644 | 2.665 | 0.843 | 158.23 | 132.20 | 49 | HVI | 0.0448 | 0.1127 | 0.0813 |
| 2007RU17 | 2.039 | 0.828 | 9.080 | 0.351 | 129.84 | 17.47 | 50 | STA | | 0.0953 | 0.0953 |
| 2007TC14 | 2.090 | 0.806 | 4.659 | 0.405 | 272.60 | 220.90 | 169 | ZPE | | 0.1589 | 0.1710 |
| 2007UL12 | 1.970 | 0.806 | 4.187 | 0.382 | 95.66 | 67.12 | 62 | BTA | | 0.1769 | 0.1858 |
| 2007UL12 | | | | | | | | NTA | | 0.1673 | 0.1691 |

**Table D.1:** continued.

| Asteroid | a[a.u.] | e | i[deg.] | q[a.u.] | Ω[deg.] | $\omega$[deg.] | $T_L$ | Shower | $D_{acs}$ | $D_{sh}$ | $D_j$ |
|---|---|---|---|---|---|---|---|---|---|---|---|
| 2007UL12 | | | | | | | | ORS | | 0.1849 | 0.1849 |
| 2007UL12 | | | | | | | | STA | 0.0221 | 0.1733 | 0.1754 |
| 2007WW3 | 3.109 | 0.653 | 6.484 | 1.079 | 345.74 | 51.05 | 40 | OCC | | 0.1958 | 0.1784 |
| 2007YP56 | 1.990 | 0.706 | 1.669 | 0.584 | 93.81 | 272.52 | 50 | SSG | | 0.1713 | 0.1676 |
| 2008BO16 | 2.432 | 0.811 | 8.475 | 0.459 | 258.36 | 130.07 | 522 | CAP | 0.0546 | 0.1509 | 0.1476 |
| 2008CA22 | 2.031 | 0.728 | 8.118 | 0.552 | 322.56 | 307.70 | 59 | EVI | | 0.1825 | 0.1820 |
| 2008LB | 2.455 | 0.607 | 4.223 | 0.965 | 213.33 | 79.16 | 57 | COR | 0.0577 | 0.0928 | 0.0881 |
| 2008RT | 2.486 | 0.567 | 21.323 | 1.077 | 13.24 | 17.65 | 234 | PPU | | 0.1577 | 0.1423 |
| 2008SH148 | 2.751 | 0.657 | 3.847 | 0.943 | 202.09 | 201.24 | 37 | OCC | | 0.1697 | 0.1654 |
| 2008VL14 | 2.203 | 0.821 | 1.909 | 0.394 | 246.65 | 37.32 | 61 | EVI | | 0.1424 | 0.1480 |
| 2008WZ94 | 1.522 | 0.774 | 6.528 | 0.344 | 320.95 | 248.93 | | NCC | | 0.1464 | 0.1572 |
| 2008XQ2 | 2.199 | 0.553 | 14.529 | 0.984 | 355.07 | 34.59 | 104 | PPU | | 0.1600 | 0.1594 |
| 2008XU2 | 2.454 | 0.620 | 2.967 | 0.932 | 334.14 | 62.41 | 45 | OCC | | 0.1715 | 0.1650 |
| 2009FU4 | 2.381 | 0.616 | 12.916 | 0.914 | 233.05 | 42.15 | 68 | TAH | | 0.1824 | 0.1761 |
| 2009HS44 | 2.574 | 0.701 | 2.439 | 0.768 | 73.14 | 209.17 | 92 | AVB | | 0.1757 | 0.1747 |
| 2009QG2 | 2.288 | 0.566 | 3.005 | 0.994 | 39.88 | 305.31 | 43 | COR | 0.0225 | 0.1190 | 0.1189 |
| 2009SB15 | 2.047 | 0.678 | 4.166 | 0.660 | 169.78 | 313.61 | 56 | AVB | | 0.1585 | 0.1471 |
| 2009SD15 | 2.346 | 0.621 | 2.904 | 0.889 | 304.23 | 356.54 | 87 | HVI | 0.0561 | 0.1978 | 0.1601 |
| 2009ST103 | 2.688 | 0.722 | 15.929 | 0.747 | 233.84 | 227.23 | 389 | AND | | 0.1352 | 0.1350 |
| 2009ST171 | 2.578 | 0.609 | 3.744 | 1.009 | 206.01 | 186.55 | 49 | OCC | | 0.1708 | 0.1698 |
| 2009SX17 | 2.338 | 0.541 | 1.403 | 1.072 | 60.32 | 304.37 | 241 | COR | 0.0364 | 0.1710 | 0.1585 |
| 2009TA1 | 2.290 | 0.664 | 12.349 | 0.769 | 271.74 | 204.09 | 99 | AND | | 0.1651 | 0.1649 |
| 2009WJ1 | 2.468 | 0.674 | 0.616 | 0.805 | 194.78 | 276.83 | 43 | AND | | 0.1898 | 0.1865 |
| 2010CF55 | 1.900 | 0.760 | 5.159 | 0.456 | 322.04 | 311.31 | 56 | EVI | | 0.0974 | 0.0974 |
| 2010CR5 | 3.186 | 0.824 | 5.395 | 0.560 | 52.58 | 320.29 | 90 | SSG | | 0.1499 | 0.1487 |

**Table D.1:** continued.

| Asteroid | a[a.u.] | e | i[deg.] | q[a.u.] | Ω[deg.] | ω[deg.] | $T_L$ | Shower | $D_{acs}$ | $D_{sh}$ | $D_j$ |
|---|---|---|---|---|---|---|---|---|---|---|---|
| 2010FL | 1.916 | 0.655 | 11.409 | 0.662 | 214.07 | 66.66 | 324 | AVB | | 0.1638 | 0.1532 |
| 2010GE35 | 2.224 | 0.617 | 5.403 | 0.852 | 233.17 | 34.33 | 95 | AVB | | 0.1922 | 0.1729 |
| 2010GH65 | 2.704 | 0.611 | 21.053 | 1.051 | 228.00 | 42.78 | 2299 | TAH | 0.0517 | 0.2045 | |
| 2010RB12 | 2.370 | 0.630 | 5.269 | 0.878 | 228.93 | 161.68 | 100 | OCC | | 0.2003 | 0.1779 |
| 2010RL43 | 2.344 | 0.622 | 0.612 | 0.886 | 2.52 | 289.17 | 36 | HVI | 0.0428 | 0.1493 | 0.0973 |
| 2010RZ11 | 2.337 | 0.634 | 1.280 | 0.855 | 292.55 | 348.88 | 46 | HVI | 0.0320 | 0.1615 | 0.1352 |
| 2010TD | 2.177 | 0.676 | 3.228 | 0.706 | 100.18 | 187.89 | 48 | HVI | 0.0557 | 0.0673 | 0.0622 |
| 2010TN167 | 1.698 | 0.588 | 5.385 | 0.700 | 264.41 | 201.38 | 56 | AND | | 0.1851 | 0.1801 |
| 2010TN55 | 2.303 | 0.789 | 0.257 | 0.486 | 243.07 | 35.22 | 81 | EVI | | 0.0998 | 0.1002 |
| 2010TP55 | 2.349 | 0.670 | 3.327 | 0.776 | 69.48 | 232.86 | 115 | HVI | 0.0493 | 0.1436 | 0.1413 |
| 2010TU149 | 2.201 | 0.828 | 1.971 | 0.378 | 91.71 | 59.71 | 59 | BTA | | 0.1227 | 0.1338 |
| 2010TU149 | | | | | | | | NTA | 0.0297 | 0.1039 | 0.1061 |
| 2010TU149 | | | | | | | | STA | | 0.0745 | 0.0781 |
| 2010TV54 | 1.916 | 0.615 | 6.195 | 0.738 | 254.98 | 202.36 | 88 | AND | | 0.1801 | 0.1794 |
| 2010UY6 | 2.654 | 0.616 | 19.881 | 1.021 | 20.18 | 9.13 | 219 | PPU | | 0.1586 | 0.1576 |
| 2010VF | 1.854 | 0.754 | 3.709 | 0.456 | 271.55 | 17.19 | 44 | EVI | | 0.1783 | 0.1784 |
| 2010VN139 | 1.874 | 0.748 | 1.511 | 0.471 | 182.85 | 335.44 | 56 | NTA | | 0.1626 | 0.1809 |
| 2010XC11 | 2.516 | 0.850 | 9.110 | 0.377 | 121.28 | 94.22 | 90 | SCC | | 0.1073 | 0.1142 |
| 2011BM45 | 1.921 | 0.803 | 5.324 | 0.378 | 63.11 | 302.33 | 259 | SSG | 0.0488 | 0.1309 | 0.1408 |
| 2011BW10 | 1.619 | 0.721 | 5.913 | 0.451 | 64.81 | 308.47 | 144 | SSG | | 0.0931 | 0.0931 |
| 2011BY18 | 2.264 | 0.783 | 3.646 | 0.490 | 240.08 | 135.25 | 100 | SSG | | 0.1700 | 0.1703 |
| 2011CG50 | 1.680 | 0.702 | 13.322 | 0.501 | 249.15 | 146.33 | 347 | CAP | | 0.1600 | 0.1573 |
| 2011CT4 | 1.726 | 0.719 | 2.648 | 0.485 | 69.53 | 304.92 | 48 | SSG | | 0.1042 | 0.1046 |
| 2011EF17 | 2.344 | 0.743 | 4.216 | 0.602 | 282.30 | 3.96 | 71 | AVB | | 0.1914 | 0.1662 |
| 2011GP65 | 2.362 | 0.645 | 11.652 | 0.839 | 274.33 | 14.73 | 63 | AVB | | 0.2016 | 0.1875 |

**Table D.1:** continued.

| Asteroid | a[a.u.] | e | i[deg.] | q[a.u.] | Ω[deg.] | $\omega$[deg.] | $T_L$ | Shower | $D_{acs}$ | $D_{sh}$ | $D_j$ |
|---|---|---|---|---|---|---|---|---|---|---|---|
| 2011HP4 | 2.181 | 0.614 | 3.439 | 0.842 | 233.84 | 41.54 | 121 | AVB | | 0.1585 | 0.1389 |
| 2011OL51 | 3.110 | 0.639 | 4.392 | 1.124 | 110.44 | 288.17 | 63 | OCC | | 0.2091 | 0.1708 |
| 2011QE38 | 2.420 | 0.578 | 1.599 | 1.022 | 65.77 | 326.55 | 117 | COR | 0.0300 | 0.0748 | 0.0721 |
| 2011TA4 | 3.095 | 0.650 | 19.698 | 1.083 | 20.79 | 11.71 | 158 | PPU | 0.0484 | 0.1587 | 0.1410 |
| 2011TC4 | 1.492 | 0.720 | 3.126 | 0.418 | 309.07 | 200.98 | 30 | BTA | | 0.1603 | 0.1809 |
| 2011TC4 | | | | | | | | NTA | | 0.1449 | 0.1538 |
| 2011TC4 | | | | | | | | STA | | 0.1783 | 0.1862 |
| 2011TJ | 1.938 | 0.637 | 4.965 | 0.703 | 218.72 | 59.94 | 184 | AVB | | 0.1096 | 0.1055 |
| 2011TX8 | 0.910 | 0.708 | 5.973 | 0.265 | 313.26 | 207.93 | 82 | BTA | | 0.1711 | 0.1896 |
| 2011YY62 | 2.467 | 0.659 | 5.411 | 0.840 | 129.74 | 262.81 | 101 | OCC | | 0.2043 | 0.1633 |
| 2012BJ14 | 2.062 | 0.743 | 6.399 | 0.529 | 85.44 | 297.51 | 80 | SSG | 0.0301 | 0.1837 | 0.1841 |
| 2012BL14 | 1.725 | 0.654 | 6.834 | 0.597 | 269.95 | 119.40 | 47 | CAP | | 0.1373 | 0.1370 |
| 2012BQ123 | 2.038 | 0.694 | 0.960 | 0.625 | 321.01 | 74.75 | 45 | CAP | | 0.1538 | 0.1516 |
| 2012BU61 | 2.525 | 0.778 | 5.225 | 0.561 | 73.69 | 296.61 | 139 | SSG | | 0.1176 | 0.1159 |
| 2012CC29 | 2.431 | 0.778 | 1.944 | 0.539 | 230.48 | 171.10 | 38 | CAP | | 0.1520 | 0.1510 |
| 2012ES10 | 1.881 | 0.756 | 6.791 | 0.459 | 73.17 | 346.34 | 101 | STA | 0.0545 | 0.1563 | 0.1738 |
| 2012FG | 2.074 | 0.633 | 2.206 | 0.760 | 288.92 | 178.22 | 46 | AND | | 0.1769 | 0.1769 |
| 2012FQ62 | 2.182 | 0.726 | 1.095 | 0.599 | 226.90 | 54.63 | 43 | AVB | | 0.1853 | 0.1578 |
| 2012JU | 2.124 | 0.582 | 7.178 | 0.887 | 229.64 | 52.12 | 147 | AVB | | 0.2057 | 0.1719 |
| 2012KA4 | 1.100 | 0.780 | 5.809 | 0.242 | 237.38 | 215.00 | 71 | APS | | 0.1888 | 0.1893 |
| 2012KA4 | | | | | | | | NIA | | 0.1722 | 0.1729 |
| 2012KA4 | | | | | | | | SMA | | 0.1047 | 0.1159 |
| 2012KX41 | 2.350 | 0.622 | 4.384 | 0.889 | 253.86 | 47.12 | | COR | 0.0596 | 0.2092 | 0.1872 |
| 2012KZ41 | 2.297 | 0.602 | 1.566 | 0.913 | 202.24 | 92.98 | 47 | COR | 0.0403 | 0.1362 | 0.1149 |
| 2012KZ41 | | | | | | | 70 | HVI | 0.0580 | 0.1905 | 0.1329 |

**Table D.1:** continued.

| Asteroid | a[a.u.] | e | i[deg.] | q[a.u.] | Ω[deg.] | ω[deg.] | $T_L$ | Shower | $D_{acs}$ | $D_{sh}$ | $D_j$ |
|---|---|---|---|---|---|---|---|---|---|---|---|
| 2012LJ | 2.323 | 0.699 | 0.687 | 0.700 | 96.34 | 239.08 | 68 | AVB | | 0.1412 | 0.1375 |
| 2012LT | 2.311 | 0.553 | 5.447 | 1.033 | 189.74 | 77.54 | 46 | COR | 0.0545 | 0.1893 | 0.1869 |
| 2012TT231 | 1.954 | 0.647 | 7.053 | 0.690 | 274.34 | 196.15 | 71 | AND | | 0.1505 | 0.1421 |
| 2012TT5 | 2.076 | 0.655 | 15.241 | 0.717 | 273.02 | 11.70 | 85 | AVB | | 0.1887 | 0.1877 |
| 2012UR158 | 2.239 | 0.855 | 3.219 | 0.324 | 238.14 | 287.70 | 358 | BTA | | 0.1609 | 0.1609 |
| 2012UR158 | | | | | | | | NTA | 0.0449 | 0.1710 | 0.1742 |
| 2012VB5 | 2.090 | 0.651 | 5.688 | 0.729 | 257.98 | 220.32 | 71 | AND | | 0.1871 | 0.1857 |
| 2012XM134 | 3.305 | 0.699 | 2.120 | 0.994 | 81.28 | 311.12 | 94 | OCC | | 0.0865 | 0.0862 |
| 2013AB65 | 1.801 | 0.748 | 2.433 | 0.453 | 252.50 | 113.65 | 32 | SSG | | 0.1580 | 0.1580 |
| 2013CT36 | 2.463 | 0.818 | 6.363 | 0.449 | 39.18 | 351.35 | 309 | ORS | | 0.1401 | 0.1474 |
| 2013GL8 | 2.431 | 0.843 | 8.538 | 0.382 | 47.45 | 331.69 | 543 | STA | | 0.1742 | 0.1762 |
| 2013HT25 | 4.524 | 0.945 | 5.185 | 0.251 | 60.89 | 24.21 | 94 | APS | | 0.1845 | 0.1845 |
| 2013JT17 | 2.422 | 0.568 | 13.073 | 1.048 | 223.11 | 54.36 | 172 | TAH | | 0.1673 | 0.1532 |
| 2013PW31 | 2.342 | 0.525 | 3.333 | 1.112 | 143.85 | 146.14 | 199 | COR | 0.0477 | 0.1379 | 0.0955 |
| 2013RN21 | 2.425 | 0.560 | 4.885 | 1.067 | 138.92 | 158.60 | 96 | COR | 0.0484 | 0.1576 | 0.1458 |
| 2013RU9 | 2.490 | 0.585 | 4.144 | 1.033 | 67.46 | 323.23 | 230 | COR | 0.0555 | 0.1152 | 0.1112 |
| 2013WX44 | 2.818 | 0.665 | 3.914 | 0.945 | 139.80 | 252.14 | 140 | OCC | | 0.1310 | 0.1260 |
| 2013XT21 | 2.482 | 0.653 | 3.074 | 0.860 | 130.59 | 262.67 | 58 | OCC | | 0.1782 | 0.1429 |
| 2013YL2 | 1.185 | 0.660 | 5.823 | 0.403 | 303.72 | 277.80 | 45 | NCC | | 0.1764 | 0.1764 |
| 2014HD198 | 2.103 | 0.642 | 0.986 | 0.754 | 69.60 | 220.27 | 44 | AVB | | 0.1878 | 0.1877 |
| 2014HE197 | 2.214 | 0.598 | 3.222 | 0.890 | 102.80 | 185.12 | 56 | COR | 0.0538 | 0.1369 | 0.1008 |
| 2014HK197 | 2.335 | 0.650 | 5.560 | 0.818 | 254.47 | 31.53 | 124 | AVB | | 0.1406 | 0.1287 |
| 2014HN199 | 2.215 | 0.653 | 2.901 | 0.768 | 268.85 | 22.14 | 199 | AVB | | 0.1849 | 0.1841 |
| 2014HN199 | | | | | | | | HVI | 0.0416 | 0.0710 | 0.0683 |
| 2014HT178 | 2.396 | 0.639 | 4.692 | 0.865 | 238.64 | 41.13 | 544 | AVB | | 0.1517 | 0.1185 |
| 2014HT197 | 2.246 | 0.609 | 2.072 | 0.877 | 234.64 | 39.54 | 44 | AVB | | 0.1962 | 0.1658 |

**Table D.1:** continued.

| Asteroid | a[a.u.] | e | i[deg.] | q[a.u.] | Ω[deg.] | $\omega$[deg.] | $T_L$ | Shower | $D_{acs}$ | $D_{sh}$ | $D_j$ |
|---|---|---|---|---|---|---|---|---|---|---|---|
| 2014HT197 | | | | | | | | COR | 0.0526 | 0.1765 | 0.1433 |
| 2014HU2 | 2.335 | 0.672 | 1.131 | 0.767 | 224.76 | 56.24 | 121 | AVB | | 0.1218 | 0.1206 |
| 2014HU2 | | | | | | | | HVI | 0.0227 | 0.1232 | 0.1218 |
| 2014JH15 | 2.316 | 0.624 | 1.525 | 0.871 | 79.01 | 205.90 | 64 | COR | 0.0575 | 0.1520 | 0.1065 |
| 2014JH15 | | | | | | | | HVI | 0.0385 | 0.1496 | 0.1105 |
| 2014KH39 | 2.343 | 0.593 | 5.452 | 0.954 | 210.97 | 74.61 | 102 | COR | 0.0543 | 0.0730 | 0.0621 |
| 2014MC6 | 2.215 | 0.629 | 10.399 | 0.821 | 197.23 | 83.94 | 159 | AVB | | 0.1898 | 0.1804 |
| 2014NK52 | 2.199 | 0.838 | 2.544 | 0.355 | 268.62 | 256.30 | 200 | BTA | | 0.1478 | 0.1514 |
| 2014NK52 | | | | | | | | NTA | 0.0262 | 0.1442 | 0.1442 |
| 2014OM207 | 2.430 | 0.584 | 2.247 | 1.012 | 168.62 | 122.71 | 45 | COR | 0.0301 | 0.0655 | 0.0645 |
| 2014OO6 | 2.202 | 0.680 | 1.382 | 0.706 | 287.34 | 111.18 | 36 | CAP | | 0.1992 | 0.1824 |
| 2014OY1 | 2.578 | 0.625 | 23.022 | 0.967 | 186.71 | 76.32 | 72 | TAH | | 0.1747 | 0.1747 |
| 2014SM142 | 2.576 | 0.596 | 26.711 | 1.041 | 16.88 | 19.54 | 302 | PPU | | 0.1683 | 0.1646 |
| 2014WN202 | 2.574 | 0.579 | 13.465 | 1.084 | 339.48 | 53.83 | 102 | PPU | | 0.2026 | 0.1889 |
| 2014XD32 | 2.083 | 0.657 | 7.362 | 0.714 | 182.39 | 326.18 | 55 | AVB | | 0.1499 | 0.1483 |
| 2014XE32 | 2.534 | 0.660 | 2.918 | 0.862 | 132.37 | 259.67 | 61 | OCC | | 0.1741 | 0.1389 |
| 2014XL6 | 2.545 | 0.620 | 2.111 | 0.966 | 324.01 | 76.25 | 51 | OCC | | 0.1708 | 0.1698 |
| 2015BA513 | 1.705 | 0.691 | 4.016 | 0.528 | 87.98 | 293.05 | 53 | SSG | | 0.1736 | 0.1741 |
| 2015BL311 | 2.368 | 0.844 | 1.717 | 0.370 | 143.20 | 220.41 | 101 | SSG | | 0.1764 | 0.1862 |
| 2015CE1 | 1.591 | 0.660 | 6.330 | 0.541 | 257.81 | 137.17 | 97 | CAP | | 0.1243 | 0.1232 |
| 2015CP | 2.398 | 0.797 | 4.808 | 0.488 | 259.30 | 137.48 | 151 | CAP | | 0.1116 | 0.1071 |
| 2015DA54 | 2.608 | 0.782 | 8.237 | 0.567 | 246.25 | 147.52 | 87 | CAP | 0.0274 | 0.0566 | 0.0563 |
| 2015DE54 | 2.140 | 0.801 | 6.831 | 0.426 | 254.75 | 143.31 | 182 | CAP | | 0.1672 | 0.1666 |
| 2015ER | 2.320 | 0.816 | 11.554 | 0.426 | 305.72 | 335.03 | 73 | EVI | | 0.1369 | 0.1380 |
| 2015FD35 | 1.517 | 0.672 | 5.888 | 0.498 | 335.74 | 302.83 | 81 | EVI | | 0.1720 | 0.1724 |

**Table D.1:** continued.

| Asteroid | a[a.u.] | e | i[deg.] | q[a.u.] | Ω[deg.] | ω[deg.] | $T_L$ | Shower | $D_{acs}$ | $D_{sh}$ | $D_j$ |
|---|---|---|---|---|---|---|---|---|---|---|---|
| 2015FQ | 2.244 | 0.715 | 2.395 | 0.639 | 86.61 | 192.43 | 58 | AVB | | 0.1936 | 0.1796 |
| 2015FQ117 | 0.861 | 0.620 | 4.560 | 0.327 | 63.09 | 293.91 | 28 | XSA | | 0.1534 | 0.1626 |
| 2015GJ13 | 2.459 | 0.712 | 2.705 | 0.708 | 97.90 | 185.01 | 47 | AVB | | 0.1806 | 0.1788 |
| 2015KK | 2.560 | 0.786 | 16.411 | 0.548 | 85.50 | 56.59 | 217 | OER | | 0.1253 | 0.1244 |
| 2015MN11 | 2.043 | 0.704 | 5.713 | 0.604 | 86.39 | 277.64 | 44 | SSG | | 0.1846 | 0.1780 |
| 2015NJ3 | 1.688 | 0.671 | 12.279 | 0.555 | 251.35 | 134.49 | 214 | CAP | | 0.1746 | 0.1743 |
| 2015PM307 | 2.225 | 0.863 | 8.090 | 0.304 | 319.04 | 142.18 | 88 | NIA | | 0.0928 | 0.1436 |
| 2015PM307 | | | | | | | | SMA | | 0.1734 | 0.1792 |
| 2015PU228 | 2.282 | 0.790 | 9.445 | 0.479 | 271.57 | 301.88 | 593 | NCC | | 0.1466 | 0.1509 |
| 2015TC144 | 2.304 | 0.777 | 3.063 | 0.514 | 59.78 | 218.83 | 123 | EVI | | 0.1549 | 0.1554 |
| 2015TL143 | 2.590 | 0.602 | 4.983 | 1.031 | 194.00 | 197.92 | 66 | OCC | | 0.1893 | 0.1855 |
| 2015TX24 | 2.267 | 0.872 | 6.042 | 0.290 | 127.03 | 33.00 | 77 | BTA | | 0.1763 | 0.1818 |
| 2015TX24 | | | | | | | | STA | | 0.1640 | 0.1803 |
| 2015VH66 | 2.280 | 0.848 | 7.364 | 0.347 | 195.40 | 329.75 | 181 | BTA | | 0.1800 | 0.1817 |
| 2015VR65 | 2.600 | 0.614 | 16.739 | 1.003 | 343.71 | 45.36 | 161 | PPU | | 0.1187 | 0.1187 |
| 2016BN14 | 2.360 | 0.756 | 10.072 | 0.577 | 270.89 | 125.69 | 166 | CAP | | 0.0572 | 0.0572 |
| 2016BP14 | 2.880 | 0.759 | 2.000 | 0.693 | 227.57 | 165.93 | 50 | CAP | | 0.1584 | 0.1414 |
| 2016BV14 | 2.359 | 0.714 | 7.706 | 0.675 | 261.31 | 137.96 | 45 | CAP | | 0.1338 | 0.1203 |
| 2016CA136 | 2.033 | 0.781 | 1.255 | 0.445 | 124.83 | 239.91 | 44 | SSG | | 0.1204 | 0.1205 |
| 2016CL137 | 1.917 | 0.712 | 0.765 | 0.552 | 250.99 | 152.21 | 19 | CAP | | 0.1787 | 0.1782 |
| 2016CM246 | 1.946 | 0.776 | 6.220 | 0.436 | 44.54 | 325.36 | 710 | SSG | 0.0258 | 0.1084 | 0.1090 |
| 2016CM246 | | | | | | | | STA | 0.0274 | 0.1502 | 0.1636 |
| 2016CW264 | 2.037 | 0.769 | 5.752 | 0.470 | 258.33 | 141.29 | 178 | CAP | | 0.1361 | 0.1322 |
| 2016ES155 | 1.433 | 0.655 | 8.057 | 0.494 | 290.21 | 352.54 | 76 | EVI | | 0.1843 | 0.1846 |
| 2016EV28 | 1.944 | 0.770 | 1.976 | 0.448 | 106.80 | 166.16 | 72 | EVI | | 0.1452 | 0.1453 |

**Table D.1:** continued.

| Asteroid | a[a.u.] | e | i[deg.] | q[a.u.] | Ω[deg.] | $\omega$[deg.] | $T_L$ | Shower | $D_{acs}$ | $D_{sh}$ | $D_j$ |
|---|---|---|---|---|---|---|---|---|---|---|---|
| 2016FC14 | 2.235 | 0.660 | 3.964 | 0.760 | 218.11 | 245.97 | 72 | AND | | 0.1356 | 0.1356 |
| 2016HN3 | 2.150 | 0.554 | 19.329 | 0.959 | 199.75 | 64.25 | 86 | TAH | | 0.1625 | 0.1623 |
| 2016JD18 | 2.794 | 0.690 | 5.398 | 0.867 | 227.21 | 57.83 | 46 | AVB | | 0.1632 | 0.1316 |
| 2016JS5 | 2.105 | 0.627 | 3.054 | 0.785 | 245.07 | 45.42 | 157 | AVB | | 0.1906 | 0.1880 |
| 2016LE10 | 2.415 | 0.618 | 3.243 | 0.922 | 42.23 | 257.33 | 49 | COR | 0.0533 | 0.1988 | 0.1876 |
| 2016LW9 | 1.133 | 0.749 | 11.284 | 0.285 | 231.17 | 227.66 | 151 | SMA | | 0.1302 | 0.1316 |
| 2016LZ8 | 2.239 | 0.527 | 2.783 | 1.059 | 203.02 | 90.69 | 115 | COR | 0.0578 | 0.1084 | 0.0948 |
| 2016MS | 2.455 | 0.555 | 1.763 | 1.092 | 136.41 | 138.45 | 102 | COR | 0.0411 | 0.1450 | 0.1196 |
| 2016NG22 | 1.886 | 0.696 | 7.546 | 0.573 | 115.97 | 263.68 | 194 | SSG | | 0.1787 | 0.1766 |
| 2016NO16 | 2.458 | 0.574 | 26.996 | 1.047 | 182.34 | 151.41 | 75 | AUD | | 0.1633 | 0.1597 |
| 2016NO16 | | | | | | | | KCG | | 0.1785 | 0.1726 |
| 2016PD40 | 2.453 | 0.538 | 3.424 | 1.134 | 228.15 | 70.58 | 132 | COR | 0.0500 | 0.1908 | 0.1487 |
| 2016PE8 | 2.470 | 0.597 | 2.352 | 0.996 | 135.75 | 138.95 | 80 | COR | 0.0478 | 0.1186 | 0.1186 |
| 2016PN38 | 2.459 | 0.621 | 3.602 | 0.933 | 55.59 | 344.45 | 54 | OCC | | 0.1856 | 0.1798 |
| 2016QY1 | 2.281 | 0.600 | 2.571 | 0.912 | 114.49 | 159.09 | 83 | COR | 0.0371 | 0.1607 | 0.1427 |
| 2016RO40 | 2.295 | 0.649 | 3.832 | 0.805 | 284.18 | 4.95 | 74 | AVB | | 0.1759 | 0.1696 |
| 2016RO40 | | | | | | | | HVI | 0.0523 | 0.1047 | 0.0930 |
| 2016RZ40 | 2.809 | 0.611 | 1.765 | 1.092 | 12.93 | 26.32 | 185 | OCC | | 0.2017 | 0.1795 |
| 2016SF | 2.132 | 0.609 | 5.621 | 0.834 | 285.24 | 0.22 | 83 | AVB | | 0.1772 | 0.1629 |
| 2016TJ18 | 2.406 | 0.585 | 17.771 | 0.998 | 348.93 | 45.00 | 100 | PPU | | 0.1145 | 0.1145 |
| 2016TP18 | 1.094 | 0.686 | 4.646 | 0.343 | 295.50 | 210.93 | 49 | BTA | | 0.1832 | 0.1843 |
| 2016TP18 | | | | | | | | NTA | | 0.1867 | 0.1871 |
| 2016TV93 | 2.828 | 0.608 | 2.016 | 1.109 | 208.98 | 187.27 | 704 | OCC | | 0.2035 | 0.1730 |
| 2016TW18 | 1.973 | 0.626 | 4.579 | 0.737 | 234.62 | 236.09 | 171 | AND | | 0.1563 | 0.1555 |
| 2016UP36 | 2.540 | 0.693 | 2.064 | 0.780 | 261.55 | 197.49 | 100 | AND | | 0.1679 | 0.1671 |

**Table D.1:** continued.

| Asteroid | a[a.u.] | e | i[deg.] | q[a.u.] | Ω[deg.] | ω[deg.] | $T_L$ | Shower | $D_{acs}$ | $D_{sh}$ | $D_j$ |
|---|---|---|---|---|---|---|---|---|---|---|---|
| 2016VK | 1.781 | 0.779 | 5.960 | 0.394 | 315.32 | 210.95 | 38 | NTA | | 0.1760 | 0.1794 |
| 2016VQ | 2.497 | 0.661 | 2.666 | 0.847 | 228.68 | 229.75 | 87 | AND | | 0.1935 | 0.1807 |
| 2016WN48 | 2.738 | 0.640 | 4.838 | 0.986 | 299.33 | 88.92 | 46 | OCC | | 0.1753 | 0.1753 |
| 2017FL101 | 2.847 | 0.785 | 4.618 | 0.612 | 276.68 | 184.66 | 218 | AND | | 0.1993 | 0.1721 |
| 2017FU64 | 2.445 | 0.707 | 6.907 | 0.717 | 247.04 | 21.26 | 58 | AVB | 0.0362 | 0.1232 | 0.1215 |
| 2017JA | 2.032 | 0.616 | 1.978 | 0.781 | 244.65 | 42.99 | 49 | AVB | | 0.1791 | 0.1769 |
| 2017KQ27 | 2.335 | 0.589 | 4.773 | 0.959 | 30.12 | 256.84 | 75 | COR | 0.0425 | 0.1358 | 0.1314 |
| 2017MA3 | 2.353 | 0.578 | 4.005 | 0.993 | 196.95 | 100.70 | 63 | COR | 0.0255 | 0.1245 | 0.1244 |
| 2017MB1 | 2.372 | 0.753 | 8.508 | 0.586 | 264.64 | 126.97 | 176 | CAP | | 0.0463 | 0.0461 |
| 2017NW5 | 3.050 | 0.709 | 28.956 | 0.887 | 186.45 | 149.71 | 60 | AUD | | 0.1791 | 0.1469 |
| 2017NW5 | | | | | | | | KCG | | 0.1602 | 0.1318 |
| 2017QB17 | 2.301 | 0.515 | 2.472 | 1.115 | 173.50 | 122.47 | 117 | COR | 0.0580 | 0.1639 | 0.1281 |
| 2017QN18 | 2.147 | 0.831 | 6.656 | 0.363 | 176.39 | 280.49 | 123 | SMA | | 0.1357 | 0.1752 |
| 2017QT1 | 2.546 | 0.751 | 1.120 | 0.635 | 100.68 | 311.22 | 67 | CAP | | 0.1806 | 0.1777 |
| 2017SA | 2.442 | 0.548 | 2.595 | 1.103 | 203.47 | 85.88 | 122 | COR | 0.0381 | 0.1132 | 0.0665 |
| 2017SB33 | 1.850 | 0.625 | 11.348 | 0.693 | 237.28 | 220.04 | 454 | AND | | 0.1740 | 0.1673 |
| 2017SG33 | 2.397 | 0.550 | 5.415 | 1.079 | 109.57 | 188.88 | 154 | COR | 0.0557 | 0.1858 | 0.1721 |
| 2017SK10 | 2.064 | 0.932 | 24.591 | 0.140 | 202.44 | 3.31 | 4098 | DLT | | 0.1207 | 0.1861 |
| 2017SP12 | 1.804 | 0.622 | 11.569 | 0.682 | 223.93 | 49.17 | 47 | AVB | | 0.1588 | 0.1525 |
| 2017UE45 | 2.829 | 0.673 | 15.106 | 0.926 | 200.39 | 275.95 | 67 | DPC | | 0.1483 | 0.1462 |
| 2017UE5 | 2.012 | 0.599 | 6.073 | 0.807 | 232.72 | 234.41 | 117 | AND | | 0.1641 | 0.1599 |
| 2017UL7 | 2.211 | 0.661 | 2.479 | 0.749 | 290.29 | 181.24 | 133 | AND | | 0.1708 | 0.1707 |
| 2017UM1 | 1.971 | 0.654 | 4.065 | 0.682 | 267.47 | 198.22 | 124 | AND | | 0.1562 | 0.1461 |
| 2017UM44 | 1.756 | 0.745 | 8.486 | 0.448 | 127.58 | 23.61 | 54 | STA | | 0.1239 | 0.1427 |
| 2017UW7 | 2.532 | 0.606 | 14.860 | 0.998 | 347.29 | 33.10 | 153 | PPU | | 0.1805 | 0.1804 |

**Table D.1:** continued.

| Asteroid | a[a.u.] | e | i[deg.] | q[a.u.] | Ω[deg.] | $\omega$[deg.] | $T_L$ | Shower | $D_{acs}$ | $D_{sh}$ | $D_j$ |
|---|---|---|---|---|---|---|---|---|---|---|---|
| 2017VC13 | 2.706 | 0.606 | 3.307 | 1.065 | 181.05 | 213.38 | 234 | OCC | | 0.1847 | 0.1717 |
| 2017VM2 | 2.613 | 0.615 | 1.969 | 1.007 | 155.44 | 238.86 | 119 | OCC | | 0.1566 | 0.1557 |
| 2017XC2 | 2.580 | 0.581 | 20.684 | 1.082 | 3.36 | 21.04 | 3424 | PPU | | 0.1600 | 0.1430 |
| 2017YC6 | 2.753 | 0.702 | 0.358 | 0.821 | 56.93 | 341.36 | 58 | OCC | | 0.1857 | 0.1241 |
| 2017YO4 | 2.236 | 0.830 | 7.400 | 0.381 | 26.74 | 189.67 | 76 | NCC | | 0.1488 | 0.1505 |
| 2017YO4 | | | | | | | | SCC | 0.0513 | 0.1525 | 0.1565 |
| 2018AK12 | 1.926 | 0.710 | 2.532 | 0.559 | 272.84 | 303.42 | 61 | NCC | | 0.1819 | 0.1859 |
| 2018BT6 | 2.279 | 0.830 | 3.020 | 0.387 | 71.93 | 307.22 | 158 | SSG | | 0.1642 | 0.1702 |

# List of papers

1. Dumitru, B. A.; Birlan, M.; Sonka, A.; Colas, F.; Nedelcu, D. A., "Photometry of asteroids (5141), (43032), (85953), (259221), and (363599) observed at Pic du Midi Observatory", Astronomische Nachrichten, vol. 339, issue 2-3, pp. 198-203, 2018 (AIS = 0.5, ISI = 1,322).

2. Dumitru, B. A.; Birlan, M.; Popescu, M.; Nedelcu, D. A., "Association between meteor showers and asteroids using multivariate criteria", Astronomy and Astrophysics, Volume 607, id.A5, 22 pp., 2017 (AIS = 1.7, ISI = 5.565).

3. Birlan, M.; Popescu, M.; Nedelcu, D. A.; Turcu, V.; Pop, A.; Dumitru, B.; Stevance, F.; Vaduvescu, O.; Moldovan, D.; Rocher, P.; Sonka, A.; Mircea, L., "Characterization of (357439) 2004 BL86 on its close approach to Earth in 2015", Astronomy and Astrophysics, Volume 581, id.A3, 7 pp., 2015 (AIS = 1.7, ISI = 5.185)

4. Birlan, Mirel; Nedelcu, Dan Alin; Sonka, Adrian; Popescu, Marcel; Dumitru, Bogdan, "Observations for Secure and Recovery Near-Earth Asteroids", Romanian Astronomical Journal, Vol. 26, No. 1, p. 25-33, 2016

5. Dumitru, B. A.; Birlan, M.; Nedelcu, A.; Popescu, M., "Investigation of meteor shower parent bodies using various metrics", Proceedings of the International Meteor Conference, Egmond, the Netherlands, 2-5 June 2016, Eds.: Roggemans, A.; Roggemans, P., ISBN 978-2-87355-030-1, pp. 69-72, 2016

# List of conferences

1. Annual Scientific Session of the Physics Faculty 2018, Romania
2. Annual Scientific Session of the Physics Faculty 2017, Romania
3. International Meteor Conference 2016, 02:05-06-2016, Netherlands
4. XXVIII Canary Islands Winter School of Astrophysics, 07:16-11-2016, Spain
5. Annual Scientific Session of the Physics Faculty 2015, Romania
6. Akdeniz Astrometry and Photometry Workshop 5-8 august 2014 Antalia, Turkey

# List of Minor Planet Electronic Circulars


1. Okumura, S.; Urakawa, S.; Sonka, A.; Dumitru, B.; Birlan, M.; Nedelcu, A.; Johnson, J. A.; Christensen, E. J.; Gibbs, A. R.; Grauer, A. D.; Hill, R. E.; Kowalski, R. A.; Larson, S. M.; Shelly, F. C.; McCarthy Obs, J. J.; Polansky, M.; Dupouy, P.; de Vanssay, J. B.; Lindner, P.; Holmes, R.; Vorobjov, T.; Buzzi, L.; Foglia, S.; Linder, T.; Inceu, V.; Hudin, L.; Mickleburgh, A., "2014 VM", Minor Planet Electronic Circ., No.2014-V25 (2014)

2. Ticha, J.; Tichy, M.; Kocer, M.; Mastaler, R. A.; Birlan, M.; Sonka, A.; Nedelcu, A.; Dumitru, B.; Euronear, T.; Kowalski, R. A.; Christensen, E. J.; Gibbs, A. R.; Grauer, A. D.; Hill, R. E.; Johnson, J. A.; Larson, S. M.; Shelly, F. C.; Linder, T.; Holmes, R.; Dupouy, P.; de Vanssay, J. B.; Bacci, P.; Emilio, R.; Belli, M.; Mangini, A.; Pistolesi, A.; Feraboli, M.; Hidas, A.; Gibson, B.; Goggia, T.; Primak, N.; Schultz, A.; Willman, M.; Bolin, B.; Chambers, K.; Chastel, S.; Denneau, L.; Flewelling, H.; Huber, M.; Magnier, E.; Schunova, E.; Wainscoat, R.; Waters, C.; Vorobjov, T.; Buzzi, L.; Foglia, S., "2014 US192", Minor Planet Electronic Circ., No.2014-V20 (2014)

3. Sonka, A.; Dumitru, B.; Nedelcu, A.; Birlan, M.; Kowalski, R. A.; Christensen, E. J.; Gibbs, A. R.; Grauer, A. D.; Hill, R. E.; Johnson, J. A.; Larson, S. M.; Shelly, F. C.; Holmes, R.; Vorobjov, T.; Buzzi, L.; Foglia, S.; Linder, T.; Hug, G.; Birtwhistle, P., "2014 VA", Minor Planet Electronic Circ., No.2014-V16 (2014)

4. Mastaler, R. A.; Sonka, A.; Dumitru, B.; Birlan, M.; Nedelcu, A.; Gibson, B.; Goggia, T.; Primak, N.; Schultz, A.; Willman, M.; Bolin, B.; Chambers, K.; Chastel, S.; Denneau, L.; Flewelling, H.; Huber, M.; Magnier, E.; Schunova, E.; Wainscoat, R.; Waters, C.; Holmes, R.; Buzzi, L.; Foglia, S.; Vorobjov, T.; Linder, T., "2014 UK192", Minor Planet Electronic Circ., No.2014-V15 (2014)

5. Birlan, M.; Sonka, A.; Nedelcu, A.; Dumitru, B.; Gibbs, A. R.; Kowalski, R. A.; Christensen, E. J.; Grauer, A. D.; Hill, R. E.; Johnson, J. A.; Larson, S. M.; Shelly, F. C.; Hug, G., "2014 UF192", Minor Planet Electronic Circ., No.2014-V10 (2014)

## ABSTRACT

Meteoroizii, asteroizii și cometele au interacționat permanent cu Pământul în timpul existenței sale. Când un obiect, cum ar fi o cometă sau un asteroid, orbitează în jurul Soarelui, poate lăsa fragmente de materie în urma lui, iar dacă acest obiect este în proximitatea Pământului, aceste fragmente sunt adunate de gravitația planetei. Studiul acestor obiecte și legătura dintre ele pot contribui la înțelegerea condițiilor de formare și evoluție a Sistemului Solar, a condițiilor de dezvoltare a vieții pe Pământ, a proceselor haotice din Sistemul Solar, a securității Pământului și, poate, în viitor, industria spațială.

Toate obiectele din Sistemul Solar sunt caracterizate de orbitele lor, iar curenții meteorici au orbite similare cu obiectele care le produc. Din acest motiv, cele mai comune metode de identificare a corpului părinte se bazează pe similaritățile orbitelor, cunoscute și ca criterii de discriminare sau criteriul-D. În această lucrarea am folosit trei metrici ale criteriului-D pentru asocierea corpului părinte. Am stabilit o valuare de prag pentru fiecare metrică folosind o nouă metodă de selectare a acestor valori. Mai mult, am investigat stabilitatea orbitală a obiectelor asociate, în sensul timpului Lyapunov și proprietăților fizice.

Datorită asemănărilor orbitale dintre curenților meteorici și corpurile care le produc, este necesar ca obiectele asociate să aparțină populației de asteroizi din apropierea Pământului. Dar pentru această populație este dificil să se obțină date. Geometria favorabilă pentru observațiile acestor obiecte are loc de cinci ori pe secol. Din acest motiv a fost creat un program observațional, care vizează obținerea datelor fizice pentru obiectele asociate care nu au date fizice.

Rezultatele mele constau intr-un eșantion care conține 296 asteroizi care au fost asociați cu 28 de curenți meteorici, dintre care 73 de asteroizi au fost asociați de toate metricile folosite. Din perspectiva dinamică, eșantionul meu conține 82\% de asteroizii Apollo, 7\% sunt clasificați ca potențiali periculoși, 15,3\% sunt pe orbite cometare, iar 84,3\% sunt pe orbite asteroidale. Din perspectiva datelor fizice, am găsit doi asteroizi care se rotesc foarte repede in jurul propriei axe, deci nu pot genera meteori. Pe de altă parte, am descoperit asociați, un asteroid binar și un asteroid care se rostogolește, obiecte care au o probabilitate mare de a fi corpuri părinte.

De asemenea, am reușit să găsesc asemănări între 5 meteoriți și 5 asteroizi asociați cu date fizice și am obținut date observaționale pentru trei asteroizi asociați.

## CUVINTE CHEIE

Meteoroizi, Meteori, Meteoroiți, Curent meteoric, Ploaie de meteori, Planete Minore (Asteroizi), metodele criteriului D

## RÉSUMÉ

Les météoroïdes, les astéroïdes et les comètes ont été en interaction permanente avec la Terre pendant son existence. Lorsqu'un objet, tel qu'une comète ou un astéroïde, tourne autour du Soleil, il peut laisser des fragments de matière derrière lui. Il y a une relation implicite entre les fragments et leurs corps parents. Le champ gravitationnel de la Terre capte les fragments et quelques fois le matériel extraterrestre est retrouve au sol sous la forme des météorites. L'étude de ces objets et le lien entre eux peuvent aider comprendre les conditions de formation et d'évolution du Système solaire, les conditions de développement de la vie sur Terre, les processus chaotiques dans le Système solaire, la sécurité de la Terre et peut-être, l'industrie spatiale.

Tous les objets dans le Système solaire sont caractérisés par leurs orbites et les flux de météoroïdes ont des orbites similaires avec les objets qui les produisent. Pour cette raison, la méthode la plus courante d'identification du corps parental est basée sur les similarités des orbites, également appelées critères de discrimination ou critères-D. Dans mon travail, j'ai utilisé trois critères D-Criteria pour l'association des corps parents. Je définis un seuil pour chaque mesure en utilisant une nouvelle méthode de sélection de seuil. En outre, j'ai étudié les objets associés stabilité orbitale, dans le sens du temps de Lyapunov et leurs propriétés physiques.

En raison des similitudes entre les flux de météorites et leurs corps parents, il est nécessaire que les associations appartiennent à la population d'astéroïdes géocroiseurs. L'observation de cette population d'objets est cependant difficile. La géométrie favorable pour les observations d'un géocroiseur  est limité a trois ou cinq fois par siècle. Pour cette raison j'ai créé un programme d'observation, qui vise à obtenir des données physiques pour les objets associés qui n'ont pas de données physiques.

Lors de mes  recherches, j'ai pu associé 296 géocroiseurs  à 28 pluies de météores; parmi eux, 73 astéroïdes satisfaisant les trois critères utilisés. Du point de vue dynamique, mon échantillon contient 82% d'astéroïdes de type Apollo et 7% sont classés comme potentiellement dangereux, 15,3% sont sur des orbites cométaires et 84,3% sur des orbites d'astéroïdes. Du point de vue des données physiques, j'ai trouvé deux astéroïdes qui sont des rotateurs rapides, donc ils ne peuvent pas générer de météores. D'un autre côté, j'ai également trouvé un astéroïde binaire associé et un astéroïde tumbling, des objets avec une forte probabilité d'être des corps parents.

J'ai également réussi à trouver des similitudes entre 5 météorites et 5 astéroïdes associés avec des données physiques et j'ai obtenu des données d'observation pour trois astéroïdes associés.

## MOTS CLÉS

Météores, Météores, Météorites, Courants des Météores, Vents de météore, Planètes mineures (astéroïdes), Méthodes D-Critères

## ABSTRACT

Meteoroids, asteroids, and comets have been permanently interacting with Earth during its existence. When an object, such as a comet or an asteroid, revolve around the Sun it may leave fragments of matter behind it and if this object is in Earth's proximity, those fragments are gathered by the planet gravity. The study of these objects and the link between them can help in the understanding of the formation and evolution conditions of the Solar System, the conditions of developing the life on Earth, the chaotic processes in the Solar System, Earth security and maybe, in future, space industry.

All objects within the Solar System are characterized by their orbits and the meteoroid streams have similar orbits with the objects that produce them. For that reason the most common method of parent body identification is based on orbits similarities, also known as discrimination criteria or D-Criteria. In my work I used three D-Criteria metrics for parent body association. I set a threshold for each metric by using a new threshold selection method. Moreover, I investigated the associated objects orbital stability, in the Lyapunov time sense and their physical properties.

Due to the similarities between meteoroid streams and their parent bodies, it is required for the associations to belong to Near Earth Asteroids population. But for this population is difficult to obtain data. The favorable geometry for these objects observations occurs five times per century. For this reason was created an observational program, that aims to obtain physical data for the associated objects that do not have physical data.

My results consist from a sample of 296 asteroids that were associated with 28 meteor showers, from which 73 asteroids satisfied all the criteria used. From the dynamical perspective, my sample contains 82% of Apollo asteroids and 7% are classified as potential hazardous, 15.3% are on commentary orbits and 84.3% are on asteroidal orbits. From the physical data perspective, I found two asteroids that are fast-rotators, therefore they can not generate meteors. On the other hand, I also found associated one binary asteroid and one tumbling asteroid, objects with a high probability of being parent bodies.

I also managed to find similarities between 5 meteorites and 5 associated asteroids with physical data and I obtained observational data for three associated

## KEYWORDS

Meteoroids, Meteors, Meteorite, Meteoroids Stream, Meteor Showers, Minor Planets (Asteroids), D-Criteria methods